

Title	FORMATION OF FUNCTIONAL SUPRAMOLECULAR MATERIALS BASED ON STIMULI-RESPONSIVE MOLECULAR RECOGNITION
Author(s)	中畑, 雅樹
Citation	大阪大学, 2015, 博士論文
Version Type	VoR
URL	https://doi.org/10.18910/52304
rights	
Note	

Osaka University Knowledge Archive : OUKA

<https://ir.library.osaka-u.ac.jp/>

Osaka University

**FORMATION OF FUNCTIONAL SUPRAMOLECULAR MATERIALS BASED ON
STIMULI-RESPONSIVE MOLECULAR RECOGNITION**

A Doctoral Thesis
by
Masaki Nakahata

Submitted to
The Graduate School of Science, Osaka University
February, 2015

Acknowledgements

This research work was carried out from 2009 to 2015 under the direction of Professor Dr. Akira Harada at the Department of Macromolecular Science, Graduate School of Science, Osaka University. The author would like to express his sincere gratitude to Professor Dr. Akira Harada for his guidance throughout this study.

Grateful acknowledgements are made to Assistant Professor Dr. Yoshinori Takashima for his continuing help, warm encouragement and kind advices. The author would like to acknowledge Professor Dr. Hiroyasu Yamaguchi and Associate Professor Dr. Akihito Hashidzume for their helpful suggestions. The author also thank to Dr. Kazuya Sakamoto, Dr. Motofumi Osaki, Dr. Daisuke Taura, Dr. Wataru Oi, Dr. Shingo Tamesue, Dr. Yongtai Zheng, Dr. Yuichiro Kobayashi, Dr. Takashi Nakamura, and Dr. Takahiro Kakuta for their helps and suggestions, and to all members of Harada laboratory for their cooperation and friendship.

Grateful acknowledgements are also made to Mr. Seiji Adachi and Dr. Naoya Inazumi for NMR measurements, Dr. Hiroshi Adachi and Dr. Akihiro Ito for MALDI-TOF-Mass measurements, and Assistant Professor Dr. Shogo Nobukawa, Lecturer Dr. Osamu Urakawa, Professor Dr. Toshiyuki Shikata, and Professor Dr. Tadashi Inoue for their helps on rheological measurements.

The author appreciates the financial support from the JSPS fellowship from MEXT of Japan.

Finally, the author is indebted to his father, Masayuki Nakahata and his mother, Etsumi Nakahata for their warm encouragement.

February, 2015

中畑 雅樹

Masaki Nakahata

Contents

Chapter 1.	General Introduction	1
Chapter 2.	Redox-Responsive Self-Healing Materials Formed from Host and Guest Polymers	23
Chapter 3.	Redox-Generated Mechanical Motion of a Supramolecular Polymeric Actuator Based on Host–Guest Interactions	49
Chapter 4.	Redox–Responsive Macroscopic Gel Assembly Based on Discrete Dual Interactions	69
Chapter 5.	Macroscopic Self-assembly Based on Complementary Interaction between Nucleobase Pairs	83
Summary and Conclusion		104
List of publications		106

Chapter 1

General Introduction

1-1. Supramolecular chemistry

In biological system, there are many kinds of biomolecules such as lipids, proteins, nucleic acids and polysaccharides which recognize each other via non-covalent interactions such as electrostatic interaction, hydrogen bonding, hydrophobic interaction and metal-ligand interaction, to form highly-ordered structures such as cells and tissues. These structures form more highly-ordered architectures such as bones, flesh, and organs in a hierarchical way through non-covalent interactions between the surfaces of them. These structures perform indispensable functions to maintain lives of living organisms, such as self-healing themselves from external damage, contraction-expansion to produce mechanical work, and transferring genetic codes to the subsequent generation. The core concept of formation of these structures is self-assembly via molecular recognition. Understanding molecular recognitions in biological system leads to construction of artificial, biomimetic system, which can express functions like living organisms, or beyond them.

The area of chemistry related to molecular assemblies composed of two or more molecules through non-covalent interaction is called “supramolecular chemistry”, which was propounded by J. M. Lehn in 1987. Originally, supramolecular chemistry was called “host-guest chemistry” as represented by crown ethers which selectively include suitable metal ions for their cavity size (Figure 1-1a). Crown ethers were discovered by C. J. Pedersen^{1,2}, who won the Nobel Prize in 1987 with J. M. Lehn³⁻⁵ and D. J. Cram^{6,7}. In recent years, the idea of “supramolecule” spread so widely including proteins consisting of multiple units, Langmuir-Blodgett films, self-assembly films, liquid crystals, and so on. Modern supramolecular chemistry has become interdisciplinary among chemistry, biology, physics, and materials science.

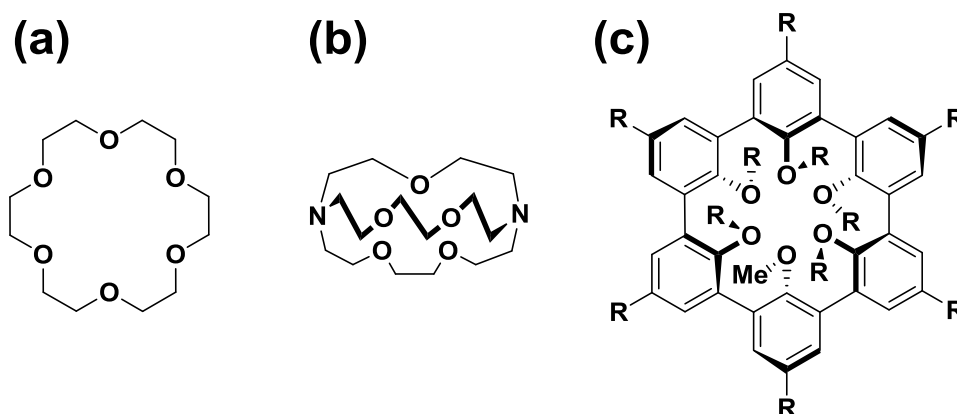


Figure 1-1. Chemical structures of crown ether (a), cryptand (b), and spherand (c).

1-2. Cyclodextrins

1-2-1. Structures and properties of cyclodextrins

Cyclodextrins (CDs, Figure 1-2) are cyclic, water-soluble compounds which are composed of D-glucose units linked with α -1,4 bonds. CD having 6, 7, and 8 glucose units are called α -CD, β -CD, and γ -CD, respectively. CD includes hydrophobic guest molecules inside their hydrophobic cavities in aqueous solution. CD is well-known as a host molecule in the field of supramolecular chemistry⁸⁻¹³. Physical properties of typical CDs are shown in Table 1-1.

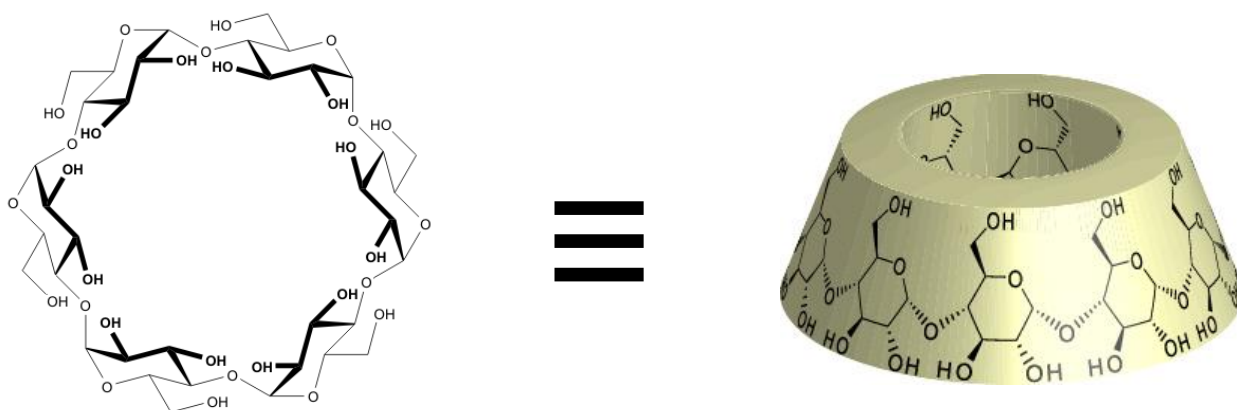


Figure 1-2. Chemical structure and schematic illustration of cyclodextrin (CD).

Table 1-1. Molecular dimensions and physical properties of CDs.

	α -CD	β -CD	γ -CD
Chemical formula	$C_{36}H_{60}O_{30}$	$C_{42}H_{70}O_{35}$	$C_{48}H_{80}O_{40}$
Number of glucose unit	6	7	8
Molecular weight	972.85	1134.98	1297.12
Depth of cavity (Å)	6.7	7.0	7.0
Diameter of cavity (Å)	4.7-5.2	6.0-6.4	7.5-8.3
Water solubility (g/100mL)	14.5	1.85	23.2

1-2-2. Interaction between cyclodextrins and polymers

Harada *et al.* have comprehensively studied a series of research about combination of CDs and polymers focusing attention on multivalent interaction with high selectivity. Generally, interaction between cyclic molecules and (supramolecular) polymers are classified into three categories; terminal recognition, main chain recognition, and side chain recognition (Figure 1-3).

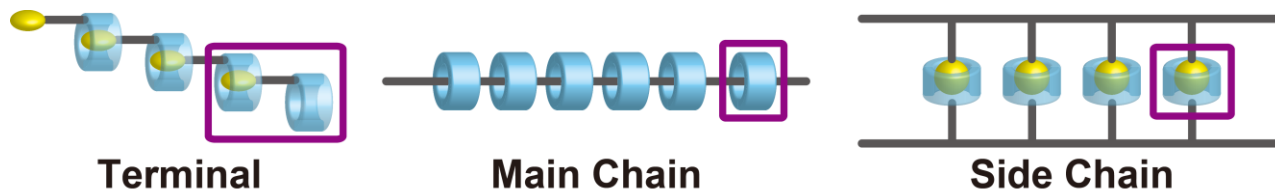


Figure 1-3. Three types of interactions between cyclic molecules and (supramolecular) polymers.

As terminal recognition, there have been a lot of examples of supramolecular polymers¹⁴⁻¹⁷ composed of modified cyclodextrins^{18,19}, which are one of the important core parts in the field of supramolecular chemistry.

As an example of main chain-type recognition, Harada *et al.* firstly reported polypseudorotaxane structure composed of many CD molecules threaded by a poly(ethylene glycol) chain in 1990²⁰. Since this discovery, they have reported a lot of examples of main chain-type supramolecular complexes, such as molecular necklace²¹, tubular polymer made from polyrotaxane²², double-stranded polyrotaxane²³, and so on^{18,19,24,25}. The polyrotaxane structure became a basis in the field of supramolecular materials science²⁶.

As side chain-type recognition, Harada *et al.* extensively studied polymers modified with CDs or guest molecules at the side chain²⁷. In 1976-77, they reported cyclodextrin-containing polymers and their cooperative binding effect and catalytic behavior toward various guest molecules (Figure 1-4)²⁸⁻³⁰.

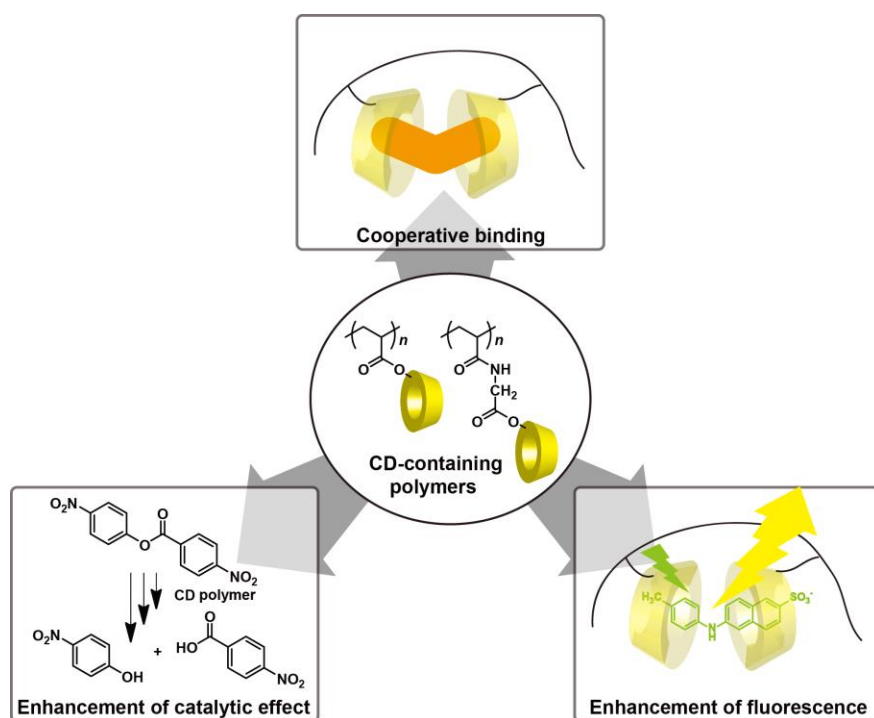


Figure 1-4. Pioneering works about CD-containing polymers²⁸⁻³⁰.

Since then, they have continuously studied interactions between CDs or CD-polymers and polymers modified with linear- or cyclo-alkyl groups³¹⁻³⁶, aromatic groups^{37,38}, and amino acids³⁹. More recently, they have studied light-responsive host-guest systems based on polymers modified with azobenzene as a photoresponsive guest⁴⁰, and have achieved unidirectional inclusion system at the side chain⁴¹, photoresponsive viscosity change⁴² and hydrogel systems⁴³. Later, other groups also began researches on polymers containing CDs and guest groups⁴⁶, supramolecular hydrogels⁴⁷⁻⁴⁹, and light-responsive systems^{50,51}. These researches are summarized in Tables 1-2, 1-3, and 1-4.

Table 1-2. Chemical structures of guest polymers forming host-guest complexes on polymer side chains.

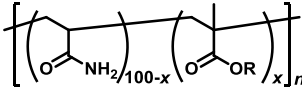
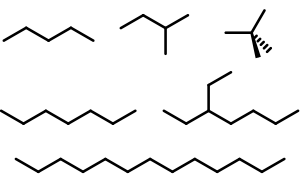
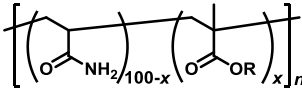
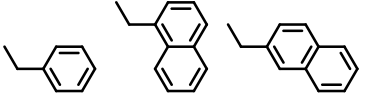
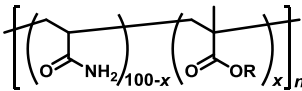
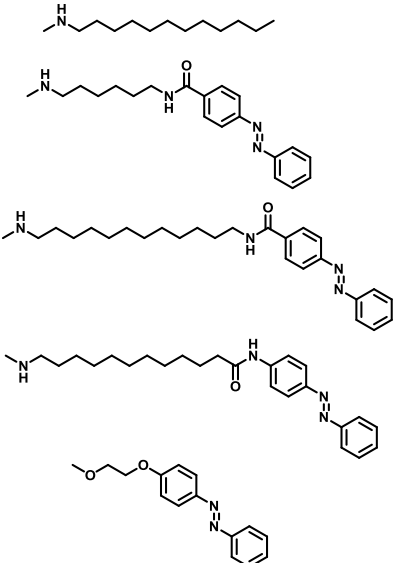
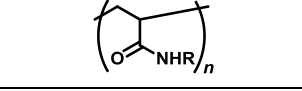
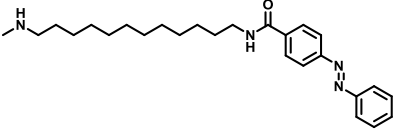
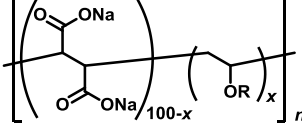
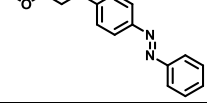
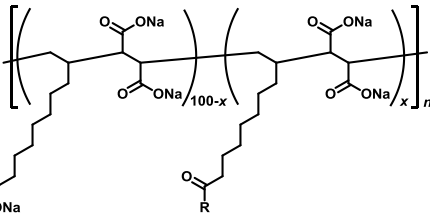
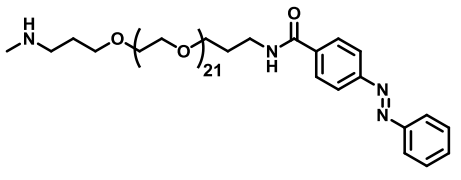
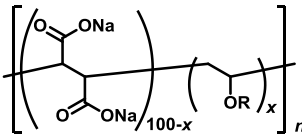
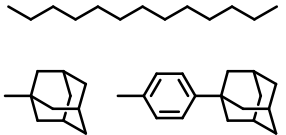
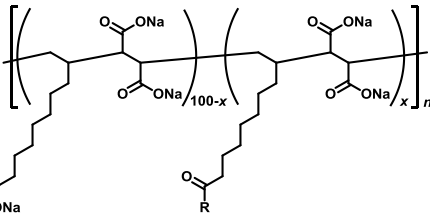
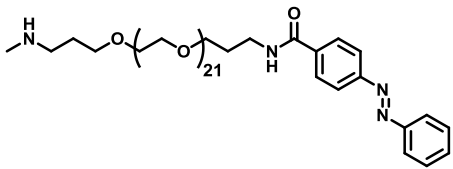
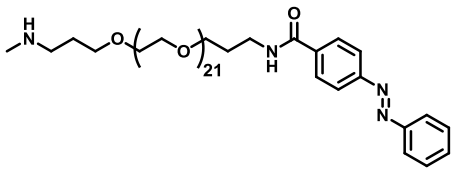
Main-chain structure	Side-chain (R) structure	Author ^{References}
		Harada ³¹
		Harada ^{37,38}
		Harada ^{32,56}
		Harada ⁴¹
		Harada ⁴¹
		Tribet ⁵¹
		Stoddart ⁵⁰
		Harada ³⁹
		Harada ^{33,34}
		Harada ³⁵
		Harada ⁴⁴

Table 1-3. Chemical structures of guest polymers forming supramolecular hydrogels with polymers modified with CDs.

Main-chain structure	Side-chain (R) structure	Author ^{References}
		Harada, Ritter ³⁶
		Ritter ⁴⁶ Lincoln ⁴⁷⁻⁴⁹
		Harada ^{33-35,44}

Table 1-4. Chemical structures of host and guest polymers that demonstrate photoresponsiveness.

CD host polymer	Guest polymer	Author ^{References}
		Harada ⁴⁰
		Harada ⁴²
		Harada ⁴³

1-2-3. Inclusion complex of CDs and ferrocene

Ferrocene (Fc) is an organometallic compound composed of Fe^{2+} and two cyclopentadienyl (Cp) ligands. This sandwich-shaped complex was discovered by T. J. Kealy and P. L. Pauson in 1951⁵². Fc is extremely stable against water, air, and heat, and is known as typical redox-active compound. Both chemical and electrochemical redox stimuli can be used for one electron oxidation of Fc to form ferrocenium cation (Fc^+). In the field of supramolecular chemistry, Fc is known to be a typical guest molecule for cyclodextrins, and forms 2:1/1:1/1:1 inclusion complexes with α -, β -, and γ -CD in aqueous solutions, respectively⁵³⁻⁵⁵. On the other hand, Fc^+ is too hydrophilic to be included into the cavity. Schematic illustrations of supramolecular complexes between CDs and Fc are shown in Figure 1-5 and association constants (K) between them are shown in Table 1-2.

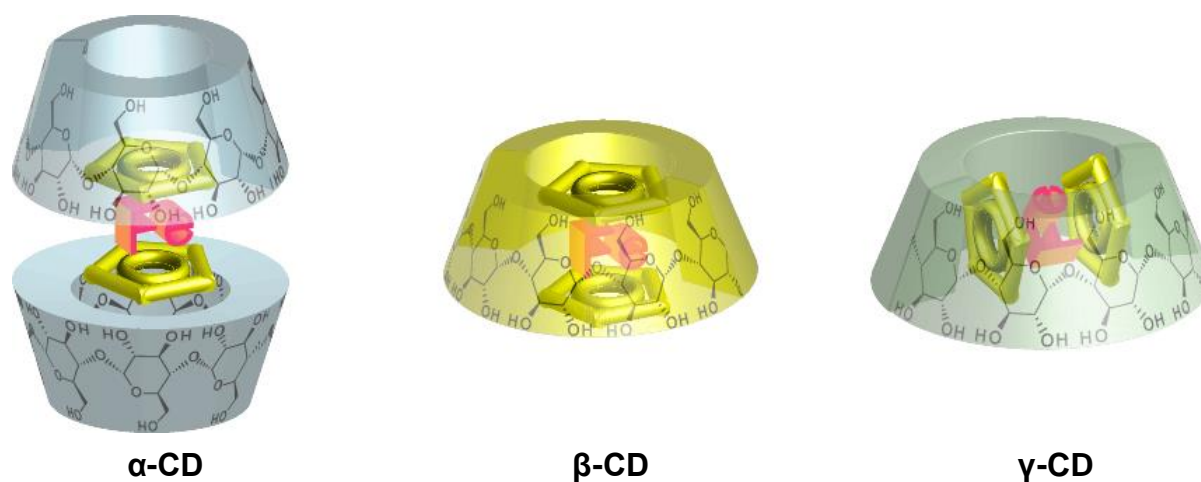


Figure 1-5. Schematic illustration of supramolecular complexes between CDs and Fc^{53} .

Table 1-2. Inclusion stoichiometry and association constants of Fc and CDs.

CD	CD : Fc	K_1 / M^{-1}	K_2 / M^{-1}
α -CD	2 : 1	$(1.39 \pm 0.21) \times 10^2$	$(2.36 \pm 0.06) \times 10^3$
β -CD	1 : 1	$(1.65 \pm 0.04) \times 10^4$	-
γ -CD	1 : 1	$(9.04 \pm 0.11) \times 10^2$	-

1-2-4. Redox-responsive supramolecular hydrogel based on CD and Fc

Recently, Harada *et al.* developed a redox-responsive hydrogel system based on molecular recognition between β -CD and Fc⁵⁶. In this research, a physical hydrogel composed of water-soluble polymers modified with linear alkyl chain was changed into sol upon addition of β -CD. Subsequent addition of Fc derivative as competitive guest for β -CD recovered gel state. Finally, oxidation of Fc resulted in the sol state again due to dissociation of inclusion complex between β -CD and Fc, generating free β -CD molecules again (Figure 1-6).

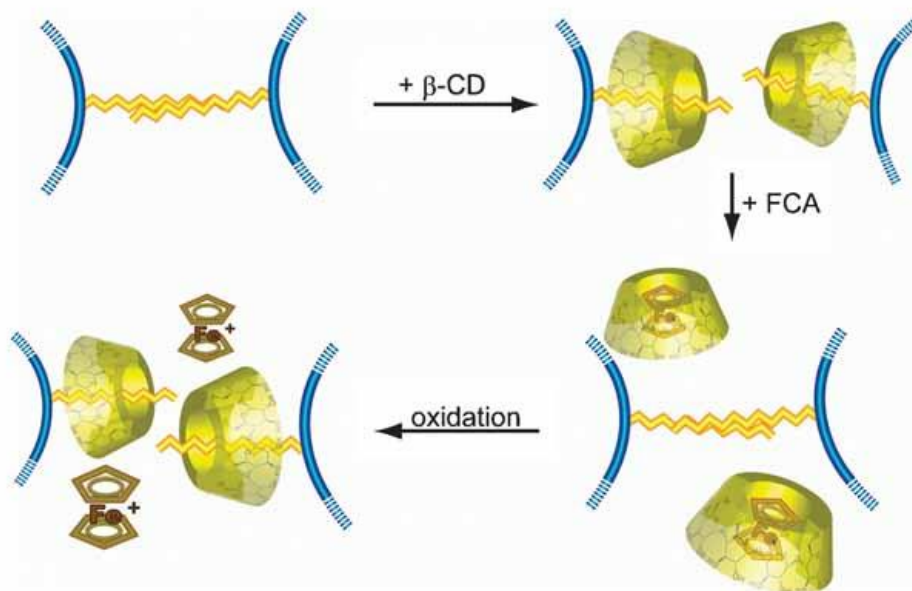
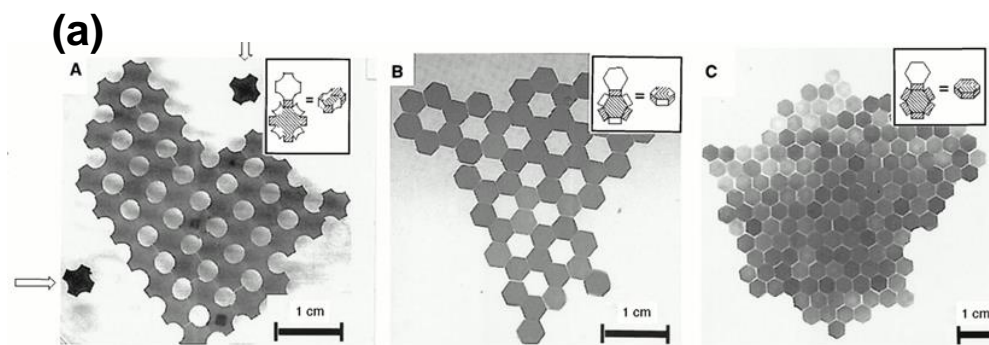


Figure 1-6. Redox-responsive supramolecular hydrogel system reported by Harada *et al*⁵⁶.

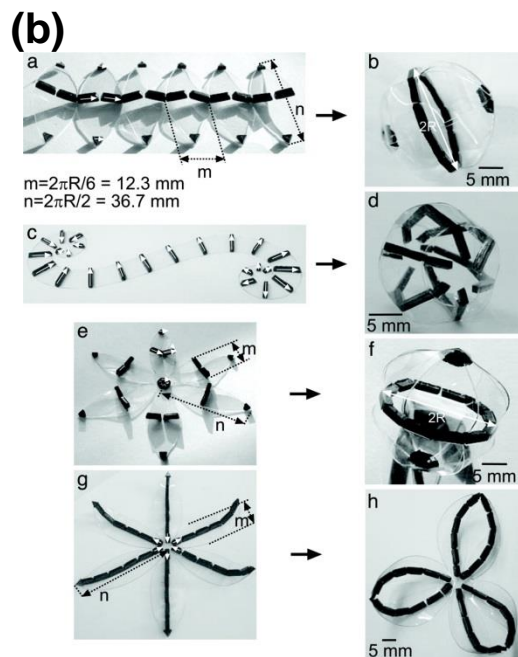
1-3. Macroscopic self-assembly through molecular recognition

At the beginning stage of supramolecular chemistry, main attention had been paid toward construction of discrete molecular assemblies on a molecular scale. Many artificial molecules and their aggregates with suitable sizes, structures and functions have been reported. Recently, it has become a big issue how to construct macroscopic materials with some functions from molecular-scale components. A lot of examples of supramolecular assemblies, polymers, and gels have been developed¹⁴⁻¹⁹. More recently, it becomes a hot topic how to construct more complicated macroscopic structures through suitable interactions from macroscopic components, analogous to biological systems where molecular aggregates such as cells adhere to each other to form more complicated structures such as tissues and organs.

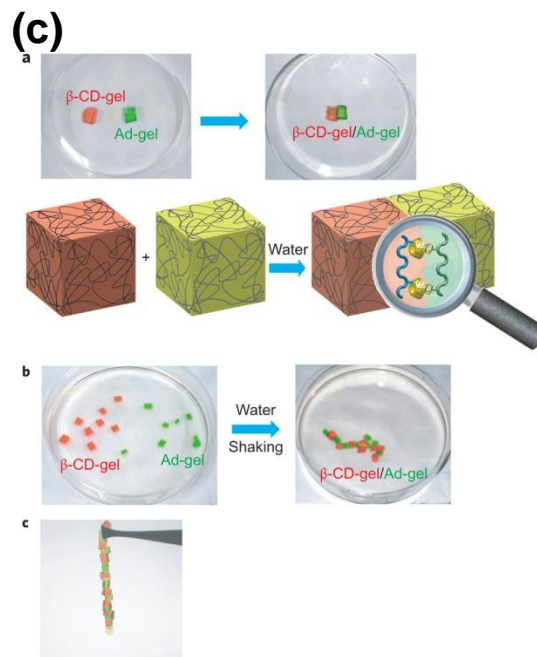
Non-specific interactions such as capillary effect, balance between hydrophile-lipophile, magnetic force, have been used to construct macroscopic assembly composed of macroscopic objects⁵⁷⁻⁶². In 2011, Harada *et al.* reported macroscopic self-assembly through molecular recognition between cyclodextrins and hydrophobic guest molecules⁶³. They used poly(acrylamide) hydrogels modified with functional molecules as macroscopic components to form assemblies. The idea of macroscopic self-assembly through molecular recognition has been one of the hottest topics in current supramolecular chemistry (Figure 1-7).



Whitesides *et al.*



Whitesides *et al.*



Harada *et al.*

Figure 1-7. Examples of macroscopic self-assemblies through non-specific (a,b) and specific (c) interactions.

1-4. Stimuli-responsive materials

In our body, a variety of stimuli-responsive supramolecules work as the driving force for our life activity. One of the typical examples is a sarcomere structure of a skeletal muscle. As illustrated in Figure 1-8, actin filaments and myosin filaments composed of proteins recognize each other in the sarcomere structure, and external stimuli-responsive sliding of the myosin filaments on the actin filaments leads to the expansion and contraction of muscle on a macroscopic scale.

Recently, external stimuli (e.g. molecule, electric field, magnetic field, heat, pH, light, redox, etc.)-responsive materials have attracted much attention by both chemists and materials scientists⁶⁴⁻⁶⁷. Stimuli-responsive materials have big potential for diverse applications such as artificial muscle^{68,69}, drug delivery systems (DDS)^{70,71}, and so on, due to its reversible switching property. These materials are closely linked to polymer science, and many kinds of intelligent polymeric materials that respond to external stimuli have been developed recently.

Here recent examples of external stimuli-responsive materials are categorized into several types based on different kinds of stimuli.

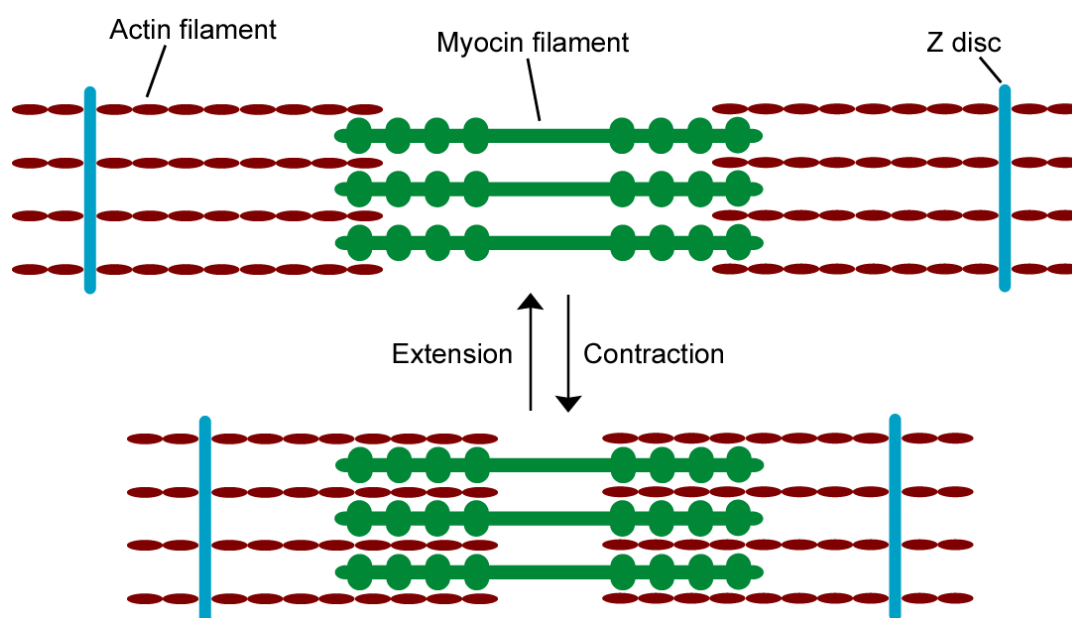


Figure 1-8. Schematic structure of sarcomere structure of skeletal muscle composed of actin filament (brown) and myosin filament (green).

1-4-1. Molecule-responsive systems

Molecules (in other words, chemical stimuli) are common stimuli to drive responsive materials based on selective molecular recognition^{72,73}. A wide range of molecules including solvents, gases, oxidizing/reducing agents (in Chapter 1-3-7), synthetic molecules, and biomolecules can be used as trigger molecules. A common approach toward molecule-responsive systems is to use scaffolds such as polymers modified with receptor molecules for a specific target molecule^{74,75}. One of the most important approaches of such molecule-responsive systems is a biomolecule-responsive system with an eye toward medical applications⁷⁶. Formation of complexes including biomolecules such as lectin-sugar⁷⁷, boronate-sugar⁷⁸⁻⁸⁰, and antibody-antigen⁸¹ has been used so far to construct biomolecule-responsive sensors, actuators, and drug delivery systems.

1-4-2. Electric/magnetic field-responsive systems

Materials which respond to external field, such as electric or magnetic field, have also been developed. External field as a stimulus has a big advantage to be applied or removed instantaneously and remotely with a specific direction. As an electroresponsive materials, not only hard materials such as metals but also ionic and conductive polymers have been used so far^{82,83}. Such electroresponsive materials have big potential applications as artificial muscles and actuators, sensors, and chemical separations⁸⁴⁻⁸⁹.

Magnetic field is also useful stimulus to be remotely applied, as long as the material includes magnetic species. Generally, as magneto-responsive materials, inorganic magnetic particles are non-covalently embedded into or covalently immobilized on polymer networks⁹⁰⁻⁹². Magneto-responsive materials have potential applications for non-invasive medical devices because they don't always need external apparatuses such as electric sources and electrodes to be inserted into the body. For example, hydrogels with magnetic nanoparticles have potentials for active scaffolds for on-demand drug and cell delivery⁹³.

1-4-3. Thermoresponsive systems

Most of chemical processes, regardless of reversible or irreversible, inevitably have dependence on temperature. In the field of materials science, many examples of thermoresponsive materials have been investigated so far. Main attention has been focused on rapid and big change such as phase transition in response to temperature change. For example, poly(*N*-isopropylacrylamide) (pNIPAAm) has lower critical solution temperature (LCST) around body temperature. This polymer has been extensively used as a scaffold in a wide range of biomedical applications such as thermoresponsive drug delivery systems⁹⁴. Other types of phase transitions such as glass transition of polymers have been utilized for shape memory materials^{95,96} which are commonly used in our life.

1-4-4. pH-responsive systems

pH is an important stimulus in aqueous media. Water soluble polymers having acid or base groups on a side chain, for example poly(acrylic acid), poly(4-vinyl pyridine), poly(allylamine) and so on, are frequently used for pH-responsive materials. It is well known that pH of cancer cells is a little acidic than surrounding cells. Using this feature, cancer-targeting drug delivery systems have been investigated^{97,98}. By modifying materials with pH-sensitive moieties, pH-responsive surfaces with variable functions such as redox activity, adhesion, and so on, have been investigated (Figure 1-9a)^{99,100}.

1-4-5. Photoresponsive systems

Light stimulus, from ultraviolet (UV) to infra-red (IR), has a big advantage that it can be irradiated from far away without direct contact, as long as the medium is transparent to it. Polymers containing light-responsive molecules which can undergo reversible or irreversible structural change have been used as light-responsive materials. The most well studied photoresponsive molecule is azobenzene¹⁰¹, which undergoes *cis*-to-*trans* isomerization under the irradiation of UV or visible (Vis) light, respectively. The main application of azobenzene-containing polymers is photoresponsive actuator which convert light energy into mechanical energy (Figure 1-9b)^{102,103}. Stilbene, cinnamate, diarylethenes, fulgide, and spiropyran also undergo structural change by irradiation of light with suitable wavelength, and they have been often used^{104,105}. The response of these photochromic actuators is relatively rapid, but they need apparatus to apply external light source for actuation and have difficulty in use *in vivo* like artificial muscle.

1-4-6. Redox-responsive systems

Oxidation and reduction, or redox reactions are chemical processes which involve transfer of electrons between species. Redox stimulus is advantageous for its rapid responsiveness, and it can be applied both chemically (via oxidizing or reducing agents) and electrochemically (via electrodes). Thiol groups, many organometallic compounds, viologens, tetrathiafulvalene and others are known as typical redox-responsive moieties. The interconversion of thiols (-SH) and disulfides (-S-S-) is one of the important reactions occurring in biological systems. Glutathione (GSH) is a typical reducing agent existing in most cells. The intracellular concentration of GSH is about 10 mM, whereas the extracellular concentration is about 0.002 mM. Thus, cell targeting drug delivery systems which release drug molecules inside cells have been investigated¹⁰⁶.

Organometallic compounds having metal center are also redox-responsive. Yoshida *et al.* utilized copolymer gel modified with ruthenium tris(2,2'-bipyridine) ($\text{Ru}(\text{bpy})_3^{2+}$) complex on a side chain. $\text{Ru}(\text{bpy})_3^{2+}$ complex acts as a catalyst for Belousov–Zhabotinsky (BZ) reaction, which is one of oscillating reactions. The polymer gel, so called self-oscillating gel, can reversibly change its volume in the course of BZ reaction in aqueous medium¹⁰⁷.

As described in chapter 1-2-3, ferrocene (Fc) is an organometallic compound which undergoes reversible one-electron oxidation and reduction by redox stimuli. As an example, polymeric materials containing Fc moieties can respond to redox stimuli to change its volume (Figure 1-9c)¹⁰⁸.

In Chapter 2, Chapter 3, and Chapter 4 of this thesis, main attention is paid to redox-responsive supramolecular materials, and various types of polymer scaffolds are modified with redox-active inclusion complex between cyclodextrin (CD) and Fc.

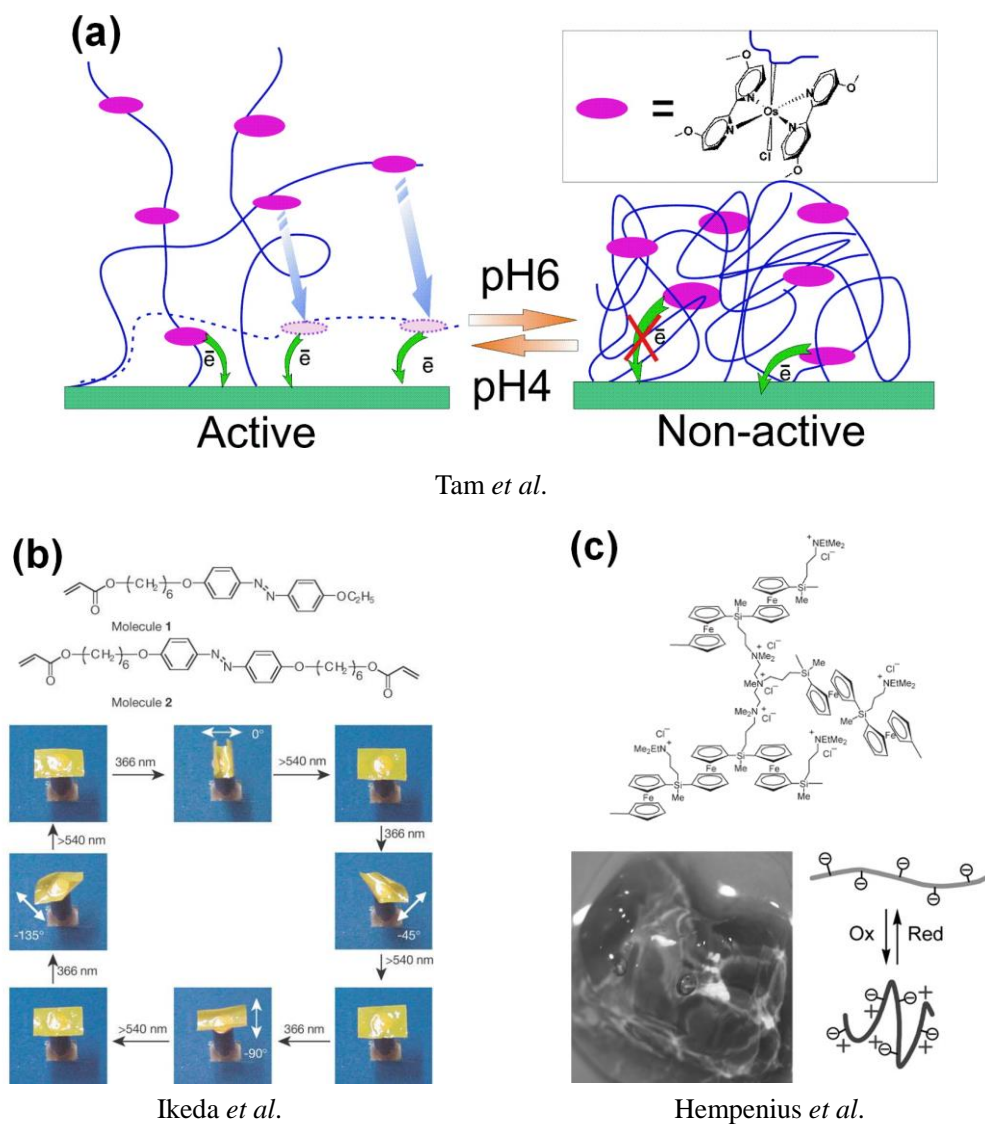
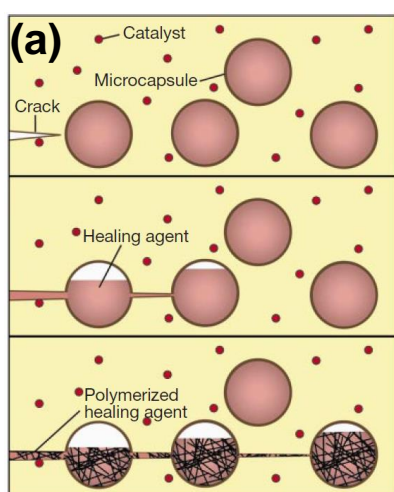


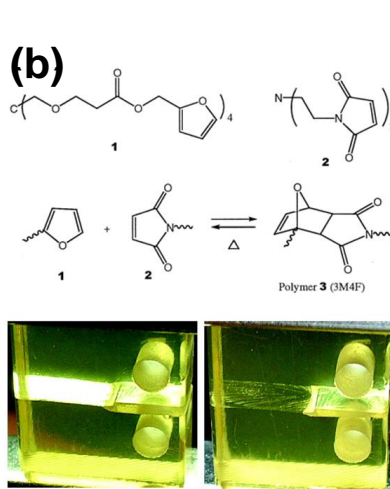
Figure 1-9. Representative examples of stimuli-responsive materials: a pH-responsive electrode (a), a photo-responsive polymer actuator (b), and a redox-responsive hydrogel (c).

1-5. Self-healing materials

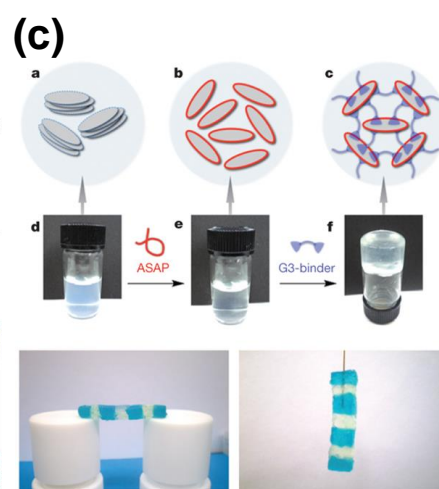
In biological system, injured body tissues automatically heal to their original form. Inspired by these features, many research works have been conducted to achieve self-healing materials using synthetic molecules¹⁰⁹⁻¹¹¹. In the field of materials science, maintenance-free self-healing materials can expand useful lifespan of various commodities. In early times, a polymer network having capsules containing “healing agent” (monomer) was reported as self-healing materials with an ability to heal a crack in it¹¹². In recent years, reversible interactions (hydrogen bonding¹¹³, ionic interaction¹¹⁴, π - π stacking¹¹⁵, metal-ligand interaction¹¹⁶, dynamic covalent bonds¹¹⁷, etc.) have been used to achieve repeatable self-healing materials. Moreover, the latest works are related to “stimuli-responsive” self-healing materials, in which the self-healing property can be controlled by external stimuli (Figure 1-10). Until now, heat¹¹⁸, pH¹¹⁹, and light^{116,120} responsive self-healing materials have been reported, but redox-responsive self-healing materials have yet to be reported so far. In *Chapter 2*, main attention is focused on the redox-responsive self-healing materials formed from host-guest polymers.



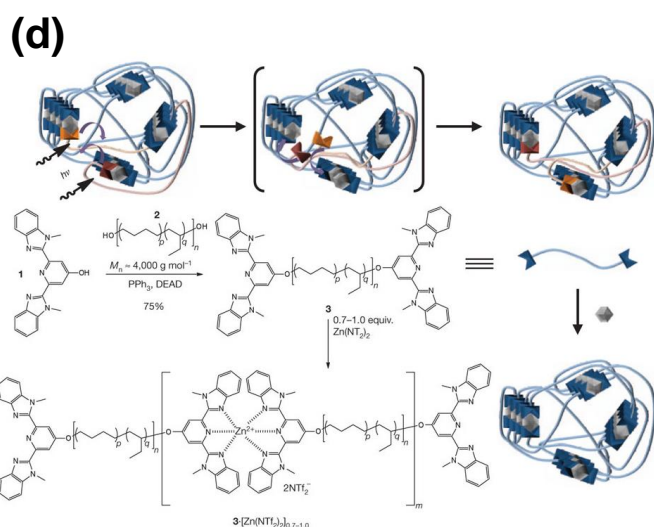
Moore *et al.*



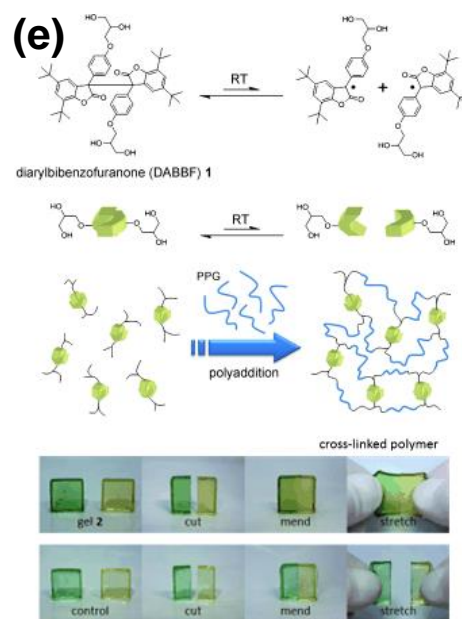
Wudl *et al.*



Aida *et al.*



Rowan *et al.*



Otsuka *et al.*

Figure 1-10. Recent examples of researches about self-healing materials.

1-6. DNA nanomaterials

DNA is one of the most important biomolecules which can produce, storage, and transfer genetic codes to the subsequent generation¹²¹⁻¹²⁶. A single-strand DNA is composed of deoxyribose modified with nucleobases (adenine (A), thymine (T), guanine (G), and cytosine (C)) linked with phosphodiester bonds. DNA forms double helix structure with complementary DNA as discovered by Watson and Crick. Combination of complementary hydrogen bonding and π - π stacking plays a crucial role in forming superstructures with extremely high fidelity, which enables transcription of a vast amount of genetic information with almost no mismatch. DNAs have been a main research target in the field of not only molecular biology but also supramolecular chemistry. In recent years, many researchers have been utilized DNAs as useful platforms to construct nanostructures in a molecular scale (Figure 1-11) such as DNA origami¹²⁷⁻¹²⁹, 3-D nanostructures¹³⁰⁻¹³³, metal arrays¹³⁴, and stimuli-responsive DNA¹³⁵.

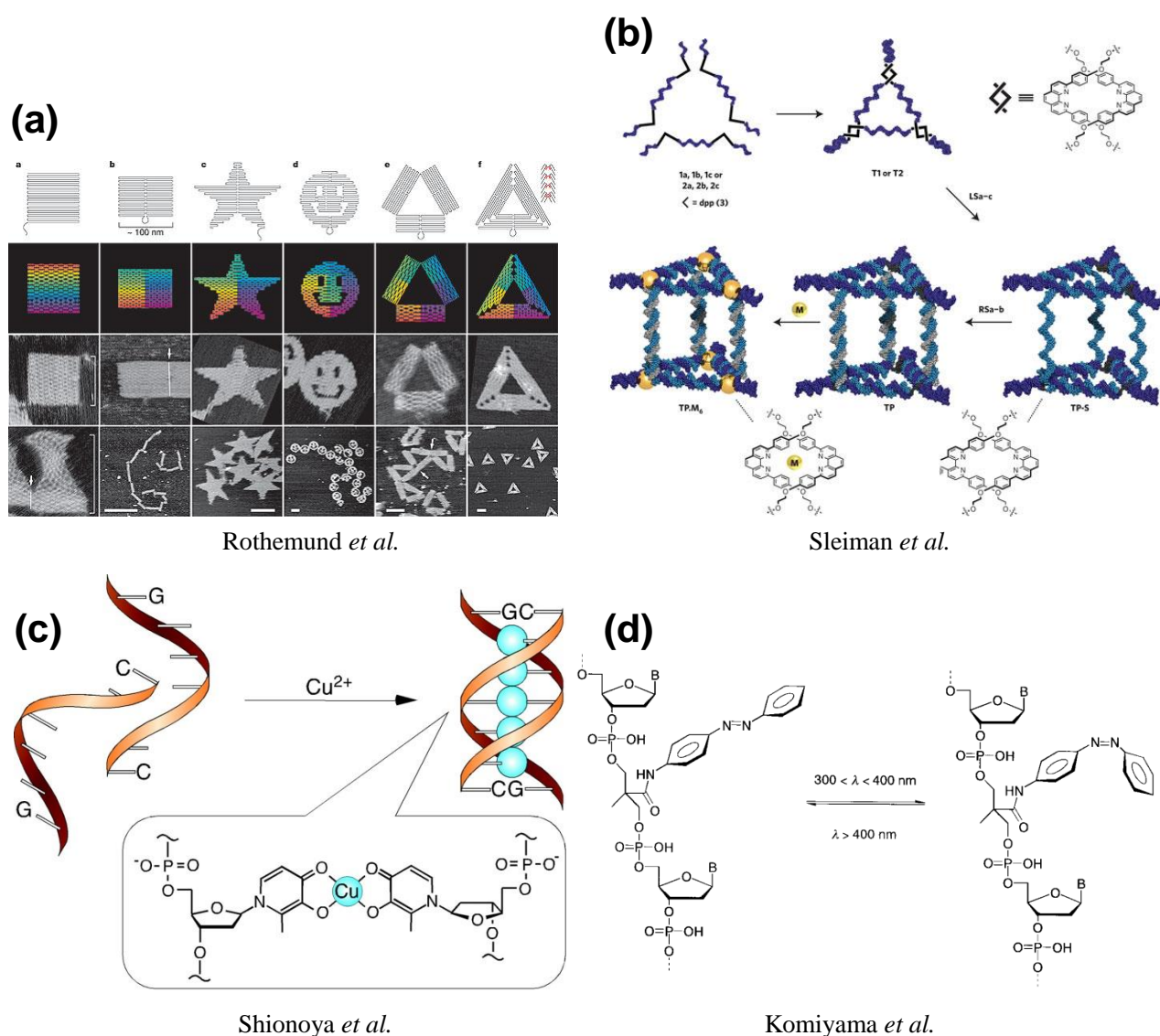
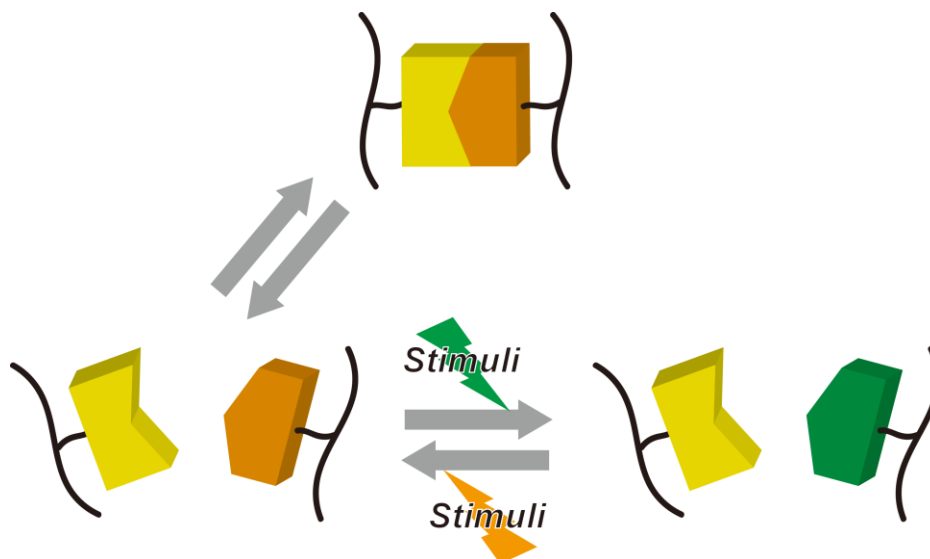


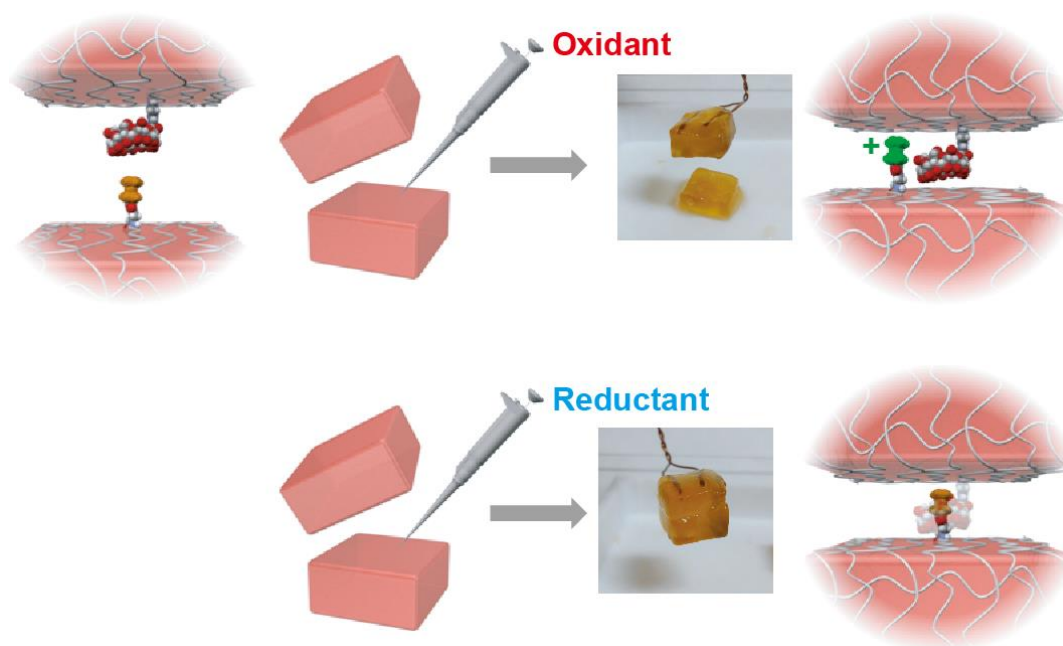
Figure 1-11. Recent examples of DNA-based nanostructures.

1-7. Scope and outline of this thesis

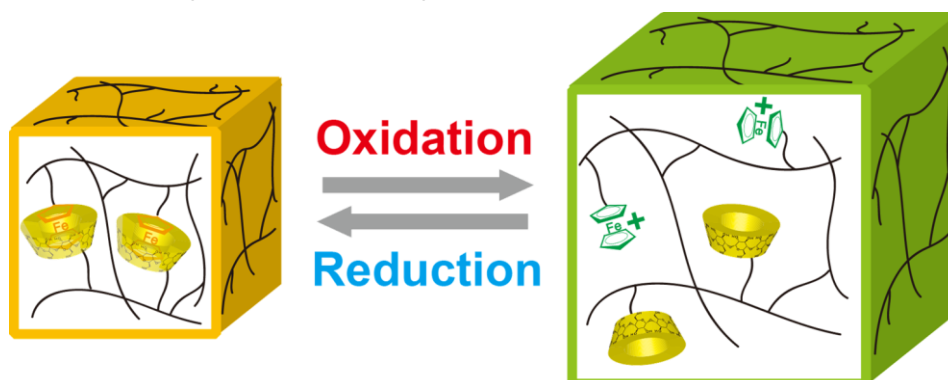
The key concept of this thesis is external stimuli-responsive molecular recognition at a side chain of polymer. Inclusion complex of CD-Fc, double strand DNA, and nucleobase pairs are selected as recognition moieties. Association and dissociation of these recognition moieties are reversible, and can be controlled by external stimuli such as chemical stimuli, especially redox stimuli. These recognition moieties are introduced into side chain of synthetic polymers to create various functional supramolecular materials depending on its material design.



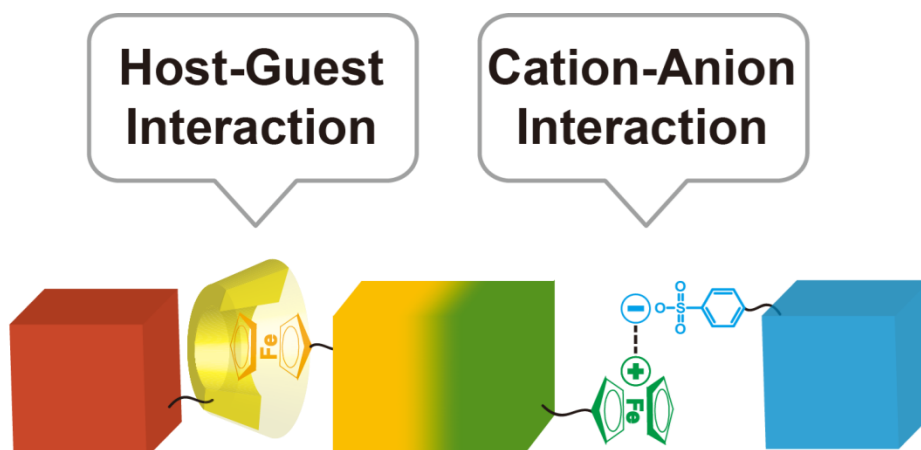
In *Chapter 2*, the formation of supramolecular hydrogels and their redox-responsive self-healing properties due to redox-responsive host-guest interactions is described. CD is employed as a host molecule because of its environmental friendliness and diverse applications. A transparent supramolecular hydrogel quickly forms upon mixing poly(acrylic acid) possessing β -CD as a host polymer with poly(acrylic acid) possessing Fc as a guest polymer. Redox stimuli control a sol-gel transition of the supramolecular hydrogel and self-healing properties between cut surfaces of the gel.



In *Chapter 3*, a redox-responsive expansion and contraction system using host-guest interactions is described. Supramolecular crosslinking points based on host-guest inclusion complexes between CD and Fc are introduced into chemically cross-linked hydrogel. By regulating the formation and dissociation of reversible supramolecular crosslinks using redox stimuli, this gel can be swollen and shrunk like our muscle.



In *Chapter 4*, a redox-responsive gel assembly system using both host-guest interactions and ionic interactions between the surfaces of macroscopic materials is described. A macroscopic self-assembly between polymeric hydrogels modified with β -CD, Fc, and styrenesulfonic acid sodium salt (SSNa) is investigated. Redox stimuli can change the oxidation state of Fc on the surface of the gel and control the assembly formation. Two discrete non-covalent interactions enable to form an ABC-type macroscopic assembly using three types of gels together.



In *Chapter 5*, a macroscopic gel assembly system using hydrogen bonds between oligonucleotides or nucleobases is described. Adhesion between hydrogels modified with complementary oligonucleotides in aqueous media, and organogels modified with complementary nucleobases are investigated. Adhesion between macroscopic objects through complementary hydrogen bonds in wide range of media from aqueous to organic is achieved.



References

1. Pedersen, C. J., *J. Am. Chem. Soc.* **1967**, 89 (26), 7017-7036.
2. Pedersen, C. J., *Angew. Chem. Int. Ed. Engl.* **1988**, 27 (8), 1021-1027.
3. Lehn, J.-M., *Science* **1985**, 227 (4689), 849-856.
4. Lehn, J.-M., *Angew. Chem. Int. Ed. Engl.* **1988**, 27 (1), 89-112.
5. Lehn, J.-M., *Angew. Chem. Int. Ed. Engl.* **1990**, 29 (11), 1304-1319.
6. Cram, D. J.; Cram, J. M., *Science* **1974**, 183 (4127), 803-809.
7. Cram, D. J., *Angew. Chem. Int. Ed. Engl.* **1988**, 27 (8), 1009-1020.
8. issue", C. s., *Chem. Rev.* **1998**, 98 (5), 1742-2076.
9. Bender, M. L.; Komiyama, M., *Cyclodextrin chemistry*. Springer-Verlag: Berlin ; New York, 1978.
10. Szejtli, J. z., *Cyclodextrins and their inclusion complexes*. Akadémiai Kiadó: Budapest, 1982.
11. Semlyen, J. A., *Large ring molecules*. Wiley: Chichester ; New York, 1996.
12. Dodziuk, H., *Cyclodextrins and Their Complexes*. Wiley-VCH: Weinheim, 2006.
13. Easton, C. J.; Lincoln, S. F., *Modified cyclodextrins : scaffolds and templates for supramolecular chemistry*. Imperial College Press ; Distributed by World Scientific Pub. Co.: London River Edge, NJ, 1999.
14. Amabilino, D. B.; Stoddart, J. F., *Chem. Rev.* **1995**, 95 (8), 2725-2828.
15. De Greef, T. F. A.; Smulders, M. M. J.; Wolfs, M.; Schenning, A. P. H. J.; Sijbesma, R. P.; Meijer, E. W., *Chem. Rev.* **2009**, 109 (11), 5687-5754.
16. Aida, T.; Meijer, E. W.; Stupp, S. I., *Science* **2012**, 335 (6070), 813-817.
17. Atwood, J. L.; Lehn, J. M., *Comprehensive supramolecular chemistry*. 1st ed.; Pergamon: New York, 1996.
18. Harada, A., *Supramolecular polymer chemistry*. Wiley-VCH: Weinheim, Germany, 2012;.
19. Harada, A.; Hashidzume, A.; Yamaguchi, H.; Takashima, Y., *Chem. Rev.* **2009**, 109 (11), 5974-6023.
20. Harada, A.; Kamachi, M., *Macromolecules* **1990**, 23 (10), 2821-2823.
21. Harada, A.; Li, J.; Kamachi, M., *Nature* **1992**, 356 (6367), 325-327.
22. Harada, A.; Li, J.; Kamachi, M., *Nature* **1993**, 364 (6437), 516-518.
23. Harada, A.; Li, J.; Kamachi, M., *Nature* **1994**, 370 (6485), 126-128.
24. Raymo, F. M.; Stoddart, J. F., *Chem. Rev.* **1999**, 99 (7), 1643-1664.
25. Wenz, G.; Han, B.-H.; Müller, A., *Chem. Rev.* **2006**, 106 (3), 782-817.
26. Okumura, Y.; Ito, K., *Adv. Mater.* **2001**, 13 (7), 485-487.
27. Hashidzume, A.; Tomatsu, I.; Harada, A., *Polymer* **2006**, 47 (17), 6011-6027.
28. Harada, A.; Furue, M.; Nozakura, S.-i., *Macromolecules* **1976**, 9 (5), 701-704.
29. Harada, A.; Furue, M.; Nozakura, S.-i., *Macromolecules* **1976**, 9 (5), 705-710.
30. Harada, A.; Furue, M.; Nozakura, S.-i., *Macromolecules* **1977**, 10 (3), 676-681.
31. Harada, A.; Adachi, H.; Kawaguchi, Y.; Kamachi, M., *Macromolecules* **1997**, 30 (17), 5181-5182.
32. Tomatsu, I.; Hashidzume, A.; Harada, A., *Macromol. Rapid Commun.* **2005**, 26 (10), 825-829.
33. Taura, D.; Hashidzume, A.; Okumura, Y.; Harada, A., *Macromolecules* **2008**, 41 (10), 3640-3645.
34. Taura, D.; Hashidzume, A.; Harada, A., *Macromol. Rapid Commun.* **2007**, 28 (24), 2306-2310.
35. Taura, D.; Taniguchi, Y.; Hashidzume, A.; Harada, A., *Macromol. Rapid Commun.* **2009**, 30 (20), 1741-1744.

36. Kretschmann, O.; Choi, S. W.; Miyauchi, M.; Tomatsu, I.; Harada, A.; Ritter, H., *Angew. Chem. Int. Ed.* **2006**, *45* (26), 4361-4365.
37. Hashidzume, A.; Ito, F.; Tomatsu, I.; Harada, A., *Macromol. Rapid Commun.* **2005**, *26* (14), 1151-1154.
38. Harada, A.; Ito, F.; Tomatsu, I.; Shimoda, K.; Hashidzume, A.; Takashima, Y.; Yamaguchi, H.; Kamitori, S., *J. Photochem. Photobiol. A: Chem.* **2006**, *179* (1-2), 13-19.
39. Hashidzume, A.; Harada, A., *Polymer* **2006**, *47* (10), 3448-3454.
40. Takashima, Y.; Nakayama, T.; Miyauchi, M.; Kawaguchi, Y.; Yamaguchi, H.; Harada, A., *Chem. Lett.* **2004**, *33* (7), 890-891.
41. Tomatsu, I.; Hashidzume, A.; Harada, A., *Angew. Chem. Int. Ed.* **2006**, *45* (28), 4605-4608.
42. Tomatsu, I.; Hashidzume, A.; Harada, A., *J. Am. Chem. Soc.* **2006**, *128* (7), 2226-2227.
43. Tamesue, S.; Takashima, Y.; Yamaguchi, H.; Shinkai, S.; Harada, A., *Angew. Chem. Int. Ed.* **2010**, *49* (41), 7461-7464.
44. Taura, D.; Li, S.; Hashidzume, A.; Harada, A., *Macromolecules* **2010**, *43* (4), 1706-1713.
45. Sarvothaman, M. K.; Ritter, H., *Macromol. Rapid Commun.* **2004**, *25* (23), 1948-1952.
46. Koopmans, C.; Ritter, H., *Macromolecules* **2008**, *41* (20), 7418-7422.
47. Li, L.; Guo, X.; Wang, J.; Liu, P.; Prud'homme, R. K.; May, B. L.; Lincoln, S. F., *Macromolecules* **2008**, *41* (22), 8677-8681.
48. Guo, X.; Wang, J.; Li, L.; Pham, D.-T.; Clements, P.; Lincoln, S. F.; May, B. L.; Chen, Q.; Zheng, L.; Prud'homme, R. K., *Macromol. Rapid Commun.* **2010**, *31* (3), 300-304.
49. Wang, J.; Pham, D.-T.; Guo, X.; Li, L.; Lincoln, S. F.; Luo, Z.; Ke, H.; Zheng, L.; Prud'homme, R. K., *Industrial & Engineering Chemistry Research* **2009**, *49* (2), 609-612.
50. Zhao, Y.-L.; Stoddart, J. F., *Langmuir* **2009**, *25* (15), 8442-8446.
51. Pouliquen, G.; Amiel, C.; Tribet, C., *J. Phys. Chem. B* **2007**, *111* (20), 5587-5595.
52. Kealy, T. J.; Pauson, P. L., *Nature* **1951**, *168* (4285), 1039-1040.
53. Harada, A.; Takahashi, S., *J. Chem. Soc., Chem. Commun.* **1984**, (10), 645-646.
54. Harada, A.; Takahashi, S., *J. Incl. Phenom.* **1984**, *2* (3-4), 791-798.
55. Wu, J.-S.; Toda, K.; Tanaka, A.; Sanemasa, I., *Bull. Chem. Soc. Jpn.* **1998**, *71* (7), 1615-1618.
56. Tomatsu, I.; Hashidzume, A.; Harada, A., *Macromol. Rapid Commun.* **2006**, *27* (4), 238-241.
57. Whitesides, G. M.; Grzybowski, B., *Science* **2002**, *295* (5564), 2418-2421.
58. Breen, T. L.; Tien, J.; J., S. R.; Oliver; Hadzic, T.; Whitesides, G. M., *Science* **1999**, *284* (5416), 948-951.
59. Boncheva, M.; Andreev, S. A.; Mahadevan, L.; Winkleman, A.; Reichman, D. R.; Prentiss, M. G.; Whitesides, S.; Whitesides, G. M., *Proc. Natl. Acad. Sci. U.S.A.* **2005**, *102* (11), 3924-3929.
60. Clark, T. D.; Ferrigno, R.; Tien, J.; Paul, K. E.; Whitesides, G. M., *J. Am. Chem. Soc.* **2002**, *124* (19), 5419-5426.
61. Du, Y.; Lo, E.; Ali, S.; Khademhosseini, A., *Proc. Natl. Acad. Sci. U.S.A.* **2008**, *105* (28), 9522-9527.
62. Bowden, N.; Terfort, A.; Carbeck, J.; Whitesides, G. M., *Science* **1997**, *276* (5310), 233-235.
63. Harada, A.; Kobayashi, R.; Takashima, Y.; Hashidzume, A.; Yamaguchi, H., *Nat. Chem.* **2011**, *3* (1), 34-37.
64. Gandhi, M. V.; Thompson, B. S., *Smart Materials and Structures*. Chapman & Hall: London, 1992.
65. Feringa, B. L.; Browne, W. R., *Molecular switches*. 2nd, completely rev. and enl. ed.; Wiley-VCH:

Weinheim, Germany, 2011.

66. Urban, M. W., *Handbook of stimuli-responsive materials*. Wiley-VCH: Weinheim, Germany, 2011.
67. Minko, S., *Responsive polymer materials : design and applications*. 1st ed.; Blackwell Pub.: Ames, Iowa, 2006.
68. Osada, Y.; De Rossi, D. E., *Polymer sensors and actuators*. Springer: Berlin ; New York, 2000.
69. Mirfakhrai, T.; Madden, J. D. W.; Baughman, R. H., *Mater. Today* **2007**, *10* (4), 30-38.
70. Jeong, B.; Gutowska, A., *Trends Biotechnol.* **2002**, *20* (7), 305-311.
71. Bajpai, A.; Shukla, S.; Saini, R.; Tiwari, A., *Stimuli Responsive Drug Delivery Systems: From Introduction to Application*. Smithers Rapra Technology: Billingham, 2010.
72. Osada, Y.; Gong, J.-P., *Adv. Mater.* **1998**, *10* (11), 827-837.
73. Schneider, H.-J.; Kato, K.; Strongin, R., *Sensors* **2007**, *7* (8), 1578-1611.
74. Schneider, H.-J.; Strongin, R. M., *Acc. Chem. Res.* **2009**, *42* (10), 1489-1500.
75. Schneider, H.-J.; Kato, K., *J. Mater. Chem.* **2009**, *19* (5), 569-573.
76. Miyata, T.; Uragami, T.; Nakamae, K., *Adv. Drug Del. Rev.* **2002**, *54* (1), 79-98.
77. Brownlee, M.; Cerami, A., *Science* **1979**, *206* (4423), 1190-1191.
78. Aoki, T.; Nagao, Y.; Sanui, K.; Ogata, N.; Kikuchi, A.; Sakurai, Y.; Kataoka, K.; Okano, T., *Polym. J.* **1996**, *28* (4), 371-374.
79. Kataoka, K.; Miyazaki, H.; Bunya, M.; Okano, T.; Sakurai, Y., *J. Am. Chem. Soc.* **1998**, *120* (48), 12694-12695.
80. Matsumoto, A.; Ikeda, S.; Harada, A.; Kataoka, K., *Biomacromolecules* **2003**, *4* (5), 1410-1416.
81. Miyata, T.; Asami, N.; Uragami, T., *Nature* **1999**, *399* (6738), 766-769.
82. Osada, Y.; Okuzaki, H.; Hori, H., *Nature* **1992**, *355* (6357), 242-244.
83. Osada, Y.; Gong, J. P.; Sawahata, K., *J. Macromol. Sci., Chem.* **1991**, *28* (11-12), 1189-1205.
84. Bar-Cohen, Y., *Electroactive polymer (EAP) actuators as artificial muscles : reality, potential, and challenges*. 2nd ed.; SPIE Press: Bellingham, Wash., 2004.
85. Wallace, G. G.; Teasdale, P. R.; Spinks, G. M.; Kane-Maguire, L. A. P., *Conductive Electroactive Polymers: Intelligent Materials Systems, 2nd ed.*. CRC: Boca Raton, 2002.
86. Mohsen, S.; Kwang, J. K., *Smart Mater. Struct.* **2005**, *14* (1), 197.
87. Kaneto, K.; Kaneko, M., *Appl. Biochem. Biotechnol.* **2001**, *96* (1-3), 13-23.
88. Qibing, P.; Marcus, R.; Scott, S.; Harsha, P.; Ron, P., *Smart Mater. Struct.* **2004**, *13* (5), N86.
89. Otero, T. F.; Cortés, M. T., *Adv. Mater.* **2003**, *15* (4), 279-282.
90. Szabó, D.; Szeghy, G.; Zrínyi, M., *Macromolecules* **1998**, *31* (19), 6541-6548.
91. Xulu, P. M.; Filipcsei, G.; Zrínyi, M., *Macromolecules* **2000**, *33* (5), 1716-1719.
92. Filipcsei, G.; Csetneki, I.; Szilágyi, A.; Zrínyi, M., Magnetic Field-Responsive Smart Polymer Composites. In *Oligomers - Polymer Composites - Molecular Imprinting*, Springer Berlin Heidelberg: 2007; Vol. 206, pp 137-189.
93. Zhao, X.; Kim, J.; Cezar, C. A.; Huebsch, N.; Lee, K.; Bouhadir, K.; Mooney, D. J., *Proc. Natl. Acad. Sci. U.S.A.* **2011**, *108* (1), 67-72.
94. Chung, J. E.; Yokoyama, M.; Yamato, M.; Aoyagi, T.; Sakurai, Y.; Okano, T., *J. Controlled Release* **1999**, *62* (1-2), 115-127.

95. Osada, Y.; Matsuda, A., *Nature* **1995**, 376 (6537), 219-219.
96. Lendlein, A.; Kelch, S., *Angew. Chem. Int. Ed.* **2002**, 41 (12), 2034-2057.
97. Schmaljohann, D., *Adv. Drug Del. Rev.* **2006**, 58 (15), 1655-1670.
98. Murthy, N.; Campbell, J.; Fausto, N.; Hoffman, A. S.; Stayton, P. S., *Bioconjugate Chem.* **2003**, 14 (2), 412-419.
99. Tam, T. K.; Ornatska, M.; Pita, M.; Minko, S.; Katz, E., *J. Phys. Chem. C* **2008**, 112 (22), 8438-8445.
100. Dejeu, J.; Gauthier, M.; Rougeot, P.; Boireau, W., *ACS Applied Materials & Interfaces* **2009**, 1 (9), 1966-1973.
101. Kumar, G. S.; Neckers, D. C., *Chem. Rev.* **1989**, 89 (8), 1915-1925.
102. Yu, Y.; Nakano, M.; Ikeda, T., *Nature* **2003**, 425 (6954), 145-145.
103. Hosono, N.; Kajitani, T.; Fukushima, T.; Ito, K.; Sasaki, S.; Takata, M.; Aida, T., *Science* **2010**, 330 (6005), 808-811.
104. Irie, M., Photoresponsive polymers. In *New Polymer Materials*, Springer Berlin Heidelberg: 1990; Vol. 94, pp 27-67.
105. Terao, F.; Morimoto, M.; Irie, M., *Angew. Chem. Int. Ed.* **2012**, 51 (4), 901-904.
106. Oh, J. K.; Siegwart, D. J.; Lee, H.-i.; Sherwood, G.; Peteanu, L.; Hollinger, J. O.; Kataoka, K.; Matyjaszewski, K., *J. Am. Chem. Soc.* **2007**, 129 (18), 5939-5945.
107. Yoshida, R., *Adv. Mater.* **2010**, 22 (31), 3463-3483.
108. Hempenius, M. A.; Cirmi, C.; Savio, F. L.; Song, J.; Vancso, G. J., *Macromol. Rapid Commun.* **2010**, 31 (9-10), 772-783.
109. Binder, W. H., *Self-Healing Polymers: From Principles to Applications*. Wiley-VCH: Weinheim, 2013.
110. Burattini, S.; Greenland, B. W.; Chappell, D.; Colquhoun, H. M.; Hayes, W., *Chem. Soc. Rev.* **2010**, 39 (6), 1973-1985.
111. Yang, Y.; Urban, M. W., *Chem. Soc. Rev.* **2013**, 42 (17), 7446-7467.
112. White, S. R.; Sottos, N. R.; Geubelle, P. H.; Moore, J. S.; Kessler, M. R.; Sriram, S. R.; Brown, E. N.; Viswanathan, S., *Nature* **2001**, 409 (6822), 794-797.
113. Cordier, P.; Tournilhac, F.; Soulie-Ziakovic, C.; Leibler, L., *Nature* **2008**, 451 (7181), 977-980.
114. Wang, Q.; Mynar, J. L.; Yoshida, M.; Lee, E.; Lee, M.; Okuro, K.; Kinbara, K.; Aida, T., *Nature* **2010**, 463 (7279), 339-343.
115. Burattini, S.; Greenland, B. W.; Merino, D. H.; Weng, W.; Seppala, J.; Colquhoun, H. M.; Hayes, W.; Mackay, M. E.; Hamley, I. W.; Rowan, S. J., *J. Am. Chem. Soc.* **2010**, 132 (34), 12051-12058.
116. Burnworth, M.; Tang, L.; Kumpfer, J. R.; Duncan, A. J.; Beyer, F. L.; Fiore, G. L.; Rowan, S. J.; Weder, C., *Nature* **2011**, 472 (7343), 334-337.
117. Imato, K.; Nishihara, M.; Kanehara, T.; Amamoto, Y.; Takahara, A.; Otsuka, H., *Angew. Chem. Int. Ed.* **2012**, 51 (5), 1138-1142.
118. Chen, X.; Dam, M. A.; Ono, K.; Mal, A.; Shen, H.; Nutt, S. R.; Sheran, K.; Wudl, F., *Science* **2002**, 295 (5560), 1698-1702.
119. He, L.; Fullenkamp, D. E.; Rivera, J. G.; Messersmith, P. B., *Chem. Commun.* **2011**, 47 (26), 7497-7499.
120. Ghosh, B.; Urban, M. W., *Science* **2009**, 323 (5920), 1458-1460.

121. Bloomfield, V. A.; Crothers, D. M.; Tinoco, I., *Nucleic acids : structures, properties, and functions*. University Science Books: Sausalito, Calif., 2000.
122. Budisa, N., *Engineering the genetic code : expanding the amino acid repertoire for the design of novel proteins*. Wiley-VCH: Weinheim, 2006.
123. Blackburn, G. M., *Nucleic acids in chemistry and biology*. 3rd ed.; RSC Pub.: Cambridge, UK, 2006.
124. Herdewijn, P., *Modified nucleosides : in biochemistry, biotechnology, and medicine*. Wiley-VCH: Weinheim, 2008.
125. Mayer, G. n., *The chemical biology of nucleic acids*. Wiley: Chichester, UK, 2010.
126. Egli, M.; Herdewijn, P.; Matsuda, A.; Sanghvi, Y. S., *Current Protocols in Nucleic Acid Chemistry*. John Wiley & Sons, Inc.: 2001.
127. Rothmund, P. W. K., *Nature* **2006**, *440* (7082), 297-302.
128. Lund, K.; Manzo, A. J.; Dabby, N.; Michelotti, N.; Johnson-Buck, A.; Nangreave, J.; Taylor, S.; Pei, R.; Stojanovic, M. N.; Walter, N. G.; Winfree, E.; Yan, H., *Nature* **2010**, *465* (7295), 206-210.
129. Pal, S.; Deng, Z.; Ding, B.; Yan, H.; Liu, Y., *Angew. Chem. Int. Ed.* **2010**, *49* (15), 2700-2704.
130. Aldaye, F. A.; Palmer, A. L.; Sleiman, H. F., *Science* **2008**, *321* (5897), 1795-1799.
131. Lo, P. K.; Mettera, K. L.; Sleiman, H. F., *Curr. Opin. Chem. Biol.* **2010**, *14* (5), 597-607.
132. Lo, P. K.; Karam, P.; Aldaye, F. A.; McLaughlin, C. K.; Hamblin, G. D.; Cosa, G.; Sleiman, H. F., *Nat. Chem.* **2010**, *2* (4), 319-328.
133. Yang, H.; McLaughlin, C. K.; Aldaye, F. A.; Hamblin, G. D.; Rys, A. Z.; Rouiller, I.; Sleiman, H. F., *Nat. Chem.* **2009**, *1* (5), 390-396.
134. Tanaka, K.; Tengeiji, A.; Kato, T.; Toyama, N.; Shionoya, M., *Science* **2003**, *299* (5610), 1212-1213.
135. Asanuma, H.; Ito, T.; Yoshida, T.; Liang, X.; Komiyama, M., *Angew. Chem. Int. Ed.* **1999**, *38* (16), 2393-2395.

Chapter 2

Redox-Responsive Self-Healing Materials Formed from Host and Guest Polymers

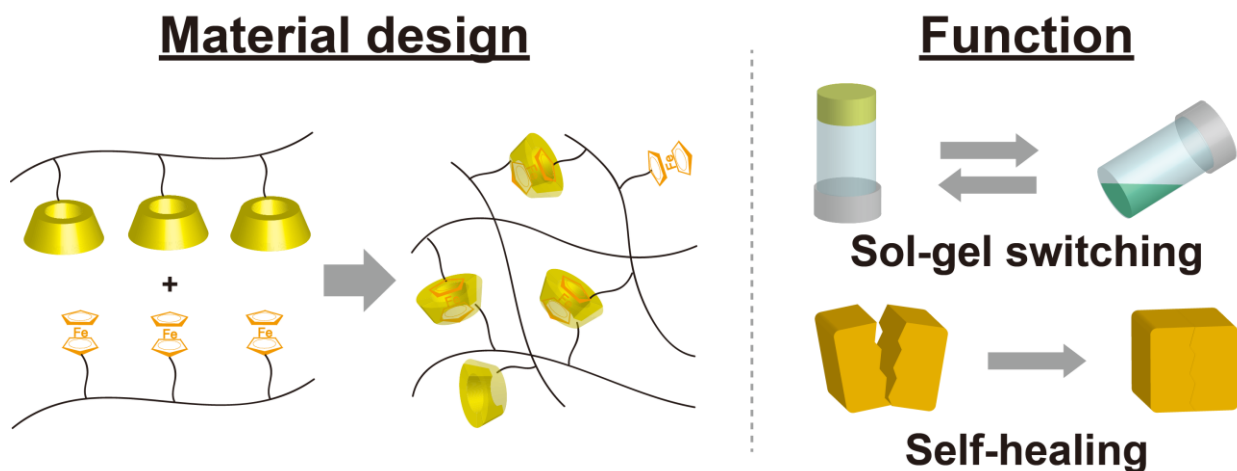


Figure 2-0. Conceptual illustration of chapter 2.

2-1. Introduction

High-performance materials such as stimulus-responsive and maintenance-free self-healing materials¹⁻⁹ have attracted much attention due to modern environmental and energy concerns. Recently developed functional soft materials possessing switching, self-healing, and self-repairing features are expected to have diverse applications (e.g., in architectural materials and external coatings). Some research groups have attempted to create switching soft materials such as remotely-actuated nanomaterials,¹⁰⁻¹⁴ artificial molecular muscles,^{15,16} drug delivery systems,^{17,18} biosensors, and shape memory materials. Although there are previous examples of supramolecular hydrogels¹⁹ where a sol–gel phase transition occurs using heat,²⁰ pH,²¹ light,²²⁻²⁵ or redox²⁶⁻³² as a stimulus, it is difficult to create multi-functional soft materials due to complicated designs and syntheses. Especially, redox stimulus-responsive self-healing materials have yet to be described.

Harada *et al.* previously reported stimulus-responsive supramolecular materials possessing host and guest polymers.³³⁻³⁵ Supramolecular materials consisting of host and guest polymers have unique features due to selective complementary interactions. Host–guest interactions are versatile, and can be used to prepare supramolecular materials, which have easily tuned switching efficiencies and functions. Self-healing and self-repairing properties may be achieved using supramolecular materials that consist of host and guest polymers. The duality of supramolecular materials, which possess both switching and self-healing properties, has attracted both supramolecular chemists and materials scientists.

Herein supramolecular materials using poly(acrylic acid) (pAA; $M_w = 25 \times 10^4$) modified with cyclodextrins (pAA-CDs)³⁶ as a host polymer and pAA with ferrocene (pAA-Fc) as a guest polymer is described. Ferrocene derivatives have attracted attention due to their redox-responsive properties. Variations in the redox potential can induce a reversible sol–gel phase transition in a supramolecular hydrogel formed by pAA-6 β -cyclodextrin (pAA-6 β CD) and pAA-Fc. Moreover, supramolecular materials formed by host–guest interactions exhibit self-healing and self-repairing properties.

2-2. Experimental section

Materials.

Poly(acrylic acid) (PAA, $M_{av} = 250,000$) and D_2O were obtained from Wako Pure Chemical Industries, Ltd. α -Cyclodextrin and β -cyclodextrin were obtained from Junsei Chemical Co., Ltd. Triethylamine (Et_3N), ethylenediamine, sodium hydroxide, potassium hydroxide, boric acid, potassium chloride, and sodium hypochlorite aqueous solution were obtained from Nacalai Tesque Inc. Benzotriazol-1-yl-oxytripyrrolidinophosphonium hexafluorophosphate (PyBOP), 3-amino-3-deoxy- α -cyclodextrin and 3-amino-3-deoxy- β -cyclodextrin, ferrocenecarboxylic acid, adamantanecarboxylic acid and oxalyl chloride were obtained from Tokyo Kasei Inc. Glutathione was obtained from KOHJIN Co., Ltd. DMSO- d_6 was obtained from Merck & Co., Inc. A highly porous synthetic resin (DIAION HP-20) used for column chromatography was purchased from Mitsubishi Chemical Co., Ltd. Dialytic tube (MWCO = 14,000) was purchased from Sanko Junyaku Inc. Water used for the preparation of the aqueous solutions (except for NMR measurements) was purified with a Millipore Elix 5 system. Other reagents were used without further purification.

Measurements.

The 1H NMR and 2D NMR (NOESY) spectra were recorded at 500 MHz with a JEOL JNM-ECA 500 NMR spectrometer. Chemical shifts were referenced to the solvent values ($\delta = 2.49$ ppm for DMSO and $\delta = 4.79$ ppm for HOD). The UV-Vis absorption spectra were recorded with a JASCO V-650 and a Hitachi U-4100 spectrometer in water with 1 cm quartz cell at room temperature. Circular dichroism spectra and UV spectra were recorded on a JASCO J820 spectrometer in water with 1 cm quartz cell at room temperature. Dynamic viscoelasticity were measured using an Anton Paar MCR301 rheometer. Mechanical properties of the gel were measured by the mechanical tension testing system (Rheoner, RE-33005, Yamaden Ltd.).

Breaking stress measurement of the pAA-6 β CD/pAA-Fc hydrogel.

One cubic centimeter cube-shaped pAA-6 β CD/pAA-Fc hydrogel (3 wt%) was cut in half using a razor-edge, and then rejoined at 24 °C (waiting time less than 5 min.). After standing for 24 h, the breaking stress was measured by a creep meter with a wedge-shaped plunger.

2-3. Preparation of host and guest polymers

Figure 2-1 depicts the chemical structures of the host polymers (pAA-CDs) and a guest polymer (pAA-Fc).

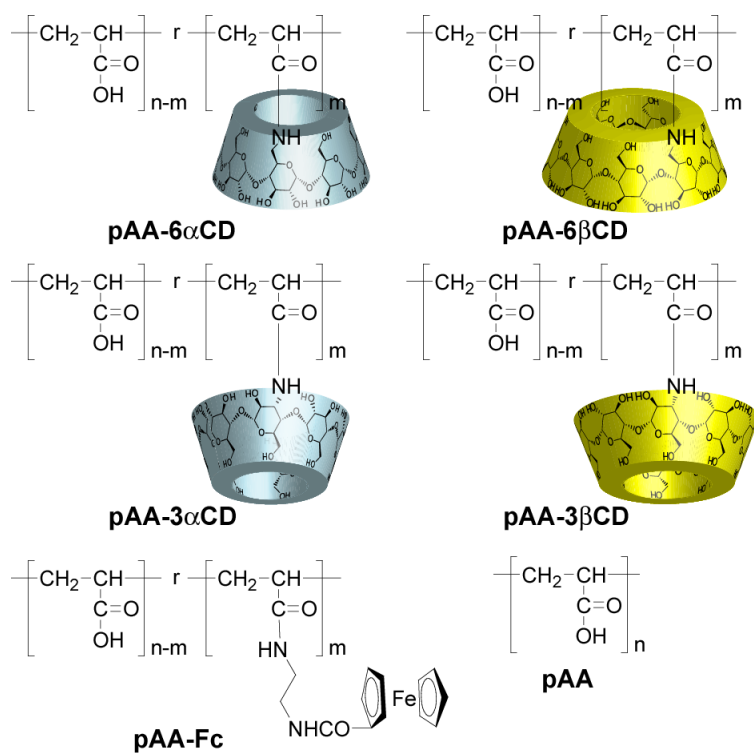
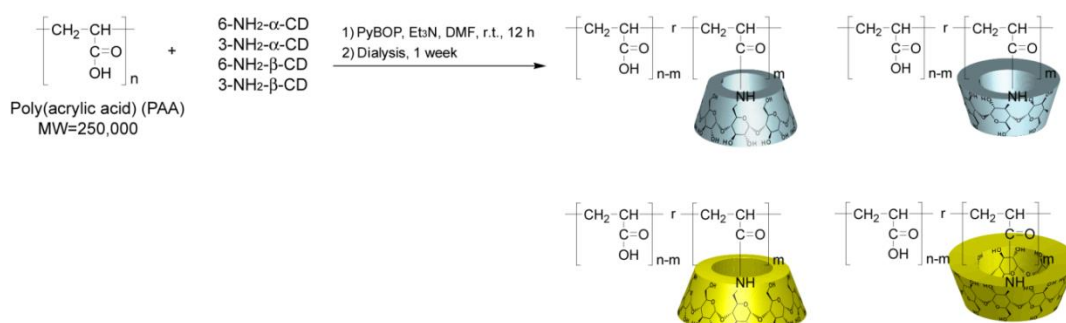


Figure 2-1. Chemical structures of the host polymers (pAA-6 α CD, pAA-6 β CD, pAA-3 α CD, and pAA-3 β CD) and the guest polymer (pAA-Fc).

Preparation and characterization of pAA-CDs.

pAA-CDs were prepared by the reaction of amino-CDs (6-amino- α CD, 3-amino- α CD, 6-amino- β CD, and 3-amino- β CD) with pAA (Scheme 2-1). According to ^1H NMR spectroscopy, amino-CDs were substituted into 4–5% of the carboxylic acid groups of pAA (Figure 2-2 and Table 2-1). These host polymers are abbreviated as pAA-6 α CD, pAA-3 α CD, pAA-6 β CD, and pAA-3 β CD for substitutions by 6-amino- α CD, 3-amino- α CD, 6-amino- β CD, and 3-amino- β CD, respectively.

Scheme 2-1. Preparation of pAA-CDs.



Poly(acrylic acid) (pAA, $M_{av} = 250,000$) was dissolved in 20 mL of *N,N*-dimethylformamide (DMF). To this solution, PyBOP (0.06 eq. of acrylic acid unit) and Et $_3$ N (0.06 eq. of acrylic acid unit) were added. After stirring for 2 h, a mono-amino-mono-deoxy-CD was added, and the solution was stirred for another 12 h at room temperature. The polymer product was reprecipitated from 200 mL of ethanol and washed with ethanol. The polymer was dissolved in water and dialyzed for 12 days with a dialytic tube (MWCO = 14,000). After dialysis, each pAA-CD was obtained by freeze-drying.

pAA-6 α CD; ^1H NMR (500 MHz, pD 9 buffer, 30 $^\circ\text{C}$): $\delta = 1.56$ to 2.12 (CH_2 (pAA)), 2.31 – 2.65 (CH (pAA)), 3.61 – 3.80 ($\text{C}_{2,4}\text{H}$ (CD)), 3.80 – 4.11 ($\text{C}_{3,5,6}\text{H}$ (CD)), 5.00 – 5.23 (C_1H (CD)).

pAA-3 α CD; ^1H NMR (500 MHz, pD 9 buffer, 30 $^\circ\text{C}$): $\delta = 1.56$ to 2.12 (CH_2 (pAA)), 2.31 – 2.65 (CH (pAA)), 3.59 – 3.80 ($\text{C}_{2,4}\text{H}$ (CD)), 3.80 – 4.11 ($\text{C}_{3,5,6}\text{H}$ (CD)), 4.97 – 5.27 (C_1H (CD)).

pAA-6 β CD; ^1H NMR (500 MHz, pD 9 buffer, 30 $^\circ\text{C}$): $\delta = 1.56$ – 2.12 (CH_2 (pAA)), 2.31 – 2.65 (CH (pAA)), 3.61 – 3.80 ($\text{C}_{2,4}\text{H}$ (CD)), 3.80 – 4.10 ($\text{C}_{3,5,6}\text{H}$ (CD)), 5.05 – 5.22 (C_1H (CD)).

pAA-3 β CD; ^1H NMR (500 MHz, pD 9 buffer, 30 $^\circ\text{C}$): $\delta = 1.56$ – 2.12 (CH_2 (pAA)), 2.31 – 2.65 (CH (pAA)), 3.52 – 3.80 ($\text{C}_{2,4}\text{H}$ (CD)), 3.80 – 4.10 ($\text{C}_{3,5,6}\text{H}$ (CD)), 4.96 – 5.23 (C_1H (CD)).

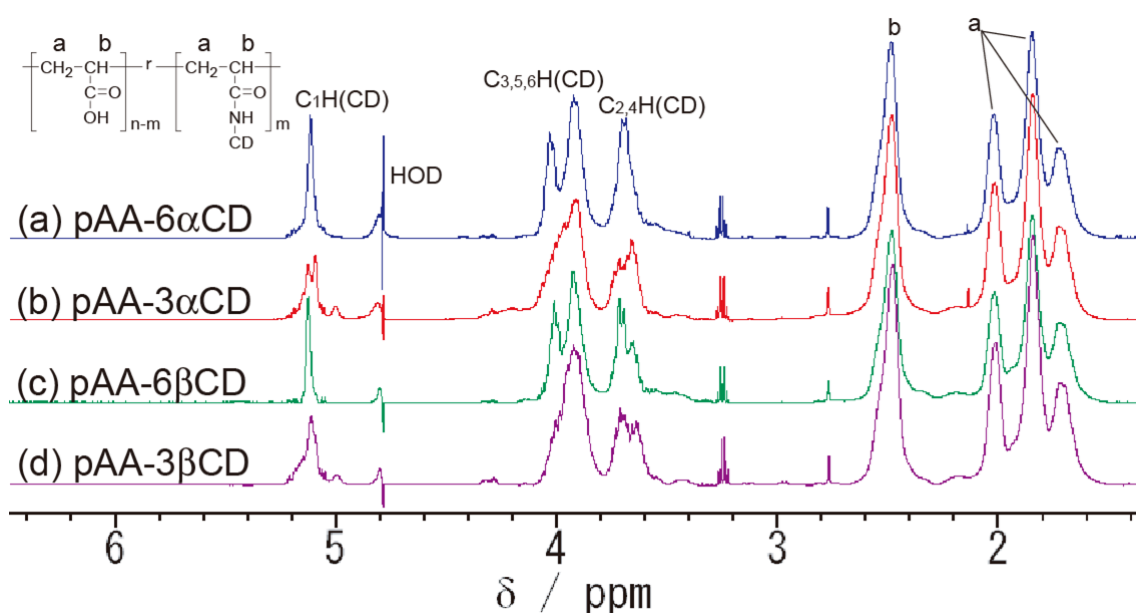
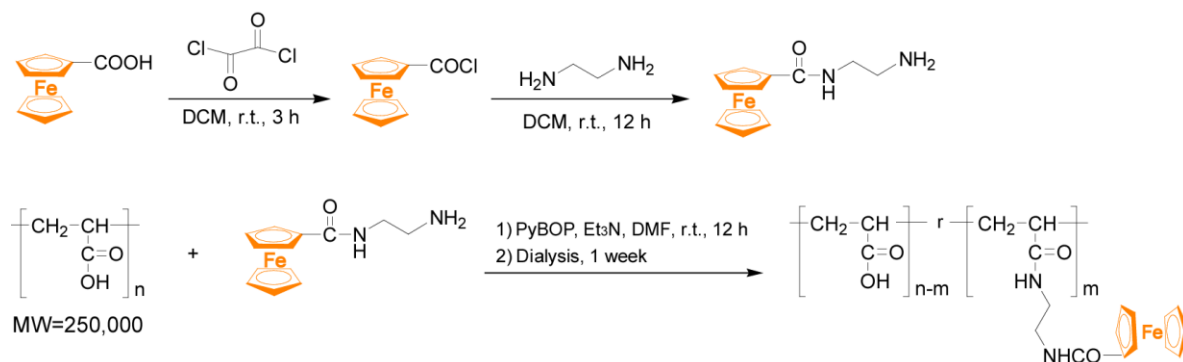


Figure 2-2. ^1H NMR spectra of (a) pAA-6 α CD, (b) pAA-3 α CD, (c) pAA-6 β CD, and (d) pAA-3 β CD. (500 MHz, pD9 buffer, 30 °C)

Preparation and characterization of pAA-Fc.

pAA-Fc was prepared by the reaction of aminoethylamide ferrocene (Fc) with pAA (Scheme 2-2), and Fc was substituted into 2.7% of the carboxylic acid groups of pAA (Figure 2-3 and Table 2-1).

Scheme 2-2. Preparation of pAA-Fc.



Synthesis and characterization of Fc-CONH-(CH₂)₂-NH₂.

A 2.00 g (8.7 mmol) of ferrocenecarboxylic acid was suspended in 120 mL of dichloromethane (DCM). Then 2 mL (23.3 mmol, 2.7 eq.) of oxalyl chloride was added dropwise, and the suspension was stirred for 3 h at room temperature. The orange suspension turned into a red solution. After evaporating the solvent, ferrocenecarboxyl chloride (red solid) was dissolved in 60 mL of DCM. 6 mL (89.9 mmol, 10 eq.) of ethylenediamine was dissolved in 60 mL of DCM, and the ferrocenecarboxyl chloride solution was added dropwise. After stirring overnight at room temperature, the solution was washed with 80 mL of 10% KOH aq., and the DCM layer was collected and evaporated. The orange solid was washed with 300 mL of hexane: ethyl acetate = 9:1, and the solid product was collected via a centrifuge and dried for 4 days at 50 °C to obtain Fc-CONH-(CH₂)₂-NH₂ as a yellow powder in 83% yield.

^1H NMR (500 MHz, D_2O , 30 °C): δ = 2.90 (2H, t, Fc-CONH-CH₂-CH₂-NH₂), 3.46 (2H, t, Fc-CONH-CH₂-CH₂-NH₂), 4.36 (5H, s, Cp), 4.61 (2H, t, Cp), 4.89 (2H, t, Cp).

Synthesis and characterization of pAA-Fc.

PyBOP (0.22 g, 0.42 mmol, 0.06 eq. of acrylic acid unit) was added to a 40 mL DMF solution of poly(acrylic acid) (pAA, M_{av} = 250,000, 500.3 mg). 0.95 g (0.35 mmol, 0.05 eq. of acrylic acid unit) of Fc-CONH-(CH₂)₂-NH₂ was dissolved in 10 mL of DMF, and 0.06 mL (0.43 mmol, 0.06 eq. of acrylic acid unit) of Et₃N was added. This solution was added dropwise to the pAA solution and stirred for 12 hours at room temperature. After stirring, the solution was diluted with water and dialyzed in water for 7 days with dialytic tube (MWCO = 14,000). After dialysis, pAA-Fc was obtained by freeze-drying.

^1H NMR (500 MHz, pD 9 buffer, 30 °C): δ = 1.40 to 1.91 (CH₂ (pAA)), 2.05 to 2.50 (CH (pAA)), 4.37 (s, Cp), 4.61 (s, Cp), 4.91 (s, Cp (overlapped with HOD)).

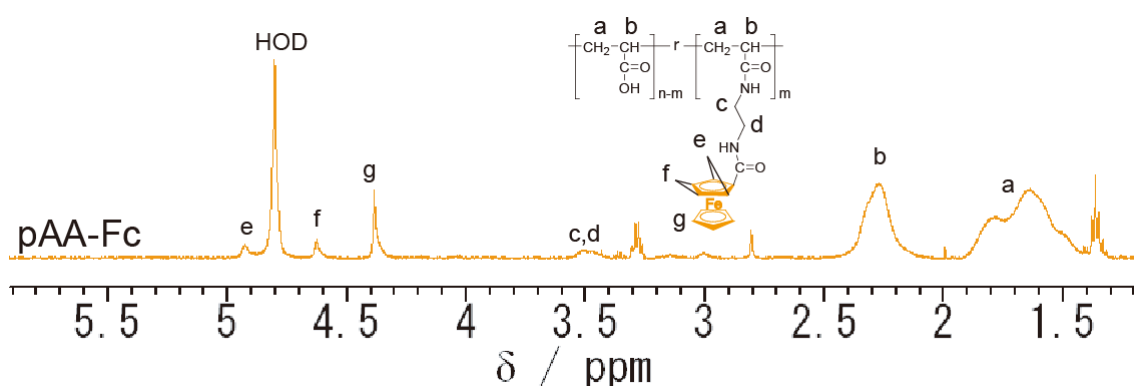


Figure 2-3. ^1H NMR spectra of pAA-Fc. (500 MHz, pD9 buffer, 30 °C)

Table 2-1. Degree of side chain modification (per acrylic acid unit) for each polymer.

Polymer	pAA-6 α CD	pAA-3 α CD	pAA-6 β CD	pAA-3 β CD	pAA-Fc
Side chain modification ratio [%]	4.6	4.4	4.0	3.6	2.7

2-4. Hydrogelation between host and guest polymers

Inset of Figure 2-4 shows photographs of hydrogelation between the host polymers and a guest polymer (2 wt%) in a pH 9 boric acid/KCl/NaOH buffer solution. The 1:1 mixture of a 2 wt% solution of pAA-6 α CD/pAA-Fc, pAA-3 α CD/pAA-Fc, pAA-3 β CD/pAA-Fc, pAA/pAA-6 β CD, or pAA/pAA-Fc in an aqueous solution had a negligible effect on the viscosity. On the other hand, the mixed solution of pAA-6 β CD/pAA-Fc selectively increased the viscosity of the solution to yield a hydrogel. These results indicate that not only the host–guest complementarity but also multipoint crosslinks play important roles in forming the supramolecular hydrogel.

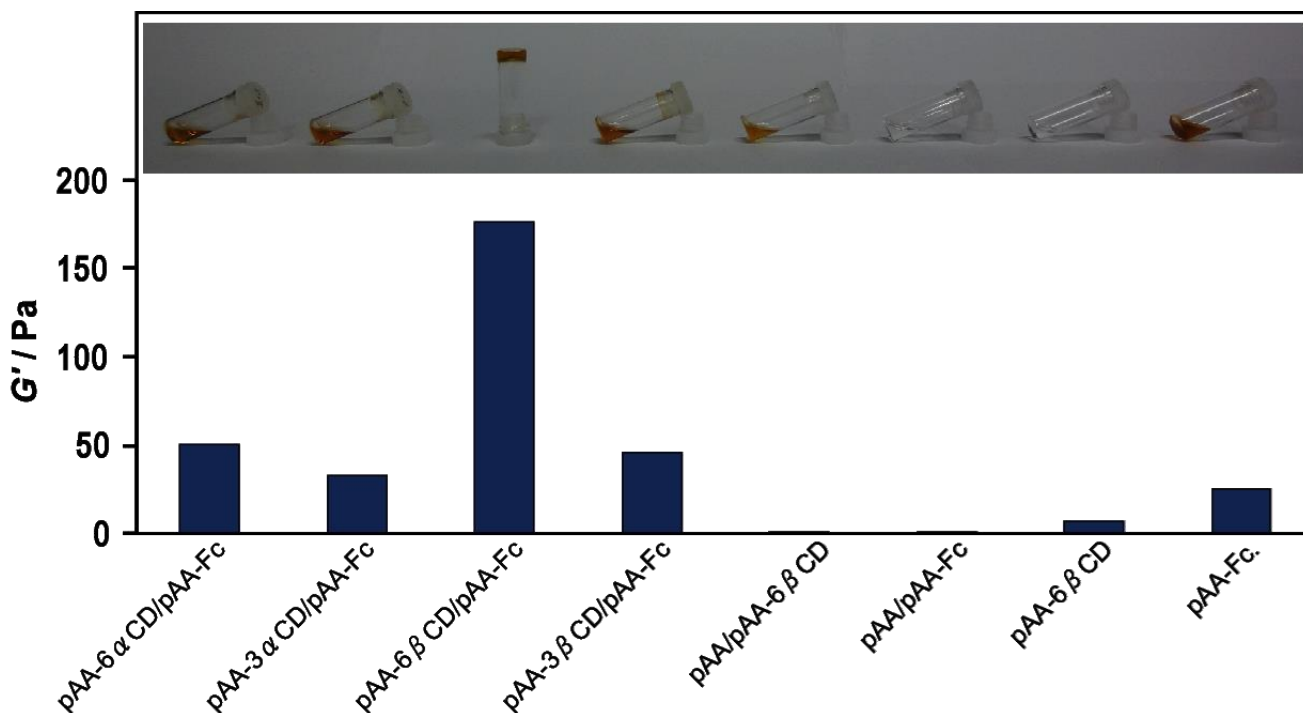


Figure 2-4. Values of storage elastic modulus (G') for each sample under 2 wt% of pH 9 buffer solutions. Inserted photograph shows hydrogelation between host polymers and a guest polymer under 2 wt% of aqueous solutions. ($\omega = 10 \text{ s}^{-1}$)

Figure 2-4 shows storage elastic moduli (G') for pAA-6 α CD/pAA-Fc, pAA-3 α CD/pAA-Fc, pAA-6 β CD/pAA-Fc, pAA-3 β CD/pAA-Fc, pAA/pAA-6 β CD, pAA/pAA-Fc, pAA-6 β CD, and pAA-Fc (1+1 wt%) in pH 9 buffer solutions, respectively. Although other samples exhibited G' less than 50 Pa, pAA-6 β CD/pAA-Fc had the highest elasticity (176 Pa), which was more than thrice the value of the comparison cases.

2D NOESY NMR confirmed the interactions between β -CD and pAA-Fc (Figure 2-5) and between the β -CD moieties of pAA-6 β CD and pAA-Fc (Figure 2-6).

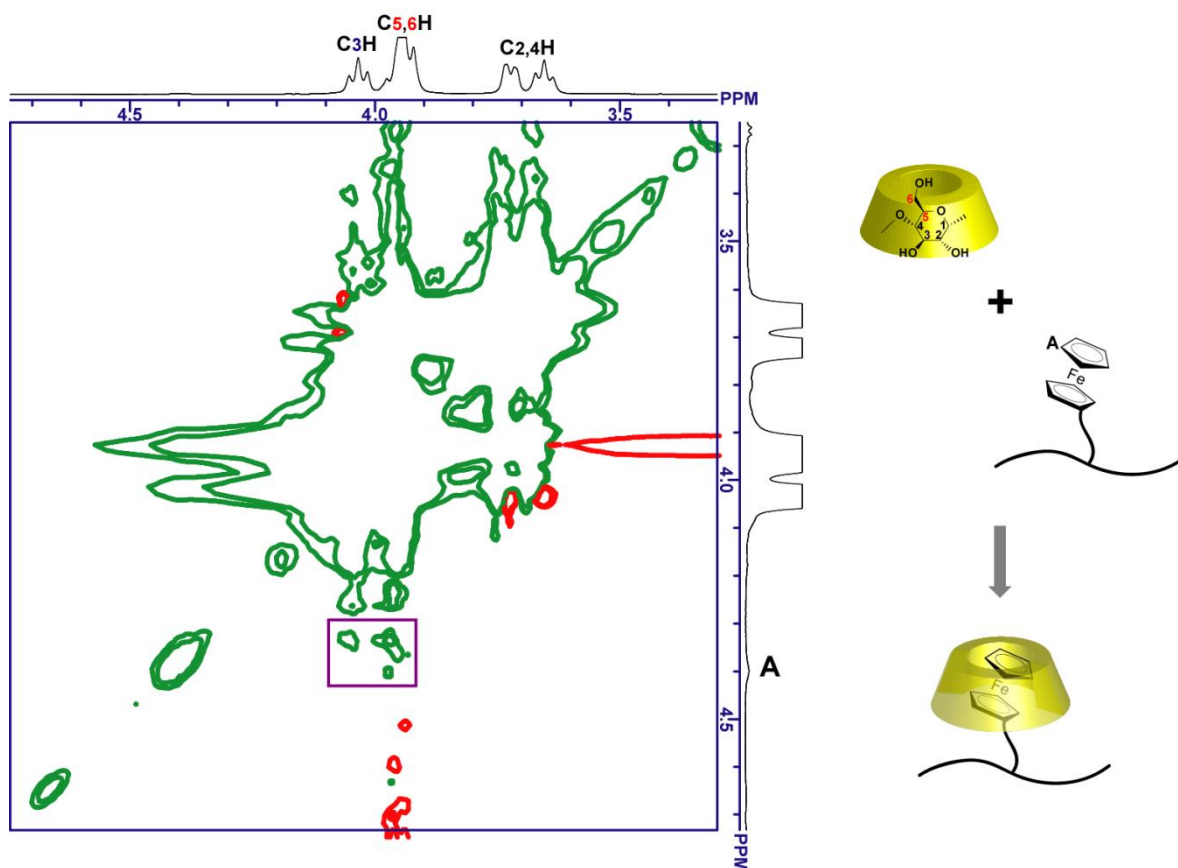


Figure 2-5. 2D NOESY NMR of β -CD with pAA-Fc. 2D NOESY NMR spectrum of the mixture of β -CD (10 mM) and pAA-Fc ([Fc] = 1 mM) (500 MHz, pD 9 buffer, 30°C, left) and proposed structure of inclusion complex at side chain of pAA-Fc (right). The NOESY NMR spectrum showed that the inner protons of β -CD were correlated to the protons of the Fc group of pAA-Fc. Peak intensities between C(5,6)H protons (wider rim of β -CD) and the A proton of the Fc group was greater than that of the C(3)H proton, indicating that the Fc group is included from the wider rim of the β -CD cavity in aqueous solutions.

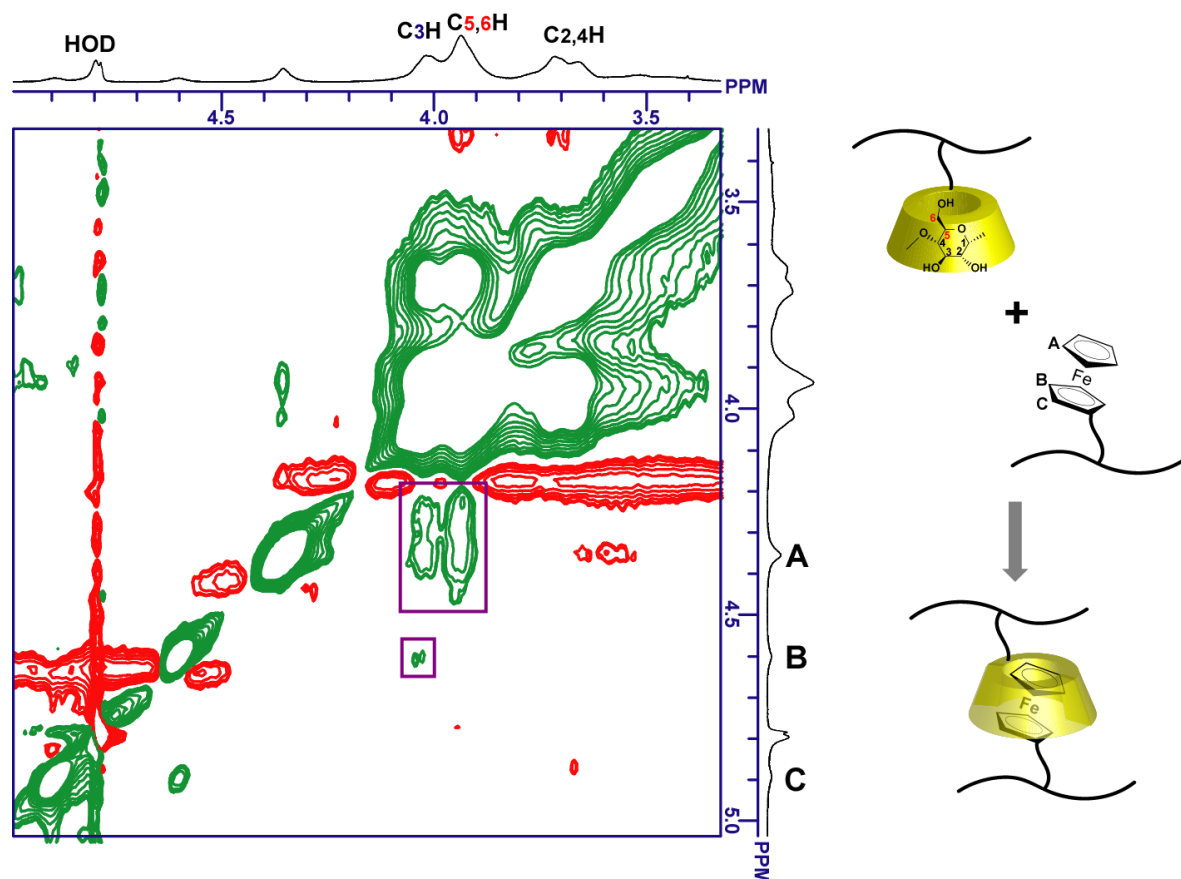


Figure 2-6. 2D NOESY NMR of pAA-6 β CD with pAA-Fc. 2D NOESY NMR spectrum of the mixture of pAA-6 β CD ([β CD] = 1 mM) and pAA-Fc ([Fc] = 1 mM) (500 MHz, pD 9 buffer, 30 °C, left) and proposed structure of inclusion complex at side chain of each polymer (right). The NOESY NMR spectrum showed that the inner protons of the β -CD unit were correlated to the protons of the Fc group of pAA-Fc, indicating that the side chain group of pAA-Fc is included in the cavity of β -CD at side chain of pAA-6 β CD in aqueous solutions.

Previous studies have suggested that the association constant of Fc in its reduced state for β -CD is larger than that for α CD (Fc/ α CD; $K_a = 0.14 \times 10^3 \text{ M}^{-1}$, Fc/ β CD; $K_a = 17 \times 10^3 \text{ M}^{-1}$).^{37,38} The K of β -CD for the Fc group of pAA-Fc was $1.1 \times 10^3 \text{ M}^{-1}$, which is suitable for a competitive host molecule for the ferrocene group of pAA-Fc. (Figures 2-7 and 2-8.)

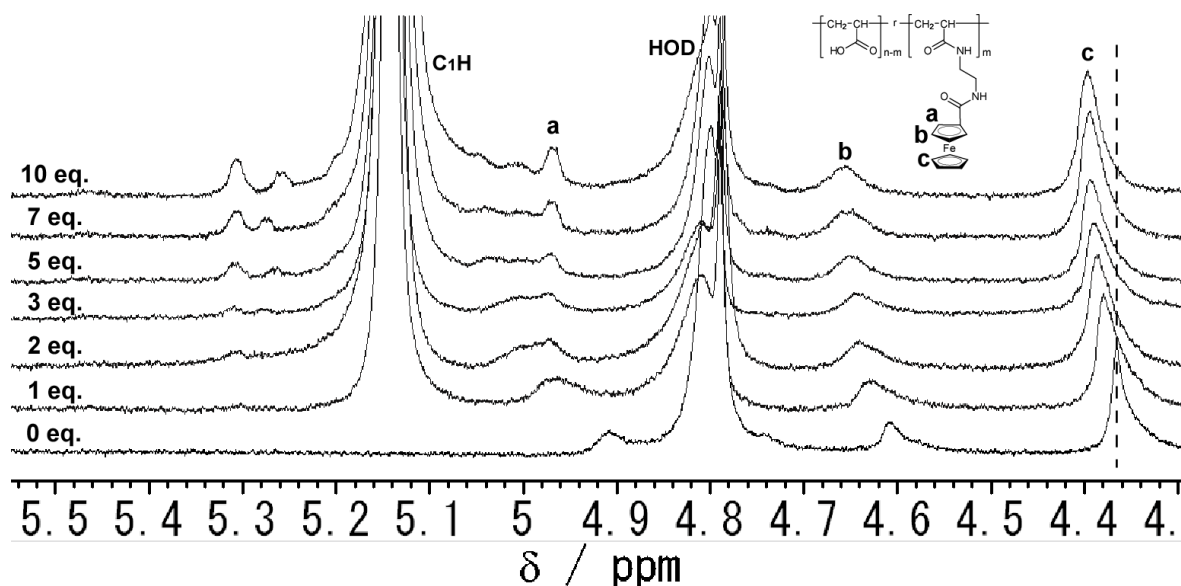


Figure 2-7. Partial ^1H -NMR spectra of pAA-Fc in the presence of β -CD. ^1H NMR spectra for pAA-Fc ($[\text{Fc}] = 1 \text{ mM}$) in the presence of various concentrations (0 mM, 1 mM, 2 mM, 3 mM, 5 mM, 7 mM, and 10 mM) of β -CD (C_{CD}) (500 MHz, pD 9 buffer, 30 $^\circ\text{C}$). As C_{CD} is increased, clear down-field shifts was observed, indicating the interaction of β -CD with Fc group.

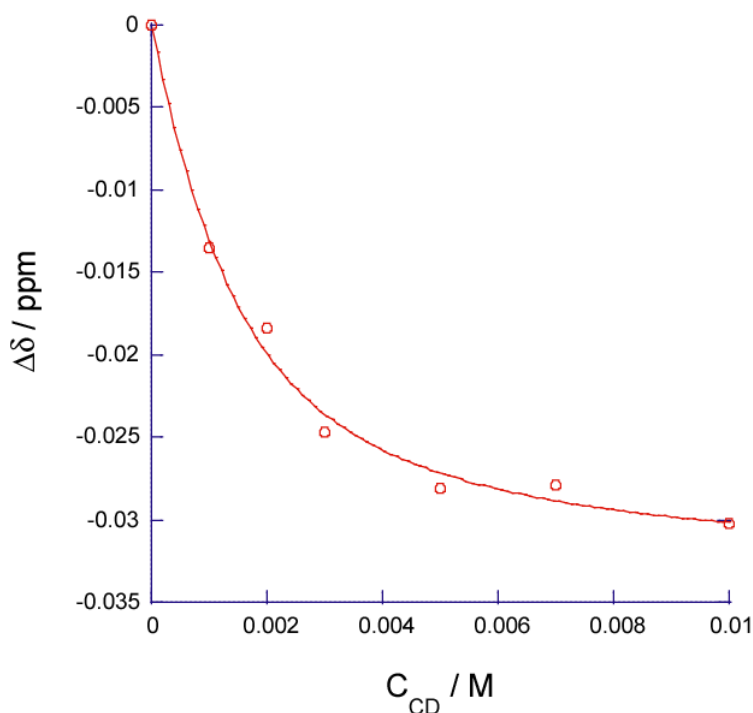


Figure 2-8. Nonlinear least-squares plot. The interaction of β -CD with the Fc group of pAA-Fc by 1H NMR to estimate apparent association constant (K) is investigated using nonlinear least-squares method. From 1H NMR spectra (Figure 2-7), the peak shifts for the signal due to the c protons of the Fc group ($\Delta\delta$) were calculated and plotted against C_{CD} . As can be seen in Figure 2-8, the plots show a good accordance with (1), indicating that the interaction of β -CD with Fc group can be analyzed based on the formation of one-to-one complexes. The apparent K value was determined to be $1.1 \times 10^3 M^{-1}$ by

$$\Delta\delta = \frac{\Delta\delta}{2K[Fc]_0} [1 + K[CD]_0 + K[Fc]_0 - \{(1 + K[CD]_0 + K[Fc]_0)^2 - 4K^2[CD]_0[Fc]_0\}^{\frac{1}{2}}] \quad (1)$$

About 72% of the Fc groups were included in the cavity of the β -CD group to form a hydrogel by applying K for the pAA-6 β CD/pAA-Fc hydrogel (2 wt%).

To clarify the complementarity between β -CD and the Fc groups (reduced state), competitive guest or host molecules were added to the pAA-6 β CD/pAA-Fc hydrogel (2 wt%). Adamantane carboxylic acid sodium salt (AdCANA) was used as a competitive guest, because the association constant for β -CD ($K_a = 35 \times 10^3 M^{-1}$)³⁹ is higher than that of ferrocene. Adding adamantane carboxylic acid sodium salt (AdCANA, 10 eq. for the β CD group of pAA-6 β CD) into the pAA-6 β CD/pAA-Fc hydrogel led to a sharp decrease in the elasticity from 176 Pa to 23.3 Pa to form the sol state (Figure 2-9a). Similarly, adding β -CD (10 eq. for the Fc group of pAA-Fc) as a competitive host into the pAA-6 β CD/pAA-Fc hydrogel induced a phase transition into the sol state (Figure. 2-9b). They inhibited the formation of an inclusion complex between the β -CD unit of pAA-6 β CD or the Fc unit of pAA-Fc.

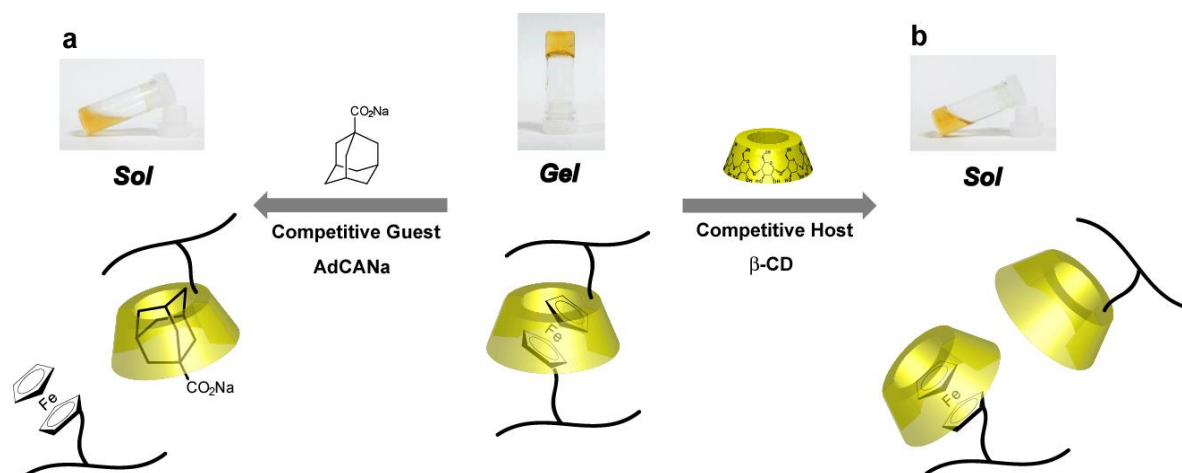


Figure 2-9. Competitive guest / host experiment. Addition of AdCANA as a competitive guest and β -CD as a competitive host into the pAA-6 β CD/pAA-Fc hydrogel (2 wt%). Adding AdCANA (10 eq. for the β CD group of pAA-6 β CD) into the pAA-6 β CD/pAA-Fc hydrogel led to a sharp drop in the elasticity from 176 Pa to 23.3 Pa to form the sol state (a). Similar to adding AdCANA, adding β -CD (10 eq. for the Fc group of pAA-Fc) as a competitive host into the pAA-6 β CD/pAA-Fc hydrogel induced a phase transition into the sol state (b).

Next, the effects of the host–guest ratio on the elasticity change were examined. The elasticity of pAA-6 β CD/pAA-Fc was estimated by varying the ratio of pAA-6 β CD and pAA-Fc in the monomer unit equivalent. Although pAA-6 β CD/pAA-Fc in the non-equivalent ratio demonstrated moderate elasticities, the 1:1 ratio of pAA-6 β CD/pAA-Fc displayed the largest G' value (176 Pa) (Figure 2-10). These results indicate that a hydrogel consisting of pAA-6 β CD/pAA-Fc is produced by the extensive complementarity between the β -CD and Fc units.

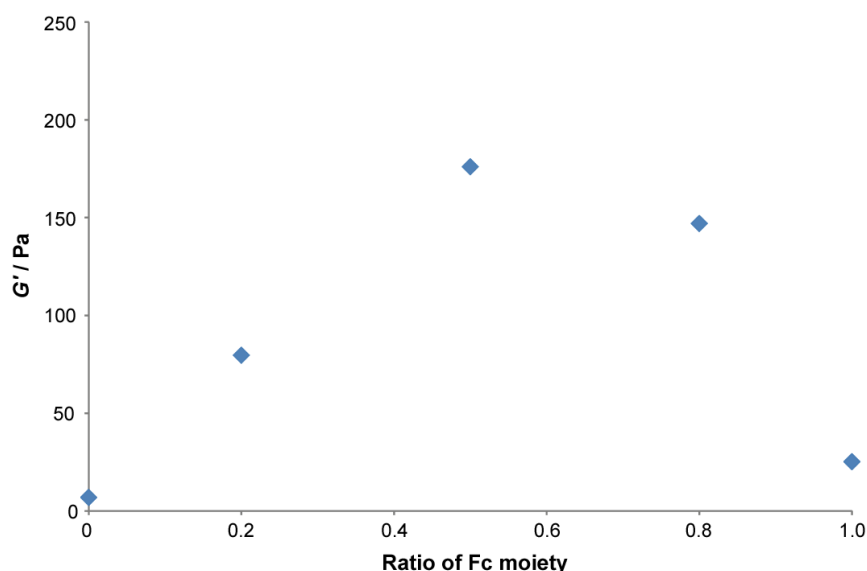


Figure 2-10. G' (storage elastic modulus) against the molar ratio of Fc. The elasticity of pAA-6 β CD/pAA-Fc was estimated by varying the ratio of pAA-6 β CD and pAA-Fc in the monomer unit equivalent ($\omega = 10$ rad / s, Strain = 0.1%, pH 9 buffer, 25 °C). Values of G' were plotted against the ratio of ferrocene moiety of pAA-Fc against β CD moiety of pAA-6 β CD.

2-5. Redox-responsive sol-gel switching

The effect of the redox reagents on the phase transition of the pAA-6 β CD/pAA-Fc hydrogel was investigated. NaClO aq. (14 mM) was chosen as an oxidant and glutathione (GSH) as a reductant. Adding NaClO aq. (0.1 mL) to the pAA-6 β CD/pAA-Fc hydrogel (0.4 mL) decreased the viscosity, transforming the hydrogel into the sol. In contrast, continuous addition of GSH (1.2 mg) to the sol recovered the elasticity, reverting it back to the hydrogel (Figure 2-11b). β -CD showed a high affinity for the reduced state of the Fc group due to its hydrophobic nature, whereas the oxidized state of the Fc group (Fc⁺) exhibited a low affinity for β -CD due to the cationic Fc⁺ group.⁴⁰ Next, the formation of pAA-6 β CD/pAA-Fc hydrogel was electrochemically controlled. The pAA-6 β CD/pAA-Fc hydrogel was electrolyzed with a potentiostat using a three-electrode system (platinum plate (working), platinum wire (counter), and Ag/AgCl electrode (reference)) and 50 mM of NaBr as a supporting electrolyte. Electrochemical oxidation of the pAA-6 β CD/pAA-Fc hydrogel decreased the elasticity, and consequently transformed the hydrogel into the sol. Subsequent reduction by heating the sol at 50 °C recovered the elasticity, yielding the hydrogel (Figure 2-11c and Figure 2-12).

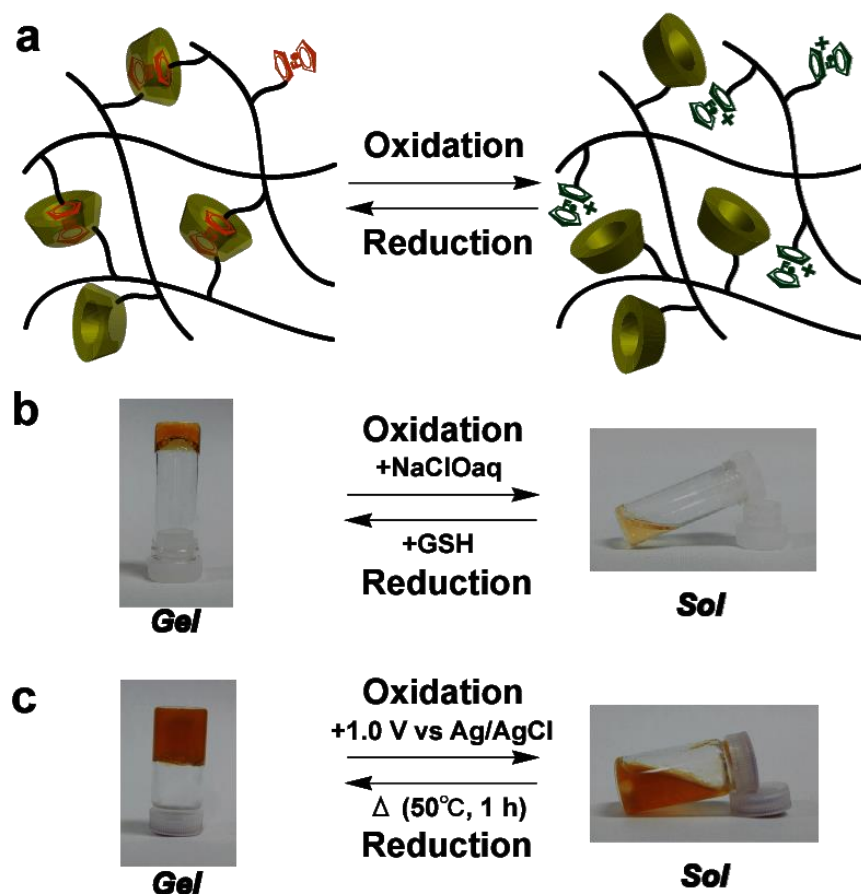


Figure 2-11. Redox responsive sol–gel transition experiment. a. Schematic illustration of Sol–gel transition. b. Sol–gel transition experiment using chemical reagents. Adding NaClO aq. to the pAA-6 β CD/pAA-Fc hydrogel induced a phase transition into the sol state and continuous addition of GSH to the sol recovered the elasticity to yield the hydrogel again. c. Sol–gel transition experiment using electrochemical reactions. Electrochemical oxidation (+1.0 V vs Ag/AgCl) transformed the hydrogel into the sol, whereas reduction recovered the viscosity, reverting it back to the hydrogel.

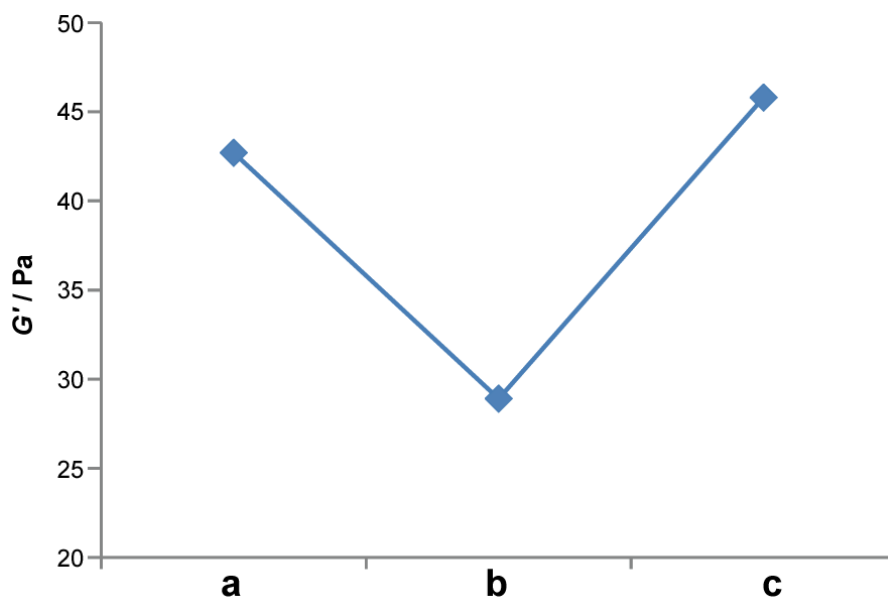


Figure 2-12. Storage elastic modulus (G') switched by redox. Storage elastic modulus (G') of pAA-6 β CD/pAA-Fc hydrogel (2 wt%) before (a), after electrochemical oxidation (+1.0 V vs Ag/AgCl, 24 h) (b), and after subsequent reduction by heating (50 °C, 1 h) (c). (ω = 10 rad / s, Strain = 1%, pH 9 buffer, 25 °C)

The redox reactions between Fc (reduced state) and Fc⁺ in its oxidized state were tracked by UV-vis (Figures 2-13, 2-14, 2-15, and 2-16) and circular dichroism (CD) spectroscopies (Figure 2-17). A mixture of pAA-6 β CD ([β CD] = 2 mM) and ferrocene carboxylic acid (FcCOOH) (2 mM) exhibited a d–d transition band around 400–450 nm, but the band disappeared upon oxidation with NaClO aq. Prior to oxidizing, the CD spectra exhibited a negative Cotton band around 400–450 nm, which was assigned to the induced Cotton band between the ferrocene group and β -CD on the side chain of pAA-6 β CD in an aqueous solution. Adding NaClO as an oxidant decreased the band, indicating that oxidized ferrocene is not included in the cavity of β -CD. Consequently, both chemical and electrochemical redox reactions for the pAA-6 β CD/pAA-Fc hydrogel yield reversible sol–gel phase transitions.

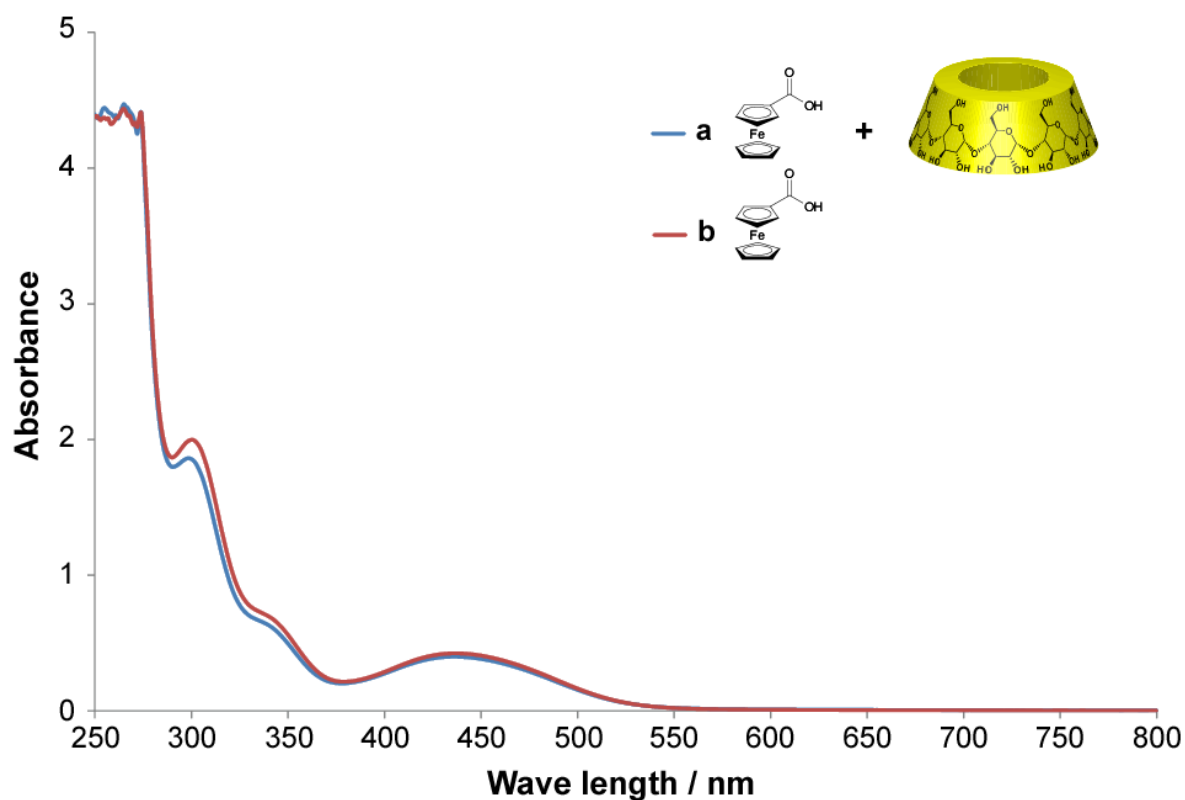


Figure 2-13. UV-Vis spectra of FcCOOH and β -CD. The UV-Vis spectra of FcCOOH (2 mM) in the presence of β -CD (2 mM) (a) and absence of β -CD (b) in aqueous solutions at 25 °C.

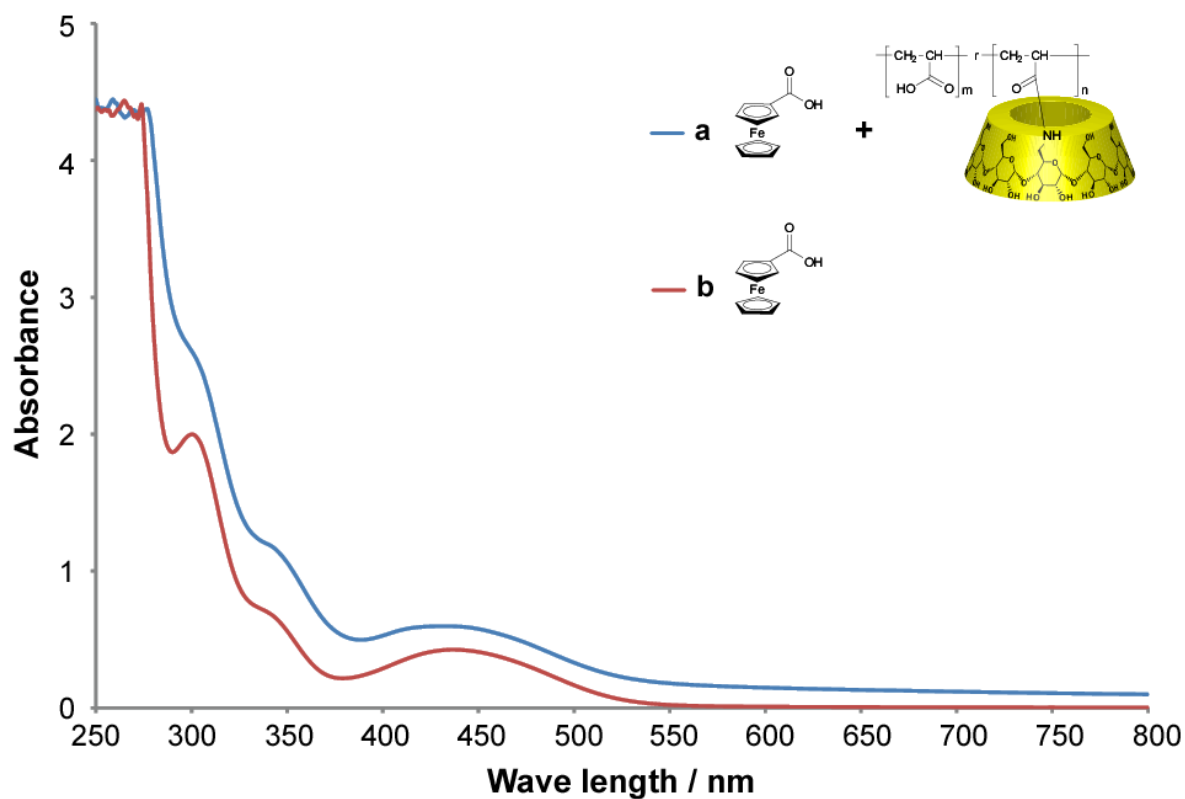


Figure 2-14. UV-Vis spectra of FcCOOH and pAA-6 β CD. The UV-Vis spectra of FcCOOH (2 mM) in the presence of pAA-6 β CD ([β CD] = 2 mM) (a) and absence of pAA-6 β CD (b) in aqueous solutions at 25 °C.

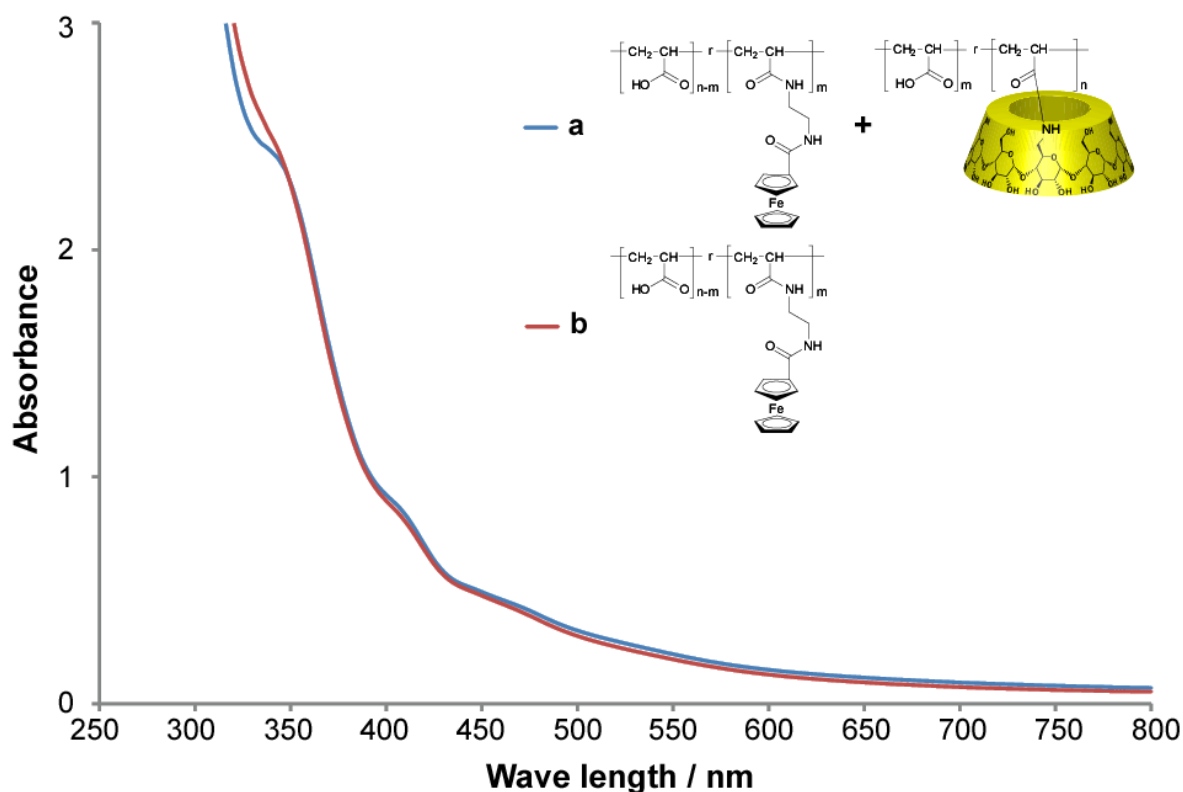


Figure 2-15. UV-Vis spectra of pAA-Fc and pAA-6βCD. The UV-Vis spectra of pAA-Fc ([Fc] = 1 mM) in the presence of pAA-6βCD ([βCD] = 1 mM) (a) and absence of pAA-6βCD (b) in aqueous solutions at 25 °C.

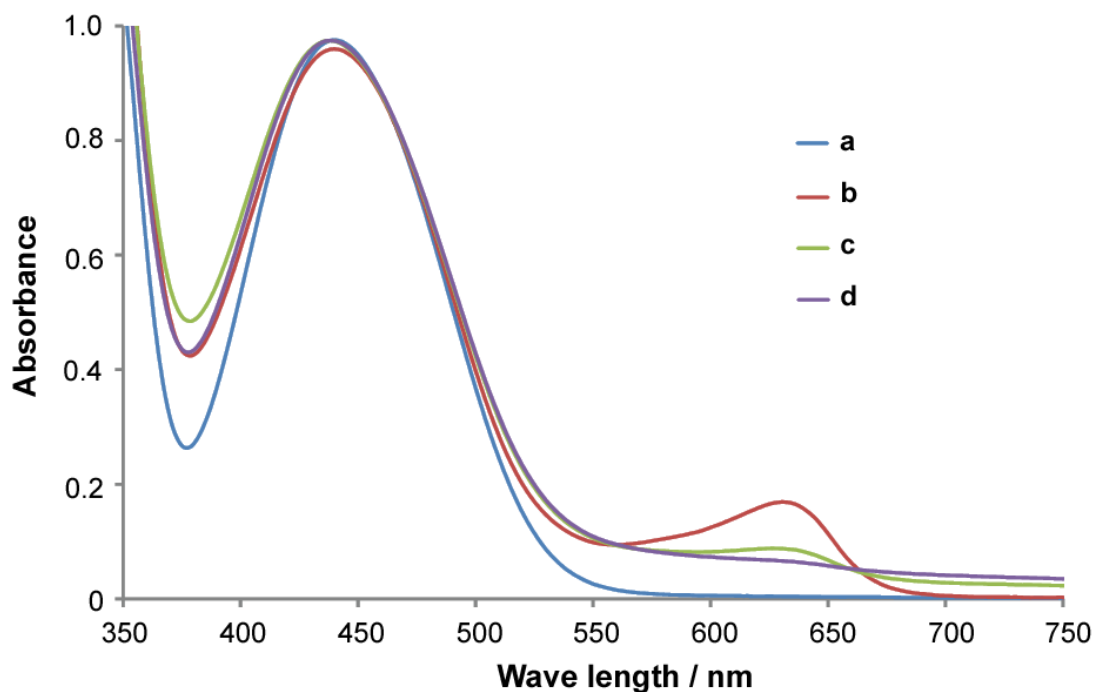


Figure 2-16. Change of UV-Vis spectra by redox. The UV-Vis spectra of Fc-COOH (5 mM) in 0.1 M NaBr aqueous solution (a), after electrochemical oxidation (+0.5 V vs Ag/AgCl, 10 min.) (b), after subsequent heating (50 °C, 10 min.) (c), and after heating (50 °C, 40 min.) (d) in aqueous solutions at 25 °C. The peak around 630 nm due to Fc⁺ in its oxidized state was observed by oxidation, and was disappeared by subsequent heating.

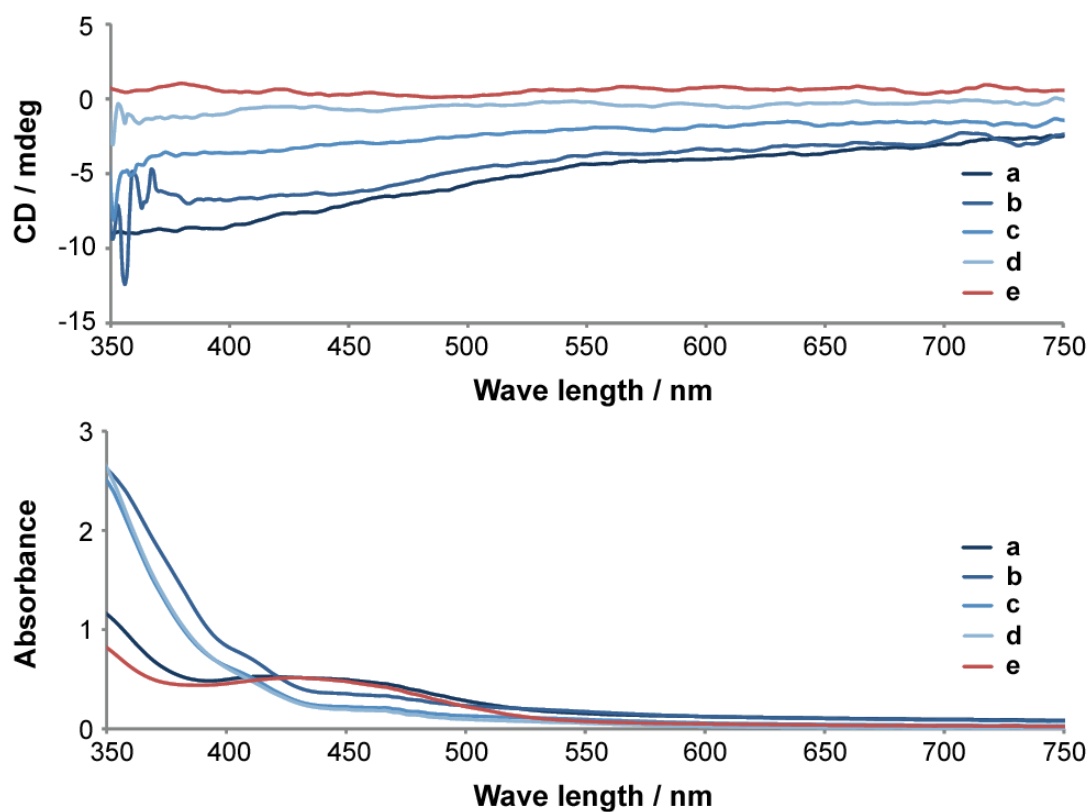


Figure 2-17. Circular dichroism spectra of Fc-COOH. UV-Vis and circular dichroism spectra of Fc-COOH (2 mM). Fc-COOH (2 mM)/PAA-6 β CD ([β CD] = 2 mM) in the absence of NaClO aq. (a) and in the presence of NaClO aq. (4.7 mM (b), 14 mM (c), and 23 mM (d)), and Fc-COOH (2 mM) (e) in aqueous solutions at 25 °C.

The negative induced Cotton band around 450 nm was observed in aqueous solutions. This Cotton band is assigned to the Fc group included in asymmetric cavity of β -CD. On the contrary, the Cotton band was disappeared on addition of NaClO aq. These results indicate that the oxidized ferricenium group was excluded from the cavity of β -CD.

2-6. Macroscopic self-healing property of pAA-6 β CD/pAA-Fc hydrogel

It is speculated that the pAA-6 β CD/pAA-Fc hydrogel would exhibit a self-healing property because a characteristic feature of the pAA-6 β CD/pAA-Fc hydrogel is the reversible host–guest interactions between the side chains of both polymers. Thus, a break test during continuous step strain measurements was conducted. As a precondition of the pAA-6 β CD/pAA-Fc hydrogel for the break test, it was confirmed that the hydrogel did not relax ($G' > G''$) in the frequency range 0.01–100 rad·s^{−1}, which was characterized by dynamic viscoelastic measurements (Figures 2-18 and 2-19).

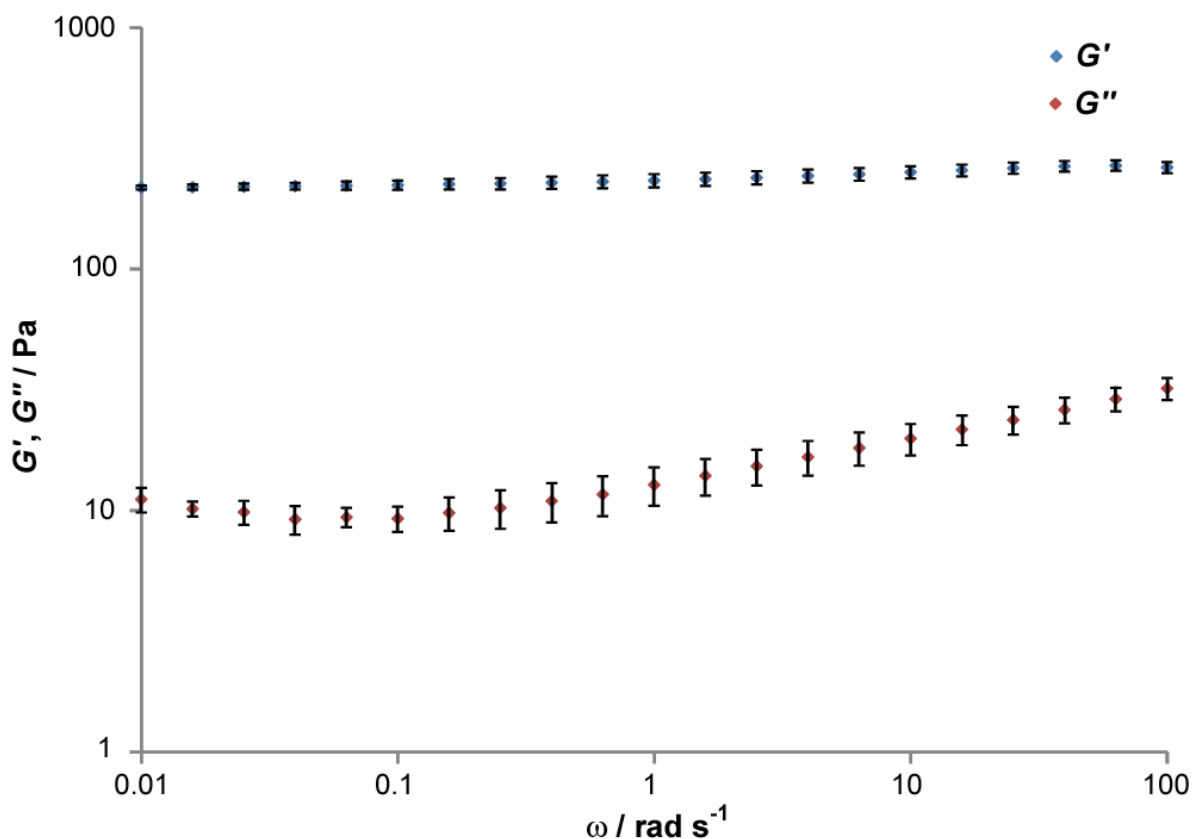


Figure 2-18. Dynamic viscoelastic measurement. Dependency of the storage and loss moduli, G' and G'' on angular frequency (ω) for an aqueous solution of the mixture of pAA-6 β CD/pAA-Fc hydrogel (2 wt%). (Strain = 0.1%, pH 9 buffer, 25 °C, n=5, error bars are standard deviation.)

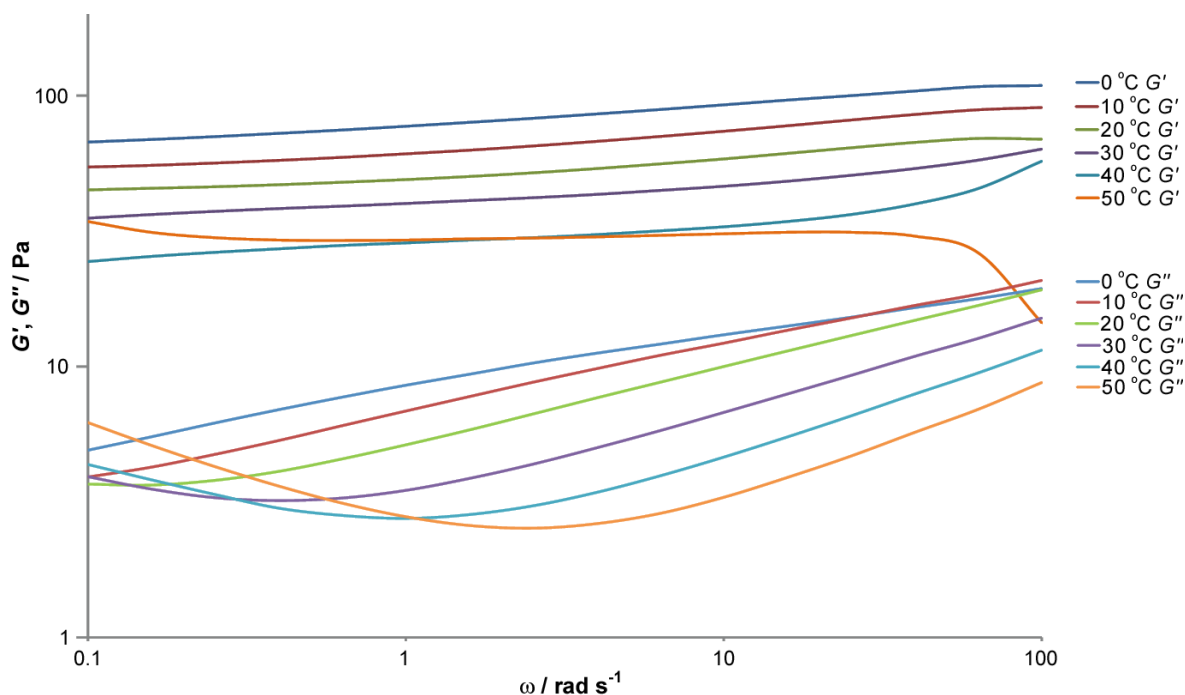


Figure 2-19. Temperature dependence of G' and G'' . Storage elastic modulus (G') and loss elastic modulus (G'') of the mixture of pAA-6 β CD/pAA-Fc hydrogel (2 wt%) according to temperature. (Strain = 1%, pH 9 buffer)

Figure 2-20 demonstrates the morphology of the pAA-6 β CD/pAA-Fc hydrogel remained the same for over 72 hours.

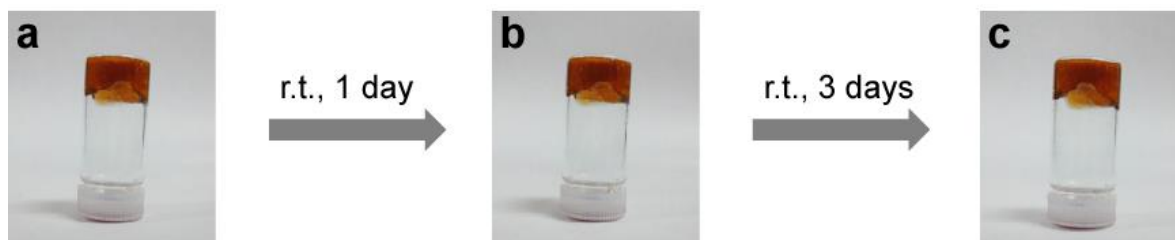


Figure 2-20. Photographs of the gel. Photographs of gels soon after making (a), after 1 day (b), and after 3 days (c). No flowing was observed.

Based on this rheological property, the self-healing ability of the pAA-6 β CD/pAA-Fc hydrogel was investigated. A cube-shaped pAA-6 β CD/pAA-Fc hydrogel (1+1 wt%) was cut in half using a razor-edge, and then rejoined (Figure 2-21). After standing for 24 hours, the crack disappeared, and the sample hydrogel sufficiently healed to form one gel.

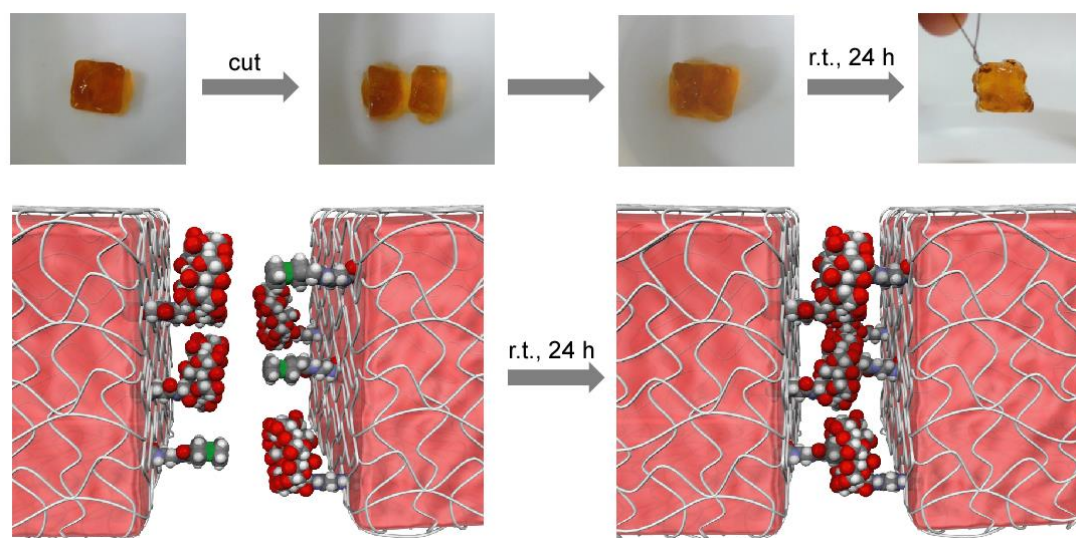


Figure 2-21. Self-healing experiments. a. After standing for 24 hours, two cut pAA-6 β CD/pAA-Fc hydrogel (1+1 wt%) pieces were rejoined, and the crack sufficiently healed to form one gel.

To demonstrate the complementary host–guest interactions between the β -CD and the Fc groups, competitive guest and host molecules were added to the cut plane of the pAA-6 β CD/pAA-Fc hydrogel (Figure 2-22). A 3 mM solution of adamantane carboxylic acid sodium salt (AdCANa) as the competitive guest, β -CD as the competitive host, or D-glucose as a reference sample was placed on the cut surfaces, and then the two gels were reattached. After 24 hours, the samples with a competitive guest or host did not heal, whereas the sample with D-glucose healed regardless of the amount of D-glucose added. These results indicate that the self-healing property is due to the ferrocene and β -CD moieties, which form an inclusion complex on the cut surfaces of hydrogels.

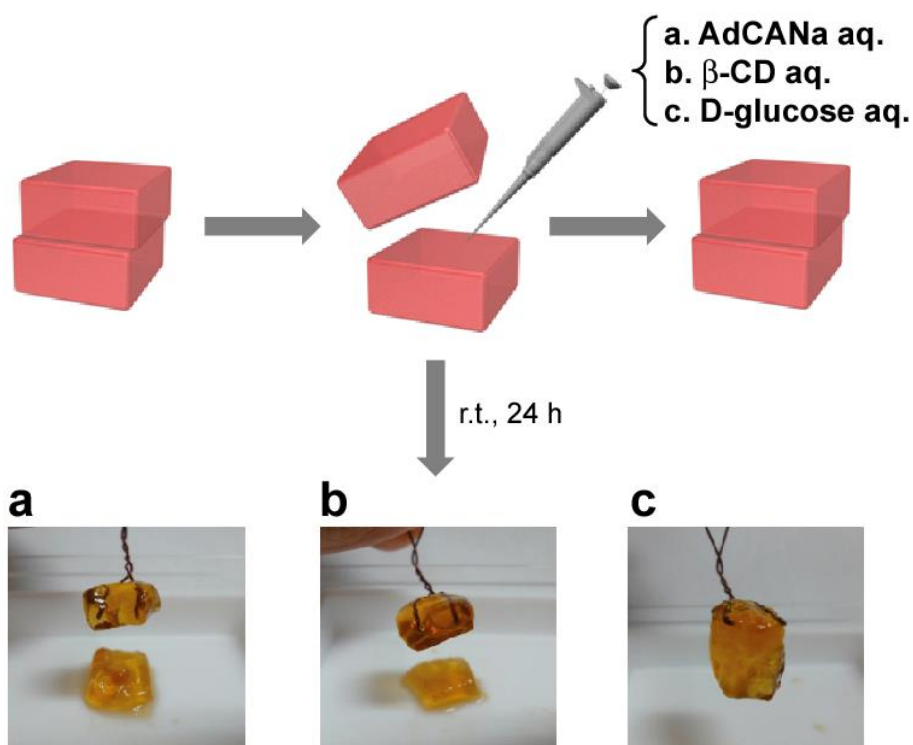


Figure 2-22. Self-healing experiments using competitive guest / host molecules. 1 cm cube-shaped 2 wt% gels were cut in half, and the cut surfaces were coated with aqueous solutions of AdCANA (3 mM, 20 μ L) (a), β -CD (3 mM, 20 μ L) (b), or D-glucose (3 mM, 20 μ L) (c). Then the two pieces were reattached according to the experimental operation. After 24 hours, gels coated with aqueous solutions of AdCANA (3 mM, 20 μ L) or β -CD (3 mM, 20 μ L) did not show healing. However, the surface coated with D-glucose aq. showed healing.

The adhesive strength of the two gels was confirmed by the wedge shape strain compression test (Figure 2-23).

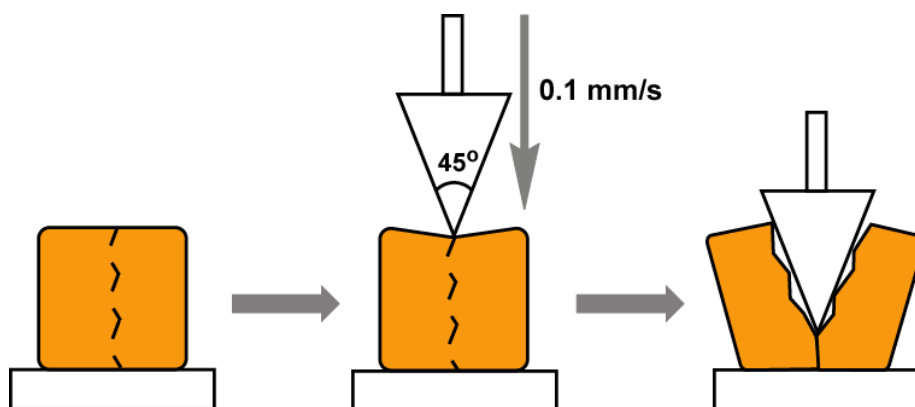


Figure 2-23. Schematic illustration of breaking stress measurement. Breaking stress of the pAA-6 β CD/pAA-Fc hydrogel was measured by a creep meter with a wedge-shaped plunger.

After the gels were rejoined for 24 hours, the adhesion strength on the joint surface reached a steady value, indicating that the interaction of the ferrocene and β -CD moieties achieved an equilibrium on the surface. The adhesion strength on the joint surface recovered 84% of the initial gel's strength after 24 hours (Figure 2-24).

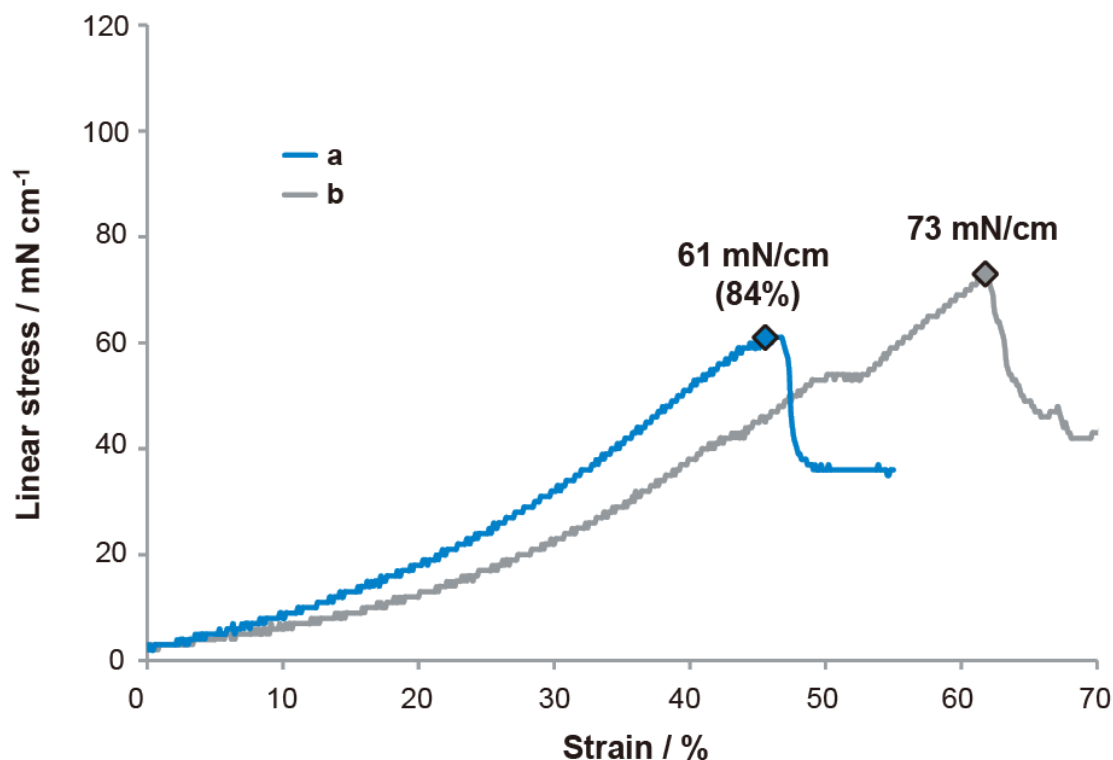


Figure 2-24. Self-healing property. Stress-strain curve of pAA-6 β CD/pAA-Fc hydrogel (3 wt%) after standing for 24 h (a) compared with the sample without crack (b). Peaks indicate the breaking points, and the stress values at that point were regarded as breaking stress.

2-7. Controlling self-healing ability by redox reaction

Finally, the self-repairing property of the pAA-6 β CD/pAA-Fc hydrogel was controlled by redox stimuli. A pAA-6 β CD/pAA-Fc hydrogel (2 wt%) was cut in half, and the cut surfaces were coated with an aqueous solution of NaClO (7 mM, 20 μL). Then the two pieces were reattached according to the experimental operation shown in Fig. 2-25. After 24 hours, healing was not observed. The NaClO applied gels did not form an inclusion complex between the β -CD and Fc^+ units. However, the surface re-adhered after spreading GSH aq. (20 mM, 20 μL), a reducing agent, onto the oxidized cut surface and allowing the gel to stand for 24 hours.

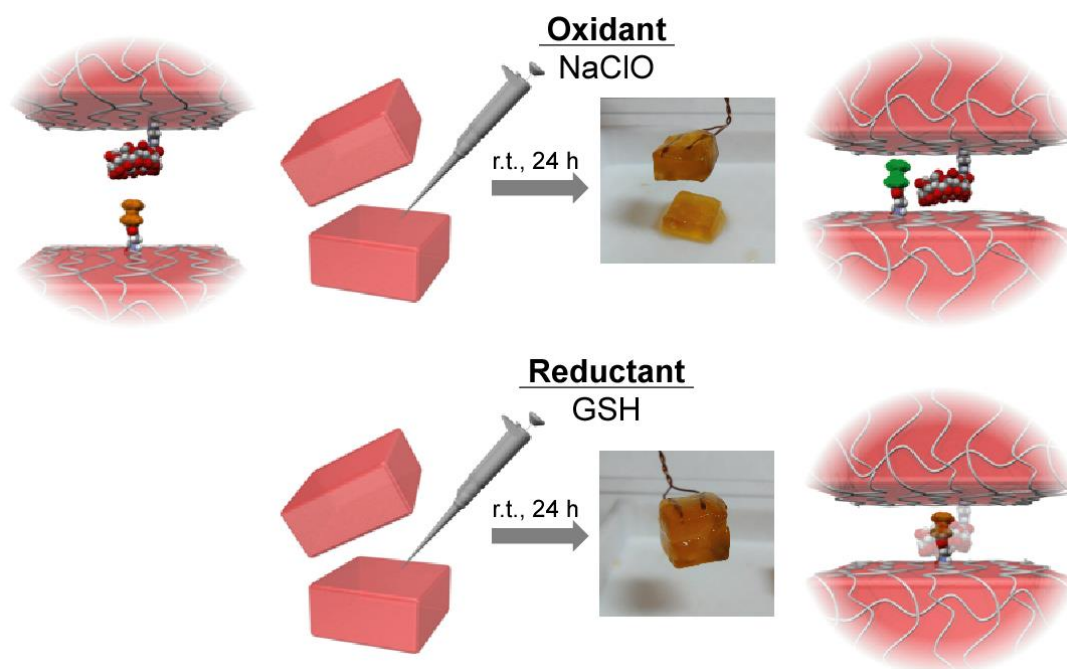


Figure 2-25. Self-healing experiments using redox reactions. Redox-responsive healing experiment of the pAA-6βCD/pAA-Fc hydrogel using oxidizing/reducing agents. A pAA-6βCD/pAA-Fc hydrogel (2 wt%) was cut in half, and NaClO aq. was spread on the cut surface. After 24 hours, healing was not observed. Re-adhesion was observed 24 h after spreading GSH aq. onto the oxidized cut surface.

Conclusion

In summary, a reversible sol–gel switching and self-healing supramolecular hydrogel system consisting of pAA-6 β CD/pAA-Fc is successfully realized. Although microscale switching of supramolecular complexes by redox is well known, a macroscale morphological change is difficult to achieve. This work demonstrates that intelligent supramolecular hydrogels may be formed using a main chain with a sufficient length and an adequate number of guest molecules to generate reversible multipoint crosslinks between pAA-6 β CD/pAA-Fc. A redox reaction alters the morphology of a supramolecular hydrogel by controlling the formation of an inclusion complex. These stimulus-responsive self-healing properties are similar to the selective cell-adhesive protein observed on a cellular surface. Stimulus-responsive self-healing properties have many general applications. Thus, it can be said that these stimulus-responsive and healing properties may eventually be used in stimulus-responsive drug-delivery carriers and peripheral vascular embolization materials with healing properties that target cancer cells and myoma.

References

1. Dry, C. M., *MRS Online Proceedings Library* **1992**, 276, null-null.
2. White, S. R.; Sottos, N. R.; Geubelle, P. H.; Moore, J. S.; Kessler, M. R.; Sriram, S. R.; Brown, E. N.; Viswanathan, S., *Nature* **2001**, 409 (6822), 794-797.
3. Chen, X.; Dam, M. A.; Ono, K.; Mal, A.; Shen, H.; Nutt, S. R.; Sheran, K.; Wudl, F., *Science* **2002**, 295 (5560), 1698-1702.
4. Toohey, K. S.; Sottos, N. R.; Lewis, J. A.; Moore, J. S.; White, S. R., *Nat. Mater.* **2007**, 6 (8), 581-585.
5. Cordier, P.; Tournilhac, F.; Soulie-Ziakovic, C.; Leibler, L., *Nature* **2008**, 451 (7181), 977-980.
6. Bergman, S. D.; Wudl, F., *J. Mater. Chem.* **2008**, 18 (1), 41-62.
7. Wool, R. P., *Soft Matter* **2008**, 4 (3), 400-418.
8. Wang, Q.; Mynar, J. L.; Yoshida, M.; Lee, E.; Lee, M.; Okuro, K.; Kinbara, K.; Aida, T., *Nature* **2010**, 463 (7279), 339-343.
9. Burnworth, M.; Tang, L.; Kumpfer, J. R.; Duncan, A. J.; Beyer, F. L.; Fiore, G. L.; Rowan, S. J.; Weder, C., *Nature* **2011**, 472 (7343), 334-337.
10. Lyshevski, S. E., *Nano- and micro-electromechanical systems : fundamentals of nano- and microengineering*. 2nd ed.; CRC Press: Boca Raton, Fla., 2005.
11. Ozin, G. A.; Manners, I.; Fournier-Bidoz, S.; Arsenaault, A., *Adv. Mater.* **2005**, 17 (24), 3011-3018.
12. Liu, C., *Foundations of MEMS*. Pearson/Prentice Hall: Upper Saddle River, NJ, 2006.
13. Huang, T. J.; Brough, B.; Ho, C.-M.; Liu, Y.; Flood, A. H.; Bonvallet, P. A.; Tseng, H.-R.; Stoddart, J. F.; Baller, M.; Magonov, S., *Appl. Phys. Lett.* **2004**, 85 (22), 5391-5393.
14. Anquetil, P. A.; Yu, H.-h.; Madden, J. D.; Swager, T. M.; Hunter, I. W. In *Recent advances in thiophene-based molecular actuators*, 2003; pp 42-53.
15. Collin, J.-P.; Dietrich-Buchecker, C.; Gaviña, P.; Jimenez-Molero, M. C.; Sauvage, J.-P., *Acc. Chem. Res.* **2001**, 34 (6), 477-487.
16. Juluri, B. K.; Kumar, A. S.; Liu, Y.; Ye, T.; Yang, Y.-W.; Flood, A. H.; Fang, L.; Stoddart, J. F.; Weiss, P. S.; Huang, T. J., *ACS Nano* **2009**, 3 (2), 291-300.
17. Eddington, D. T.; Beebe, D. J., *Adv. Drug Del. Rev.* **2004**, 56 (2), 199-210.
18. Itoga, K.; Yamato, M.; Kobayashi, J.; Kikuchi, A.; Okano, T., *Biomaterials* **2004**, 25 (11), 2047-2053.
19. Piepenbrock, M.-O. M.; Lloyd, G. O.; Clarke, N.; Steed, J. W., *Chem. Rev.* **2009**, 110 (4), 1960-2004.
20. Jeong, B.; Kim, S. W.; Bae, Y. H., *Adv. Drug Del. Rev.* **2002**, 54 (1), 37-51.
21. Yoshida, R., *Adv. Mater.* **2010**, 22 (31), 3463-3483.
22. Murata, K.; Aoki, M.; Suzuki, T.; Harada, T.; Kawabata, H.; Komori, T.; Ohseto, F.; Ueda, K.; Shinkai, S., *J. Am. Chem. Soc.* **1994**, 116 (15), 6664-6676.
23. Jung, J. H.; Ono, Y.; Shinkai, S., *Angew. Chem. Int. Ed.* **2000**, 39 (10), 1862-1865.
24. Lee, C. T.; Smith, K. A.; Hatton, T. A., *Macromolecules* **2004**, 37 (14), 5397-5405.
25. Tomatsu, I.; Hashidzume, A.; Harada, A., *J. Am. Chem. Soc.* **2006**, 128 (7), 2226-2227.
26. Ahmed, S. A.; Sallenave, X.; Fages, F.; Mieden-Gundert, G.; Müller, W. M.; Müller, U.; Vögtle, F.; Pozzo, J.-L., *Langmuir* **2002**, 18 (19), 7096-7101.
27. Kawano, S.-i.; Fujita, N.; Shinkai, S., *J. Am. Chem. Soc.* **2004**, 126 (28), 8592-8593.

28. Tsuchiya, K.; Orihara, Y.; Kondo, Y.; Yoshino, N.; Ohkubo, T.; Sakai, H.; Abe, M., *J. Am. Chem. Soc.* **2004**, *126* (39), 12282-12283.
29. Hempenius, M. A.; Cirmi, C.; Song, J.; Vancso, G. J., *Macromolecules* **2009**, *42* (7), 2324-2326.
30. Zuo, F.; Luo, C.; Ding, X.; Zheng, Z.; Cheng, X.; Peng, Y., *Supramol. Chem.* **2008**, *20* (6), 559-564.
31. Ritter, H.; Mondrzik, B. E.; Rehahn, M.; Gallei, M., *Beilstein J. Org. Chem.* **2010**, *6*, 60.
32. Tomatsu, I.; Hashidzume, A.; Harada, A., *Macromol. Rapid Commun.* **2006**, *27* (4), 238-241.
33. Tamesue, S.; Takashima, Y.; Yamaguchi, H.; Shinkai, S.; Harada, A., *Angew. Chem. Int. Ed.* **2010**, *49* (41), 7461-7464.
34. Deng, W.; Yamaguchi, H.; Takashima, Y.; Harada, A., *Angew. Chem. Int. Ed.* **2007**, *46* (27), 5144-5147.
35. Ogoshi, T.; Takashima, Y.; Yamaguchi, H.; Harada, A., *J. Am. Chem. Soc.* **2007**, *129* (16), 4878-4879.
36. Guo, X.; Abdala, A. A.; May, B. L.; Lincoln, S. F.; Khan, S. A.; Prud'homme, R. K., *Macromolecules* **2005**, *38* (7), 3037-3040.
37. Harada, A.; Takahashi, S., *J. Incl. Phenom.* **1984**, *2* (3-4), 791-798.
38. Wu, J.-S.; Toda, K.; Tanaka, A.; Sanemasa, I., *Bull. Chem. Soc. Jpn.* **1998**, *71* (7), 1615-1618.
39. Rekharsky, M. V.; Inoue, Y., *Chem. Rev.* **1998**, *98* (5), 1875-1918.
40. Moozyckine, A. U.; Bookham, J. L.; Deary, M. E.; Davies, D. M., *J. Chem. Soc., Perkin Trans. 2* **2001**, (9), 1858-1862.

Redox-Generated Mechanical Motion of Supramolecular Polymeric Actuator Based on Host-Guest Interactions

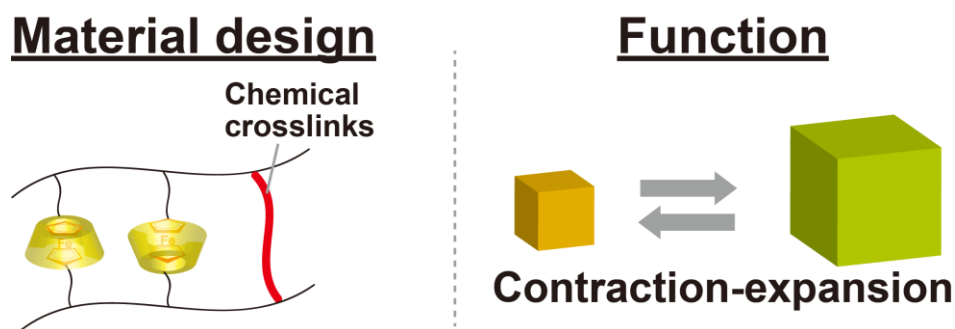


Figure 3-0. Conceptual illustration of chapter 3.

3-1. Introduction

The expansion and contraction of natural muscles have inspired the design and construction of actuators capable of responding to external stimuli with controllable dimensions and shapes¹⁻³. The development of actuators based on materials that reversibly change their shape in response to external stimuli should help improve people's quality of lives in such areas as medical treatment and micromachine application. Recently, stimuli-responsive materials have been reported to create artificial muscles and actuators⁴⁻⁷. Stimuli-responsive materials using polymeric actuators⁸⁻¹³, crystal¹⁴⁻¹⁶, and liquid crystal¹⁷⁻²⁷ systems have been achieved shape deformations in response to external stimuli, such as temperature^{28,29}, chemicals³⁰, pH^{31,32}, ionic strength^{33,34}, electric field/voltage/current^{8,35-38}, light intensity^{39,40}, and so on. However, reports using redox responsive materials are relatively scarce⁴¹⁻⁴⁴. Furthermore, supramolecular polymeric actuators with combination of redox responsiveness and host-guest interactions are extremely-limited.

In chapter 2, a supramolecular hydrogels possessing host and guest polymers with a self-healing property was reported⁴⁵. A supramolecular hydrogel consisting of a β -cyclodextrin (β CD) polymer and ferrocene (Fc) polymer crosslinked by host-guest interactions exhibits redox responsive properties. The formation of inclusion complexes serving as crosslink points for the polymers yield self-healable hydrogels. In contrast, the dissociation of inclusion complexes results in transformation into a sol. It was hypothesized that partial chemical bonds prevent a gel from changing to a sol, because the chemical bonds keep a gel structure. Changing crosslink densities (effective network chains) affect to the expansion-contraction ability of hydrogels. Accordingly, the reversible complex formation by external stimuli may induce an expansion-contraction. Although some previous papers have altered the expansion-contraction properties via ionic strengths, adjusting the crosslink density via a redox-responsive host-guest complex has yet to be reported. Especially, there is no report of evaluating mechanical work of host-guest supramolecular polymeric actuators via external stimuli.

Herein, a redox-driven supramolecular hydrogel actuator through a host-guest interaction is described. The hydrogel actuator consists of a poly(acrylamide) (pAAm) network crosslinked by *N,N'*-methylenebis(acrylamide) (MBAAm) and a complex of β CD-Fc, a redox-responsive host-guest pair. The actuator shows an expansion-contraction in response to oxidation and reduction of the Fc moieties. The mechanical work stored in the actuator is evaluated.

3-2. Experimental section

Materials.

Acrylamide (AAM), 2,2'-azobis[2-(2-imidazolin-2-yl)-propane] dihydrochloride (VA-044), CDCl_3 , and D_2O were purchased from Wako Pure Chemical Industries, Ltd. α -Cyclodextrin, β -cyclodextrin, and γ -cyclodextrin (αCD , βCD , and γCD , respectively) were obtained from Junsei Chemical Co., Ltd. Triethylamine (Et_3N), ethylenediamine, potassium hydroxide, sodium hydroxide, tris(hydroxymethyl)aminomethane, hydrochloric acid, and *N,N'*-methylenebis(acrylamide) (MBAAM) were obtained from Nacalai Tesque Inc. Ferrocenecarboxylic acid (FcCOOH), oxalyl chloride, acryloyl chloride, and ceric ammonium nitrate (CAN) were purchased from Tokyo Chemical Industry Co., Ltd. Tetrahydrofuran (THF) was obtained from Kanto Chemical Co., Inc. Glutathione (GSH) was obtained from Kohjin Co., Ltd. $\text{DMSO-}d_6$ was obtained from Merck & Co., Inc. A highly porous synthetic resin (DIAION HP-20) used for column chromatography was purchased from Mitsubishi Chemical Co., Ltd. Water used for the preparation of the aqueous solutions was purified with a Millipore Elix 5 system. Other reagents were used without further purification. $\text{Fc-CONH-(CH}_2)_2\text{-NH}_2$ was prepared according to our previous report⁴⁵.

Measurements.

The ^1H NMR spectra were recorded at 500 MHz with a JEOL JNM-ECA 500 NMR spectrometer. The 2D ROESY NMR spectra were recorded at 600 MHz with a VARIAN INOVA 600 NMR spectrometer. The solid-state ^1H Field Gradient Magic Angle Spinning (FGMAS) NMR spectra were recorded at 400 MHz with a JEOL JNM-ECA 400 NMR spectrometer. Sample spinning rate was 8 kHz. In all NMR measurements, chemical shifts were referenced to the solvent values ($\delta = 2.49$ ppm and 4.79 ppm for $\text{DMSO-}d_6$ and D_2O , respectively). The IR spectra were measured using a JASCO FT/IR-410 spectrometer. Positive-ion matrix-assisted laser desorption/ionization time-of-flight mass spectrometry (MALDI-TOF-MS) experiments were performed using a Bruker autoflex speed mass spectrometer using 2,5-dihydroxy-benzoic acid as a matrix. Mass number was calibrated by four peptides, i.e., angiotensin II ($[\text{M}+\text{H}]^+ 1046.5418$), angiotensin I ($[\text{M}+\text{H}]^+ 1296.6848$), substance P ($[\text{M}+\text{H}]^+ 1347.7354$), and bombesin ($[\text{M}+\text{H}]^+ 1619.8223$). Mechanical properties of the gels were measured by the mechanical tension testing system (Rheoner, RE-33005, Yamaden Ltd.). The size of gel was measured using a digital inverted microscope (EVOS AME i2111, Advanced Microscopy Group).

Preparation of gels.

Preparation of $\beta\text{CD-Fc}$ gel (x,y,z).

Typical procedure for $\beta\text{CD-Fc}$ gel (3,3,1). $\beta\text{CD-AAM}$ (36 mg, 0.030 mmol) and Fc-AAM (9.8 mg, 0.030 mmol) were mixed in a mixed solvent of water/DMSO (95/5, v/v) (1 mL) and stirred at 70 °C overnight to give a transparent solution. MBAAM (1.5 mg, 0.010 mmol), AAM (66.1 mg, 0.93 mmol), and VA-044 (3.2 mg, 0.01 mmol) were added and dissolved. The solution was purged with argon gas for 1 h and was then heated at 50 °C overnight to form a gel. The gel was washed repeatedly with water.

Preparation of βCD gel (x,z).

Typical procedure for βCD gel (3,1). $\beta\text{CD-AAM}$ (36 mg, 0.030 mmol), MBAAM (1.5 mg, 0.010 mmol), AAM (68.2 mg, 0.96 mmol), and VA-044 (3.2 mg, 0.01 mmol) were dissolved in a mixed solvent of water/DMSO (95/5,

v/v) (1 mL). The solution was purged with argon gas for 1 h and was then heated at 50 °C overnight to form a gel. The gel was washed repeatedly with water.

Preparation of Fc gel (y,z).

Typical procedure for Fc gel (3,1). β CD (34 mg, 0.030 mmol) and Fc-AAm (9.8 mg, 0.030 mmol) were mixed in a mixed solvent of water/DMSO (95/5, v/v) (1 mL) and stirred at 70 °C overnight to give a transparent solution. MBAAm (1.5 mg, 0.010 mmol), AAm (66.1 mg, 0.93 mmol), and VA-044 (3.2 mg, 0.01 mmol) were added and dissolved. The solution was purged with argon gas for 1 h and was then heated at 50 °C overnight to form a gel. The gel was washed repeatedly with DMSO and water to remove β CD.

Preparation of polyacrylamide (pAAm) gel (z).

Typical procedure for pAAm gel (1). MBAAm (1.5 mg, 0.010 mmol), AAm (68.2 mg, 0.96 mmol), and VA-044 (3.2 mg, 0.01 mmol) were dissolved in a mixed solvent of water/DMSO (95/5, v/v) (1 mL). The solution was purged with argon gas for 1 h and was then heated at 50 °C overnight to form a gel. The gel was washed repeatedly with water.

3-3. Preparation and characterization of CD-Guest gels

Prior to preparing the host–guest gel (β CD–Fc gel), the Fc guest monomer (Fc-AAm) was dissolved by the β CD host monomer (β CD-AAm) in a mixed solvent of water and dimethyl sulfoxide (DMSO) (95/5, v/v) to form an inclusion complex. 2D NMR techniques demonstrated the association behavior between β CD-AAm and Fc-AAm as a model system. Figure 3-1 shows the 2D ROESY NMR spectrum of β CD-AAm/Fc-AAm in $D_2O/DMSO-d_6$ (95/5, v/v).

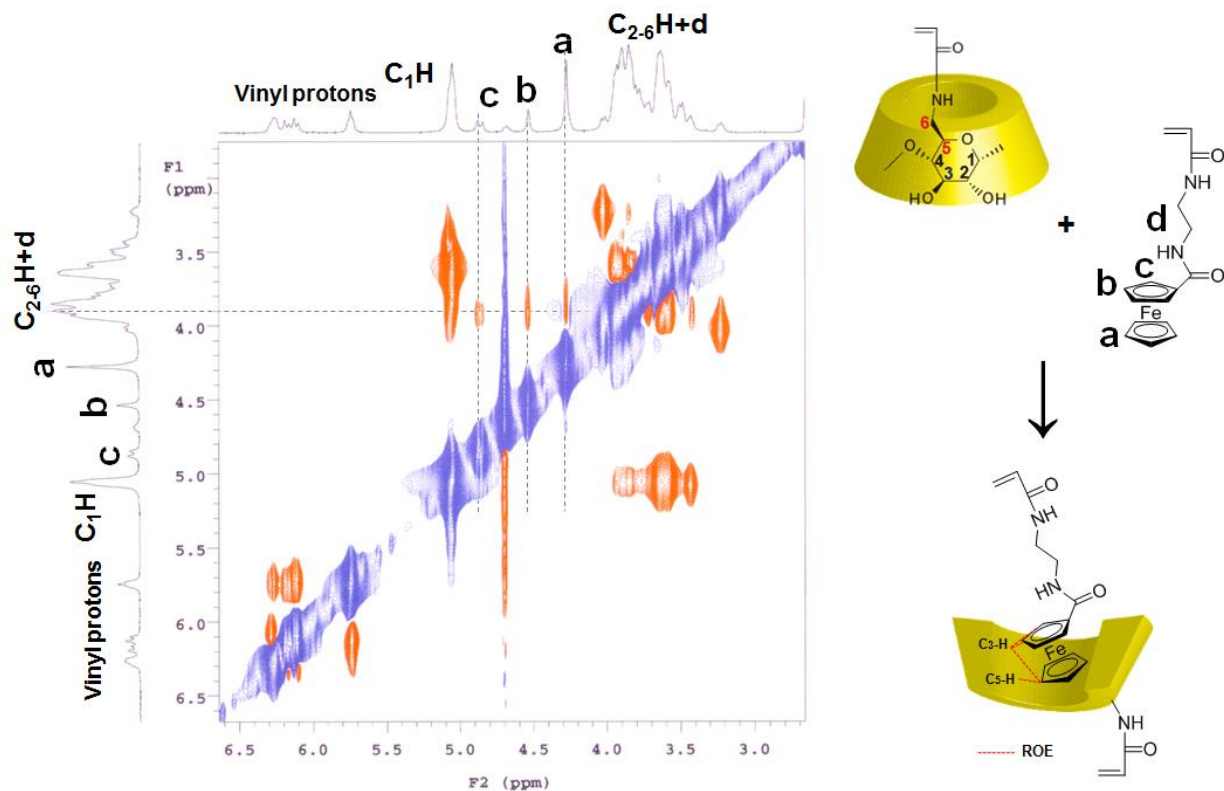


Figure 3-1. 2D ROESY NMR spectrum and proposed structure of the inclusion complex for a mixture of β CD-AAm (1 mM) and Fc-AAm (1 mM) ($D_2O/DMSO-d_6$ (95/5, v/v), 600 MHz, 30 °C).

The protons of the inner cavity of β CD were correlated to the Fc protons, indicating complexation between the β CD and Fc moieties.

Figure 3-2 shows a typical example of the ^1H NMR spectra for Fc-AAm in the presence of varying concentrations of β CD-AAm (C_{CD}). As C_{CD} is increased, the peak which is attributed to the **a** protons of the Fc group clearly shifted to a lower field, indicating the interaction of β CD with the Fc group. The peak shift ($\Delta\delta$) are plotted against C_{CD} . As can be seen in Figure 3-3, the curve using eq. (1) fitted the plots, indicating that the interaction of β CD with the Fc group can be analyzed based on the formation of one-to-one complexes. The apparent K value was determined to be $(9.3 \pm 0.5) \times 10^2 \text{ M}^{-1}$.

$$\Delta\delta = \frac{\Delta\delta}{2K[Fc]_0} [1 + K[CD]_0 + K[Fc]_0 - \{(1 + K[CD]_0 + K[Fc]_0)^2 - 4K^2[CD]_0[Fc]_0\}^{\frac{1}{2}}] \quad (1)$$

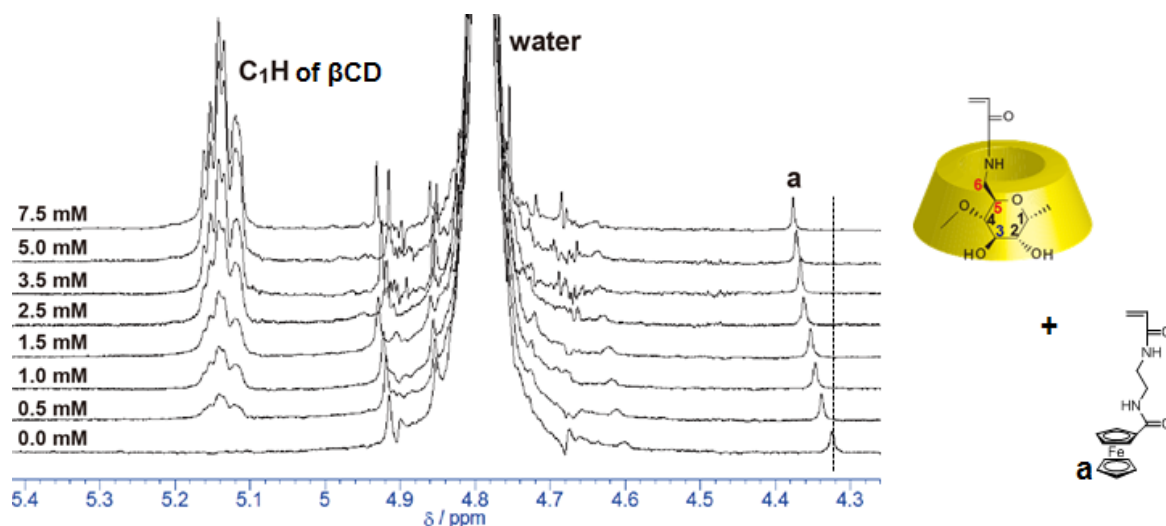


Figure 3-2. Partial ^1H NMR spectra of Fc-AAm (0.2 mM) in the presence of varying concentrations ($C_{\text{CD}} = 0, 0.5, 1.0, 1.5, 2.5, 3.5, 5.0,$ and 7.5 mM) of β CD-AAm. ($\text{D}_2\text{O}/\text{DMSO-}d_6$ (95/5, v/v), 500 MHz, 30°C).

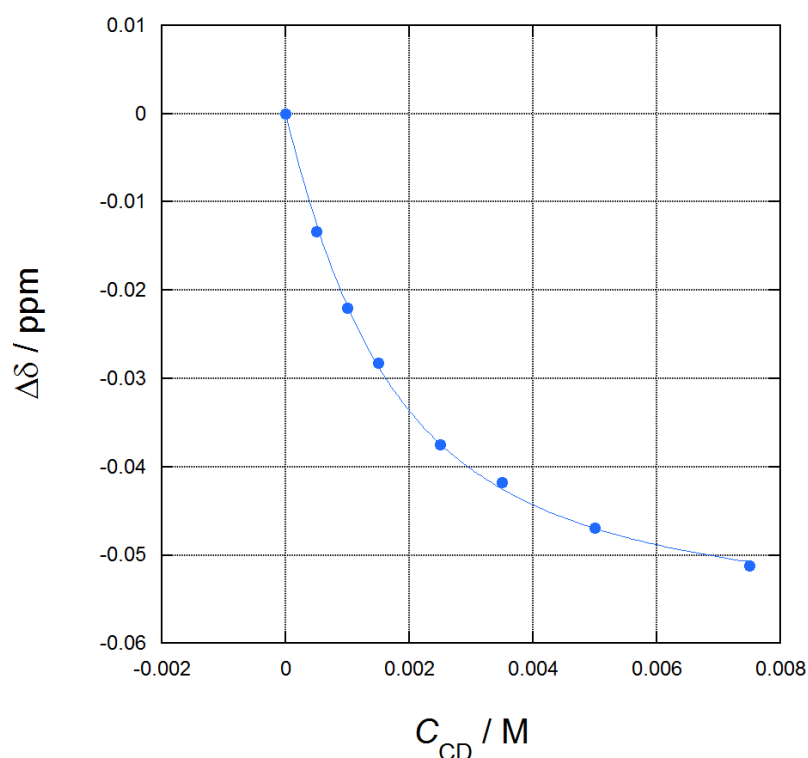
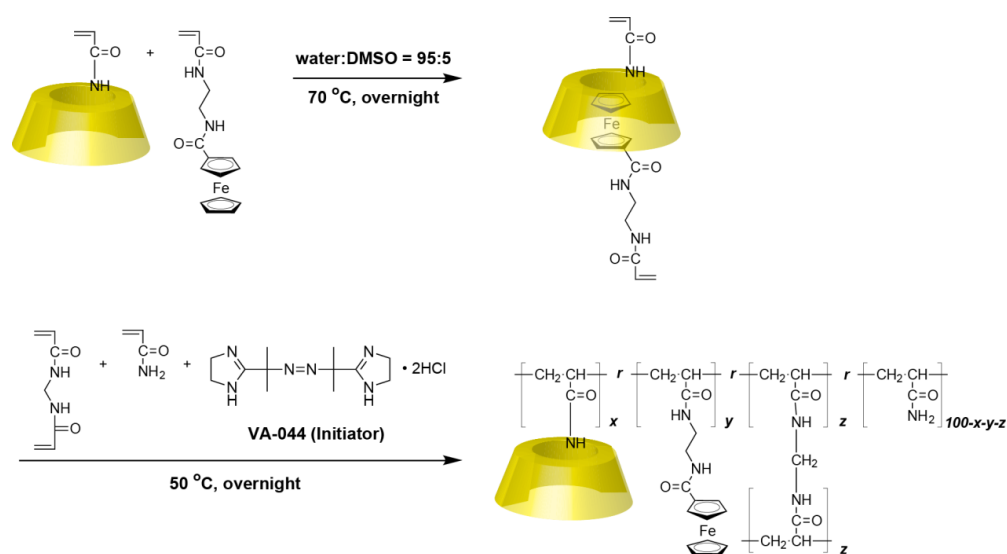


Figure 3-3. The peak shift ($\Delta\delta$) for the signal due to the **a** protons of the Fc group as a function of C_{CD} . The best fitted curve using eq. (1) is also drawn.

This value indicated that about 72, 79, and 83% of both monomers formed inclusion complexes before polymerization in cases of β CD–Fc gels(1,1, z), (2,2, z), and (3,3, z), respectively (See also Figure 1).

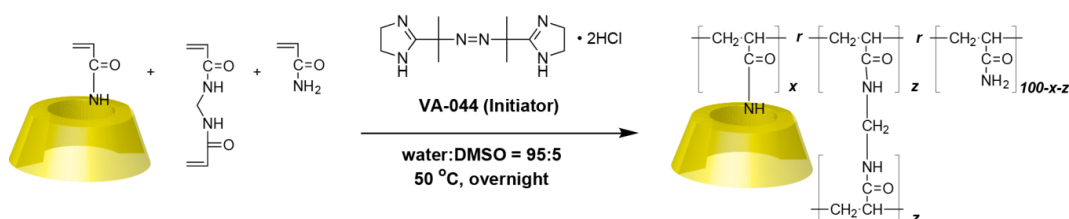
The β CD–Fc gel was prepared by homogeneous radical copolymerization of the inclusion complex with acrylamide (AAm) and MBAAm using 2,2'-azobis[2-(2-imidazolin-2-yl)-propane] dihydrochloride (VA-044) as a water-soluble radical initiator (See Scheme 3-1)⁴⁶.

Scheme 3-1. Preparation of β CD–Fc gel (x,y,z).

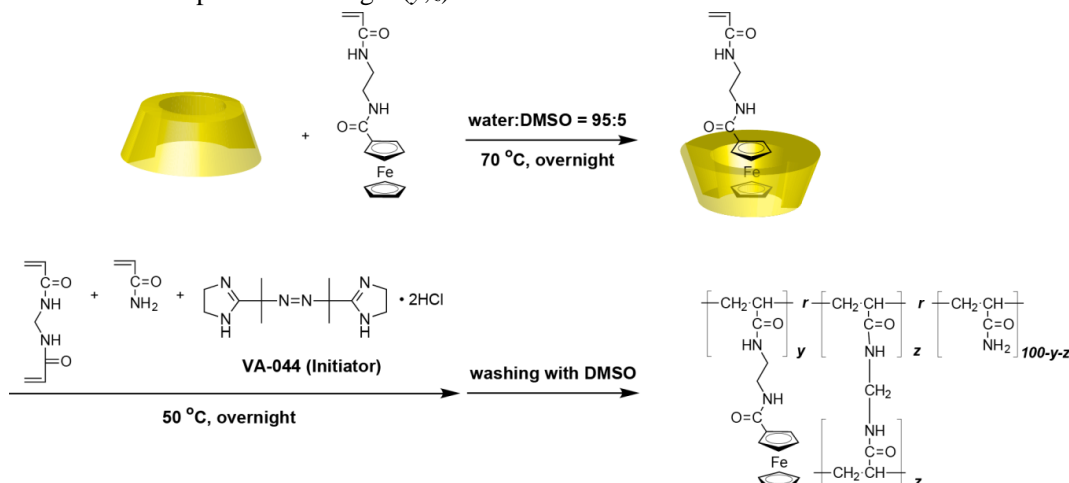


As reference gels, a host gel (β CD gel), a guest gel (Fc gel), and a blank gel (pAAm gel) were prepared via the similar methods as described above (See Schemes 3-2, 3-3, and 3-4).

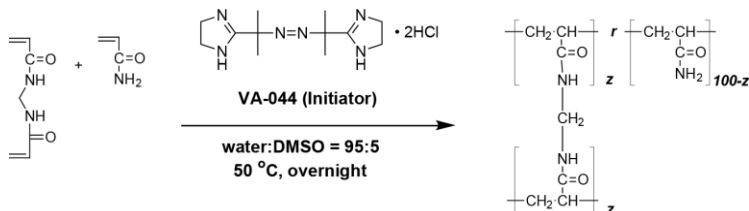
Scheme 3-2. Preparation of β CD gel (x,z).



Scheme 3-3. Preparation of Fc gel (y,z).



Scheme 3-4. Preparation of pAAm gel (z).



These hydrogels were purified by washing with DMSO and water to remove the unreacted compounds. Figure 4 depicts the chemical structures of the β CD–Fc gel (x,y,z), β CD gel (x,z), Fc gel (y,z), and pAAm gel (z).

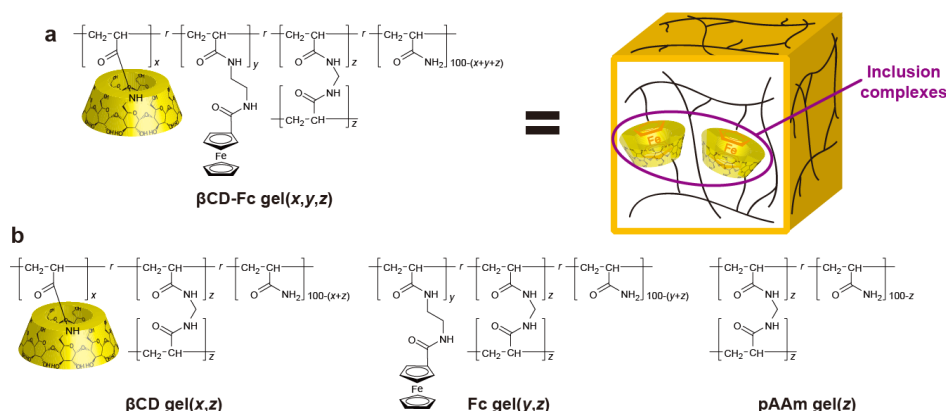


Figure 3-4. a: Chemical structure and schematic illustration of β CD–Fc gel (x,y,z). **b:** Chemical structures of reference gels, β CD gel (x,z) (without the Fc unit), Fc gel (y,z) (without the β CD unit), and pAAm gel (z) (without β CD and Fc units).

Here x , y , and z represent the mol% of β CD-AAm, Fc-AAm, and MBAAm units. The ^1H solid state field gradient magic angle spinning (FGMAS) NMR and FT-IR spectroscopies characterized the chemical structures and content of each monomeric unit of the β CD-Fc gels, β CD gel(3,1), Fc gel(3,1), and pAAm gel(1) (Figures 3-5 and 3-6).

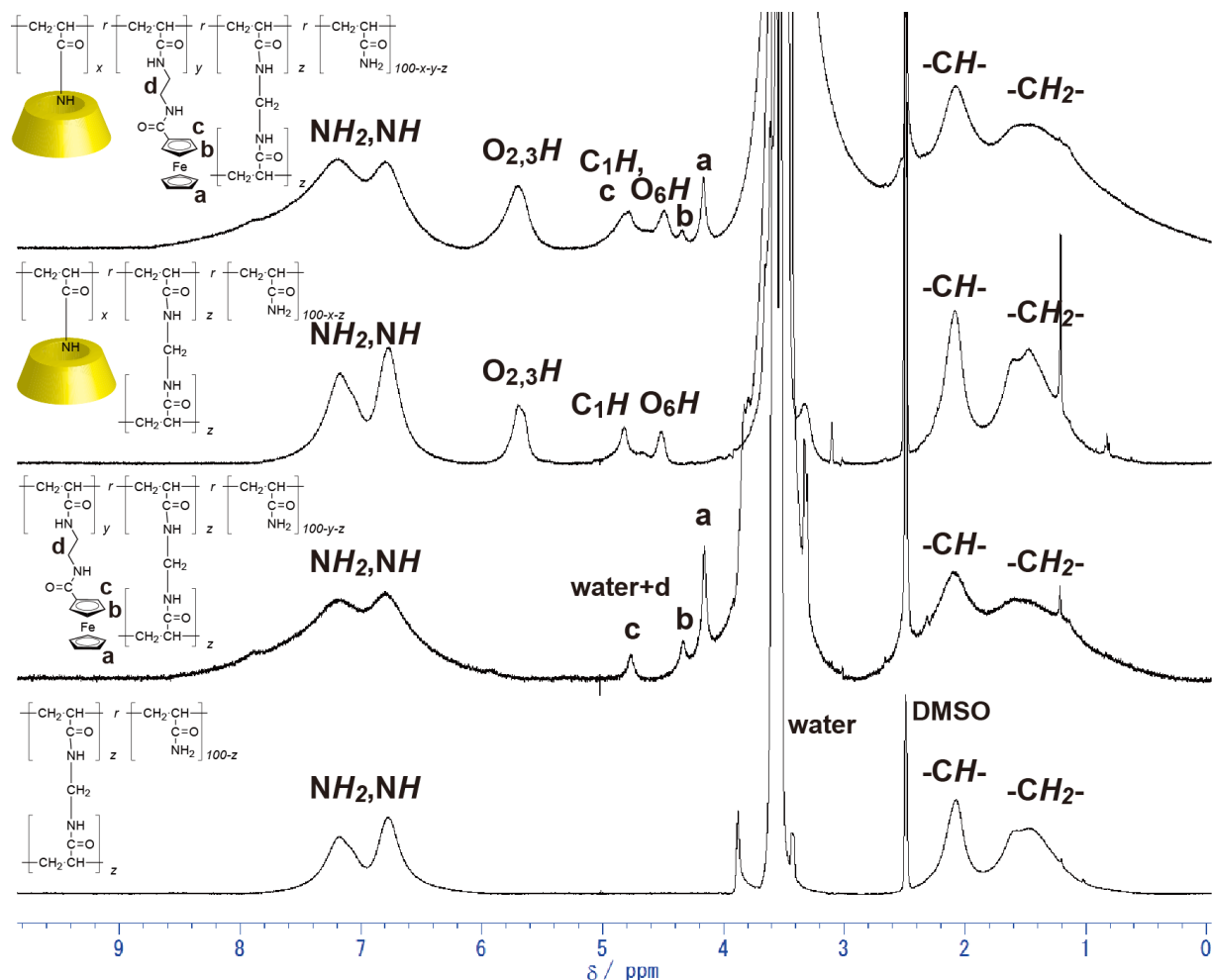


Figure 3-5. Solid-state ^1H FGMAS NMR spectra of β CD-Fc gel (3,3,1), β CD gel (3,1), Fc gel (3,1), and pAAm gel (1), respectively. (Immersed in $\text{DMSO-}d_6$, 400 MHz, 30 $^{\circ}\text{C}$, rotation frequency = 8 kHz)

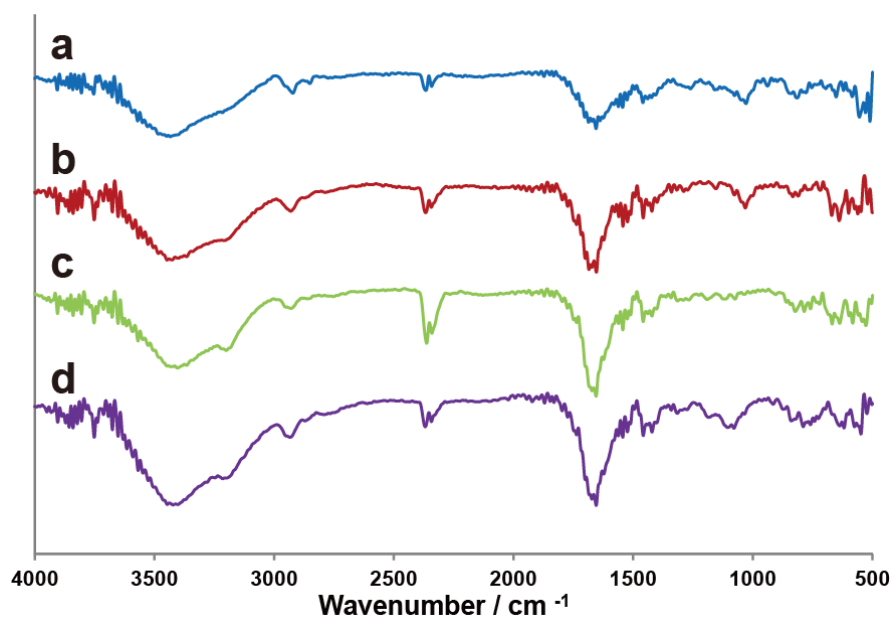


Figure 3-6. FT-IR spectra of (a) β CD-Fc gel (3,3,1), (b) β CD gel (3,1), (c) Fc gel (3,1), and (d) pAAm gel (1), respectively. (KBr disc, r.t.)

β CD-Fc gel(3,3,1): 3435, 3159 cm^{-1} (O-H stretching vibration, N-H asymmetric stretching vibration, and N-H symmetric stretching vibration), 2922 cm^{-1} (methylene C-H stretching vibration) 1655 cm^{-1} (C=O stretching vibration, N-H bending vibration).

β CD gel(3,1): 3427, 3190 cm^{-1} (O-H stretching vibration, N-H asymmetric stretching vibration, and N-H symmetric stretching vibration), 2931 cm^{-1} (methylene C-H stretching vibration) 1653 cm^{-1} (C=O stretching vibration, N-H bending vibration).

Fc gel(3,1): 3404, 3199 cm^{-1} (N-H asymmetric stretching vibration, and N-H symmetric stretching vibration), 2929 cm^{-1} (methylene C-H stretching vibration) 1655 cm^{-1} (C=O stretching vibration, N-H bending vibration).

pAAm gel(1): 3402, 3159 cm^{-1} (N-H asymmetric stretching vibration, and N-H symmetric stretching vibration), 2922 cm^{-1} (methylene C-H stretching vibration) 1655 cm^{-1} (C=O stretching vibration, N-H bending vibration).

3-4. Stress-strain measurements.

A tensile test analyzed the influence of the host–guest interaction on the mechanical property of the hydrogels. A rectangular gel sample was tore using a mechanical tension testing system, and the rupture strengths of the gels were determined from the obtained stress–strain curves. Figure 3-7 shows the stress–strain curves of β CD–Fc gel (3,3,1), β CD gel (3,1), Fc gel (3,1), and pAAm gel (1), respectively. The β CD–Fc gel (3,3,1) exhibited the highest rupture stress and rupture strain. These results indicate that the non-covalent crosslink density of the β CD–Fc gels improves the mechanical strength and stretching property.

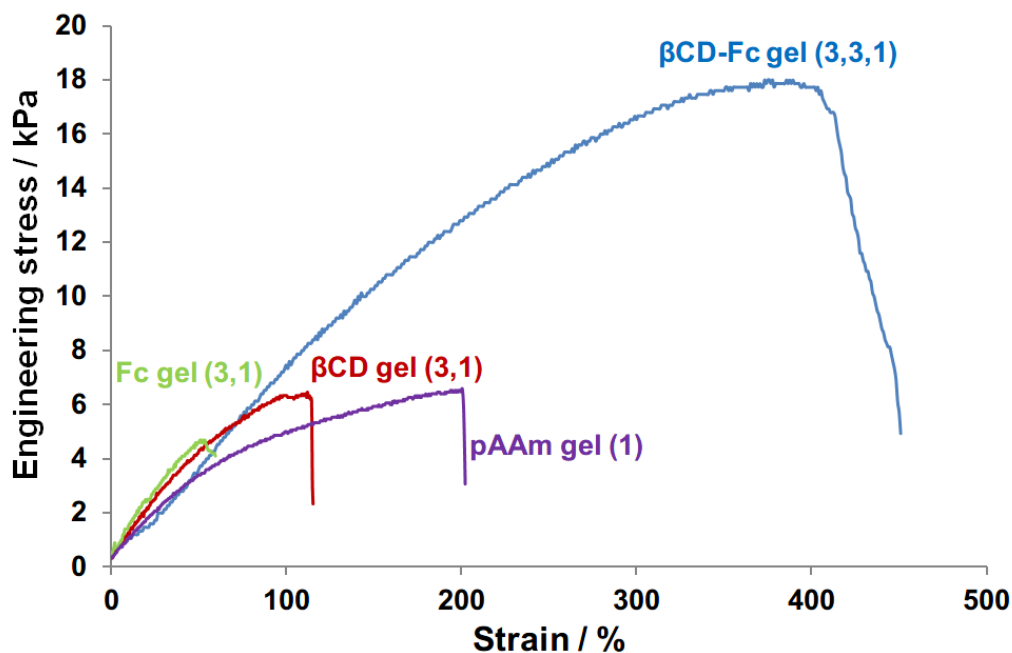


Figure 3-7. Stress-strain curves of β CD–Fc gel(3,3,1) (blue), β CD gel(3,1) (red), Fc gel(3,1) (green), and pAAm gel(1) (purple), respectively. From the maxima, the stresses at rupture were determined.

3-5. Confirmation of the formation of inclusion complex inside the gel

First, the formation of supramolecular complexes between the β CD and Fc units inside the hydrogel and the influence of competitive molecules on the size of the gel were investigated. The cube-shaped β CD–Fc gels (size: $1\times1\times1\text{ mm}^3$) were immersed in 3 mL of 0.1 M Tris/HCl buffer solutions (pH 7) of competitive molecules for two hours. Adamantane carboxylic acid sodium salt (AdCANa) and cyclodextrins (α CD, β CD, and γ CD) are selected as competitive guest and competitive host molecules, respectively. A digital inverted microscope measured the size changes of gels⁴⁷. The ratio of the lengths (r) was determined as $r = L_f / L_i \times 100\%$ (L_f : length of the hydrogel after equilibrium swelling, L_i : length of gel before). Figures 2a and 2b show photographs of the β CD–Fc gel(3,3,1) before and after immersion in 10 mM aqueous solutions of AdCANa and β CD. The size of β CD–Fc gel(3,3,1) increased after immersion into an aqueous solution of competitive molecules. Immersing the β CD–Fc gel(3,3,1) in 10 mM AdCANa aq. increased the r to $121 \pm 1\%$ of the original length (Fig. 2c). When β CD–Fc gel(3,3,1) was immersed in 10 mM aqueous solutions of CDs (α CD, β CD, and γ CD), the r increased to $101 \pm 1\%$, $106 \pm 1\%$, and $102 \pm 0.3\%$, respectively (Fig. 2c). The r when immersed in β CD aq. was larger than those of α CD and γ CD. Previous studies have suggested that the association constant of Fc for β CD

was larger than those for α CD and γ CD ($\text{Fc}/\alpha\text{CD}$; $K = 0.14 \times 10^3 \text{ M}^{-1}$, $\text{Fc}/\beta\text{CD}$; $K = 17 \times 10^3 \text{ M}^{-1}$, $\text{Fc}/\gamma\text{CD}$; $K = 0.90 \times 10^3 \text{ M}^{-1}$)⁴⁸. The r was larger for the AdCANa case than that for β CD because the association constant (K) of the adamantane derivative for β CD ($K = 35 \times 10^3 \text{ M}^{-1}$)⁴⁹ was much larger than that for Fc. These results indicate that β CD–Fc gels shrink in water due to the formation of inclusion complexes between β CD and Fc units which function as crosslinker inside the hydrogel before immersing in aqueous solutions of competitive molecules. After immersing, the addition of competitive molecules decompose the inclusion complexes to swell β CD–Fc gels (Figure 3-8).

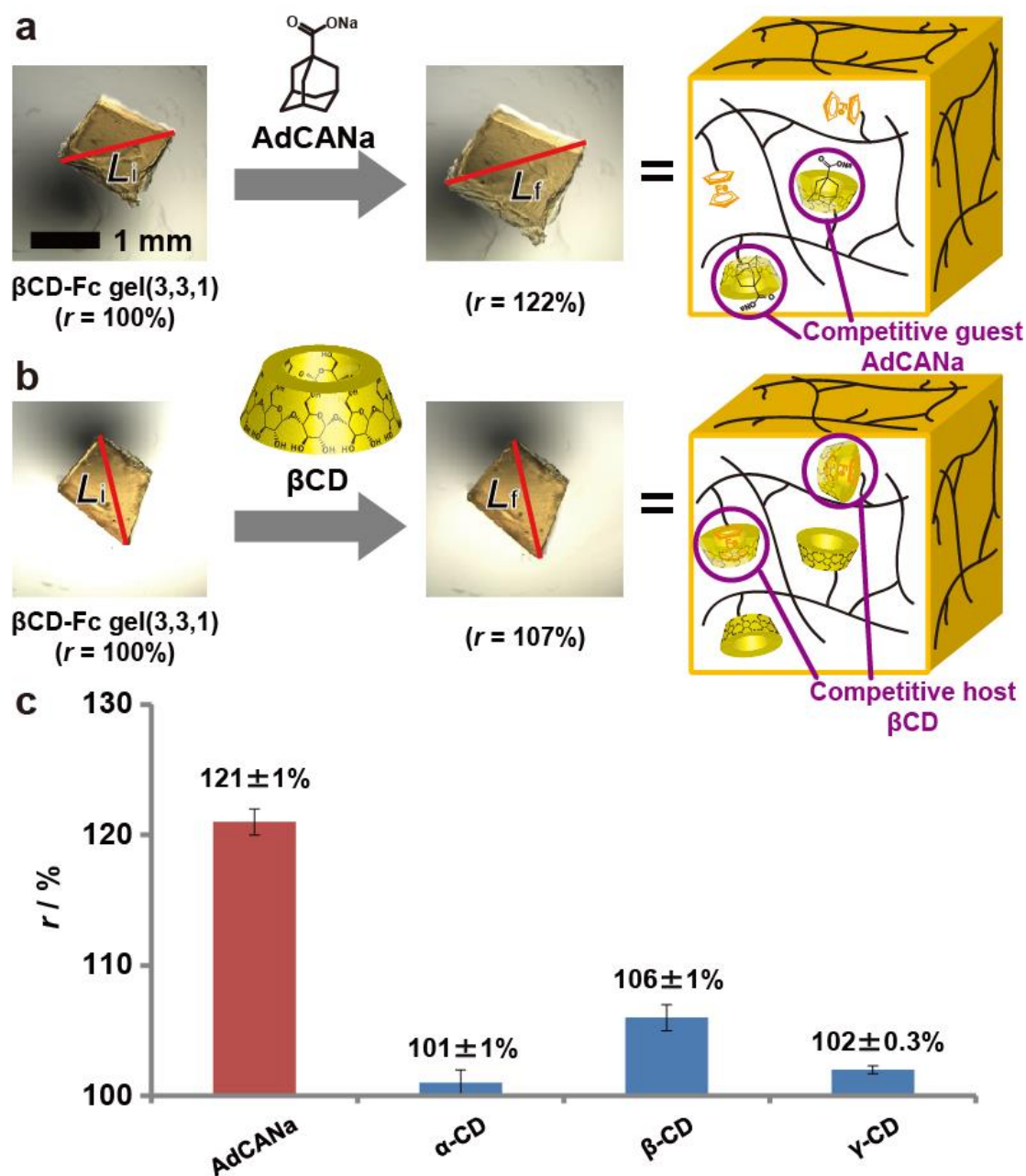


Figure 3-8. **a, b:** Photographs (left) and schematic illustration (right) of the length change of β CD–Fc gel(3,3,1) by the addition of (a) AdCANa and (b) β CD. Red lines indicate the lengths of gels. Scale bar indicates 1 mm. **c:** The r of the β CD–Fc gels immersed in solutions of competitive guest molecules (AdCANa) and competitive host molecules (α CD, β CD, and γ CD). More than three independent studies confirmed the size change of the β CD–Fc gels.

3-6. Redox-responsiveness of the gel

Next, the size of the β CD-Fc gels was regulated using redox reagents. Cube-shaped gels were immersed in a 0.1 M Tris/HCl buffer (pH 7) before the redox reactions. The Tris/HCl buffer suitably controlled the crosslink density of the β CD-Fc gels by eliminating the electric repulsion between the oxidized ferrocenium cation (Fc^+) units. Ceric ammonium nitrate (CAN) was chosen as an oxidant. The following immersion procedure was used. (1) The β CD-Fc gel immersed in the Tris/HCl buffer (0.1 M) was placed into the Tris/HCl buffer with CAN (50 mM). (2) After standing for an hour, the oxidized β CD-Fc gel was returned into the Tris/HCl buffer. Figure 3-9a shows photographs of β CD-Fc gel(3,3,1) before and after the oxidation.

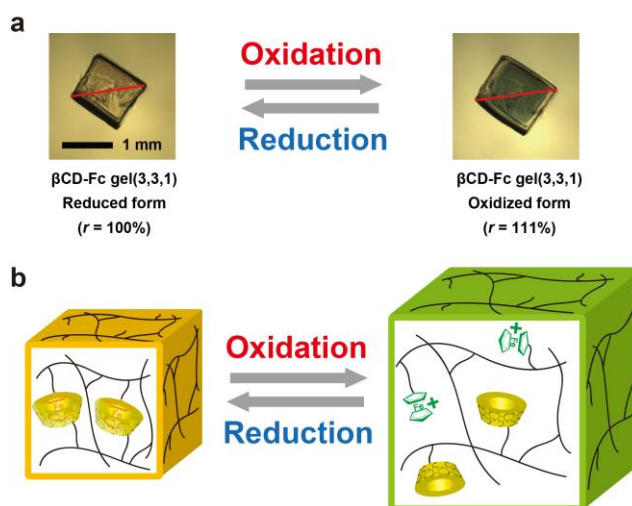


Figure 3-9. a: Photographs of the β CD-Fc gel(3,3,1) soon after immersed in the Tris/HCl buffer with CAN (50 mM) (left) and after one hour (right). Red lines indicate the lengths of gels. Scale bar indicates 1 mm. b: Schematic illustration of redox-responsive expansion-contraction of β CD-Fc gel.

The oxidized hydrogel changed from orange to green, which is a characteristic color of Fc^+ .

The redox reaction of the ferrocene moiety was traced by UV-Vis spectroscopy (Figure3-10).

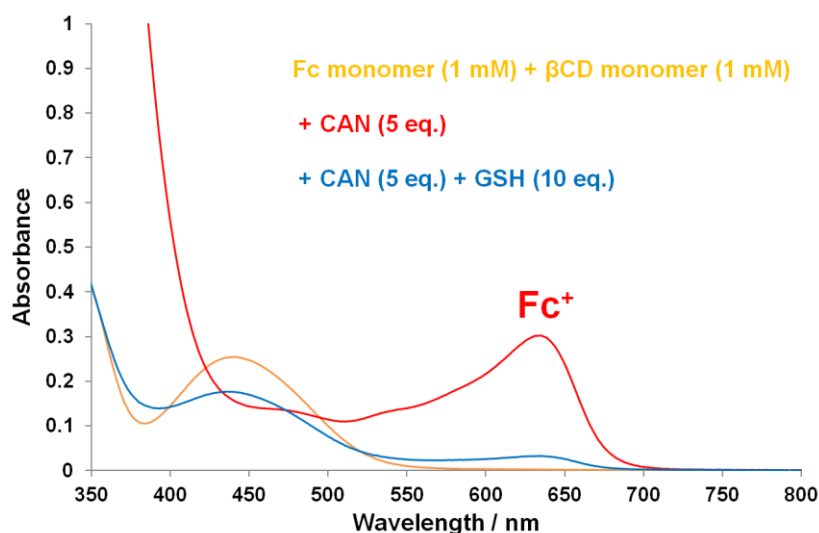


Figure 3-10. UV-Vis spectra of Fc-AAm (1 mM) / β CD-AAm (1 mM) (orange), with CAN (5 mM) (red), and with CAN (5 mM) / GSH (10 mM) (blue), respectively. The absorption band around 630 nm is attributed to the ferrocenium cation.

The oxidation with the Tris/HCl buffer with CAN increased the length of the hydrogel, whereas the continuous reduction of the β CD–Fc gel restored the initial length. This behavior was reversible for at least three oxidation–reduction cycles (Figure 3-11).

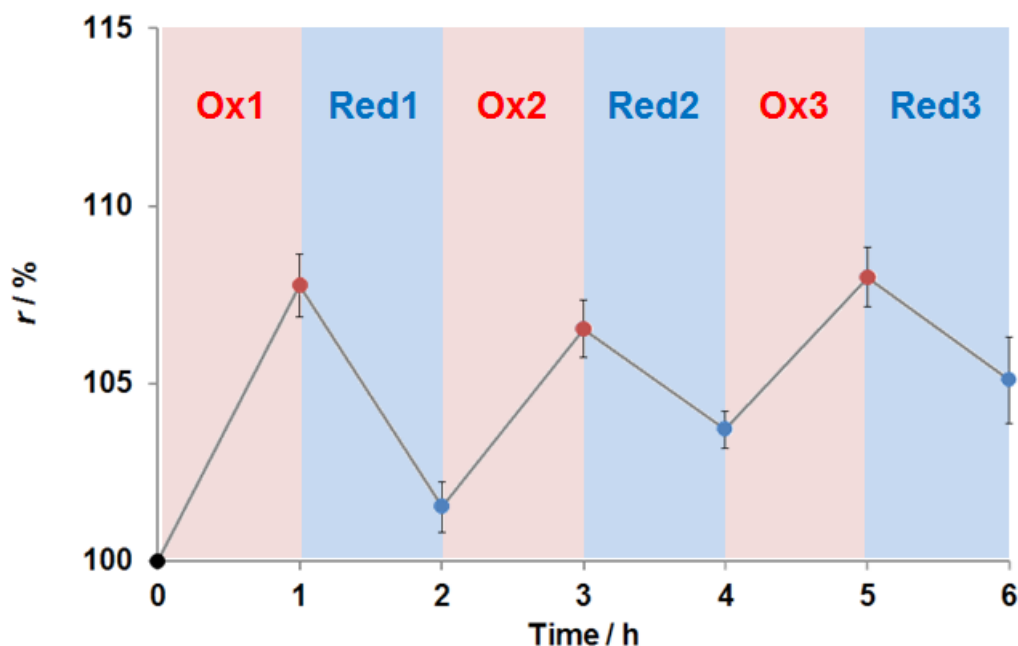


Figure 3-11. The r of β CD-Fc gel (3,3,1) throughout three cycles of oxidation (50 mM CAN) and reduction in the Tris/HCl buffer solutions (0.1 M, pH 7). ($n=3$, error bars are standard deviation.)

β CD showed a high affinity for the reduced state of the Fc group due to its hydrophobic nature, but the oxidized state of the Fc group (Fc^+) exhibited a low affinity for β CD due to the cationic nature, which resulted in dissociation of the inclusion complex of β CD/Fc⁵⁰. In contrast, β CD gel(3,1), Fc gel(3,1), and pAAm gel(1) did not exhibit expansion behaviors in response to the CAN (Figure 3-12).

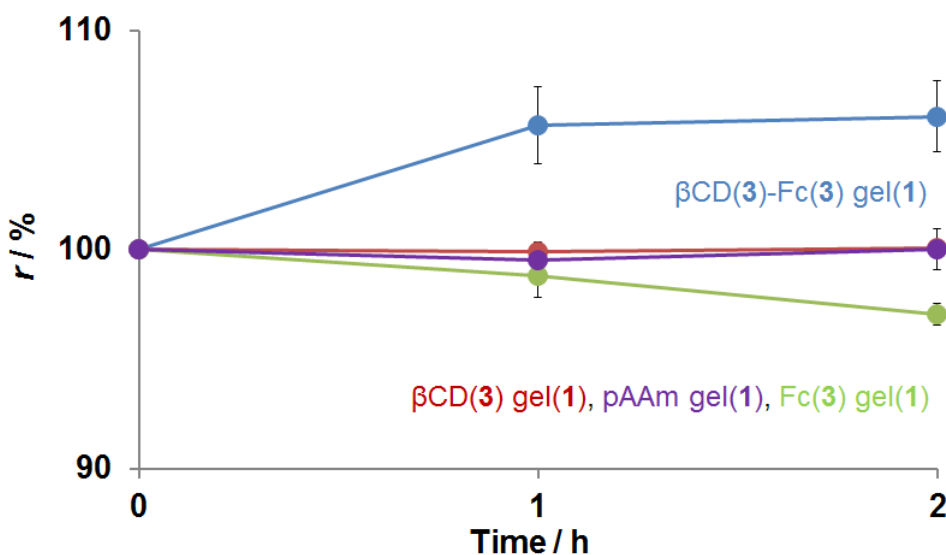


Figure 3-12. The r of β CD-Fc gel (3,3,1) (blue), β CD gel (3,1) (red), Fc gel (3,1) (green), and pAAm gel (1) (purple) in response to immersion into the Tris/HCl buffer with CAN (50 mM). ($n=3$, error bars are standard deviation.)

The influences of the host–guest induction ratio were investigated. Figure 3-13 shows the r of β CD–Fc gels (1,1,1), (2,2,1), and (3,3,1), respectively, in response to the Tris/HCl buffer with CAN (50 mM). This result indicates that a larger host/guest ratio induced a larger length change in the β CD–Fc gels.

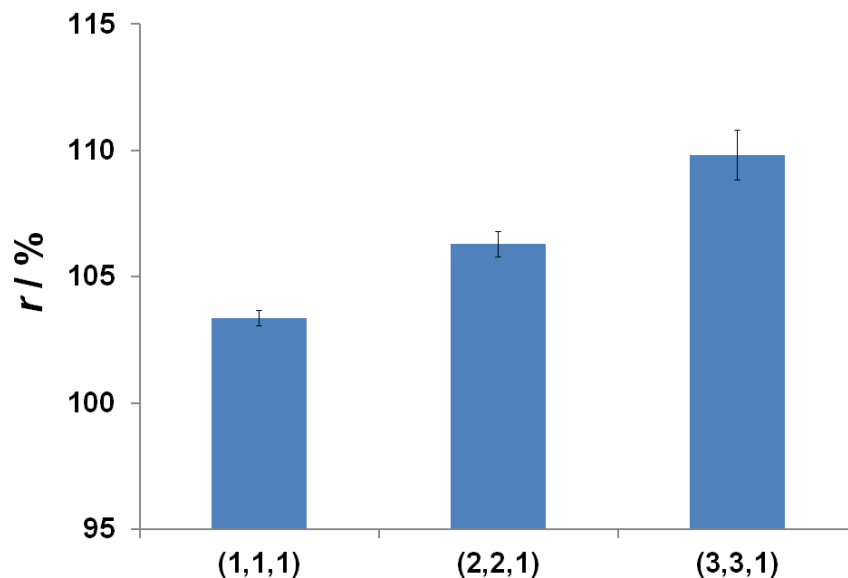


Figure 3-13. The r of β CD–Fc gels (1,1,1), (2,2,1), and (3,3,1) after immersed for two hours in the Tris/HCl buffer with CAN (17, 33, and 50 mM, respectively). ($n=3$, error bars are standard deviation.)

The influences of the chemical crosslinking ratio were also investigated. Figure 3-14 shows the influence of crosslink ratio for the r of β CD–Fc gels (3,3,0), (3,3,1), and (3,3,2), respectively, in the Tris/HCl buffer (0.1 M) with CAN (50 mM). A smaller crosslink ratio of β CD–Fc gels led to a larger length change ratio. These results indicate that the β CD–Fc gel with a lower content of the chemical crosslink unit and a higher content of the host/guest units gives a larger volume change in response to redox stimuli.

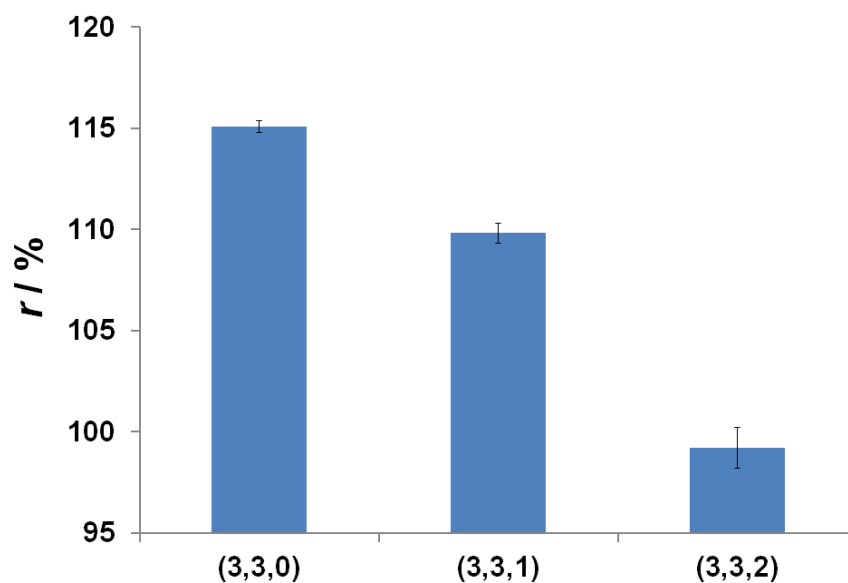


Figure 3-14. Length change ratios of β CD–Fc gels (3,3,0), (3,3,1), and (3,3,2) after immersed for two hours in the Tris/HCl buffer with CAN (50 mM). ($n=3$, error bars are standard deviation.)

The stress–strain measurements clearly represented the increase and decrease of the supramolecular crosslink density in response to redox stimuli (Supplementary Fig. 3-15 and Table 3-1).

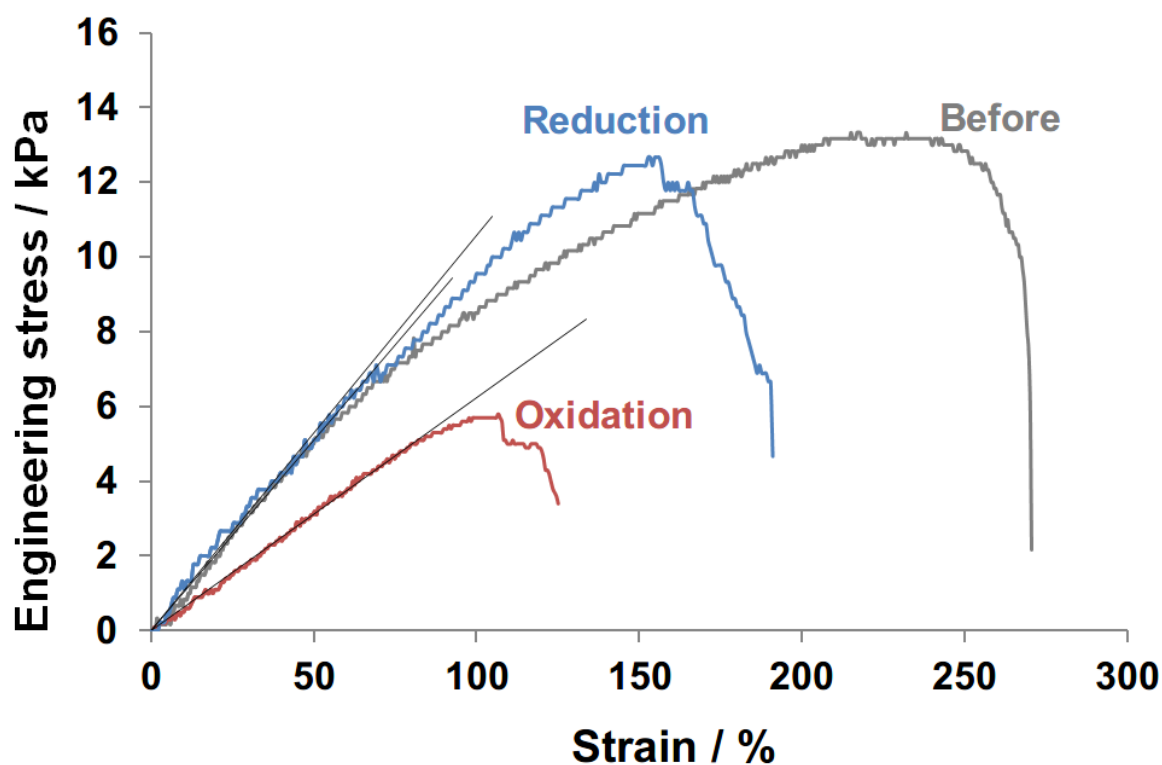


Figure 3-15. Stress-strain curves of β CD-Fc gel (3,3,1) before (gray) and after immersion into the Tris/HCl buffer with CAN (50 mM) (red). After immersion into the Tris/HCl buffer with GSH (50 mM) (blue), the stress-strain curve came back to the original shape. Approximation lines on the linear regime of each curve are also shown.

Table 3-1. Tensile elastic modulus (E) of β CD-Fc gel (3,3,1) throughout one cycle of oxidation-reduction.

	E / kPa
Before	10.2
Oxidation	6.23
Reduction	10.5

The water content change of the β CD-Fc gel in response to redox stimuli was measured by the following procedure.

[1] The weight of the hydrogel in its swelling equilibrium (W_{wet}) was measured.

[2] The weight of the freeze-dried gel (W_{dry}) was measured.

[3] The water content was determined by a following equation.

$$(\text{Water content}) = (W_{\text{wet}} - W_{\text{dry}}) / W_{\text{wet}} \times 100 (\%)$$

Table 3-2 shows the water content of the β CD-Fc gel (3,3,1) before and after immersion into Tris/HCl buffer with CAN (50 mM). As shown in the Table 3-2, the oxidation of the Fc moiety increases the water content of the hydrogel. These results indicate that the expansion and contraction of the hydrogel corresponds to the uptake and release of water.

Table 3-2. The water content of β CD-Fc gel (3,3,1) before and after immersion into Tris/HCl buffer with CAN (50 mM).

	Water content (% , w/w)
Before	77.2 ± 0.3
Oxidation	84.5 ± 0.1

The deformation of inclusion complex between β CD and Fc decreases the crosslink density to swell the hydrogel, whereas the formation of the inclusion complex increases it to shrink, implying that the change in the crosslink density in response to the redox stimuli lead to the uptake and release of water from the gel, which altered the volume of the β CD-Fc gel (Fig. 3-9b and Table 3-2).

3-7. Mechanical work done by the gel actuators

Finally, the mechanical work done by the β CD-Fc gel (3,3,1) through the redox-responsive contraction–expansion was estimated. A weight (291 mg) was attached to the bottom of a rectangular β CD-Fc gel (size: $10 \times 5 \times 1 \text{ mm}^3$) (Fig. 4a).

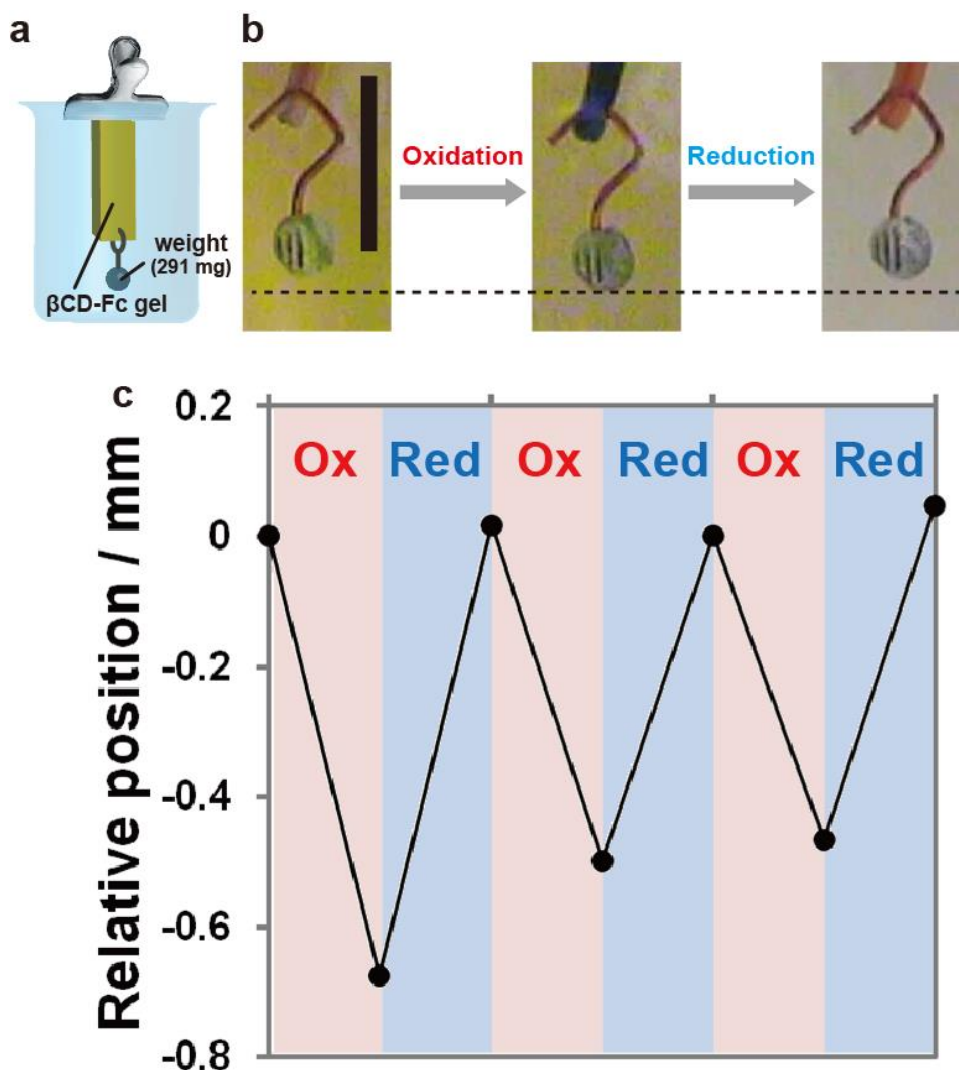


Figure 3-16. **a:** Schematic illustration of the hydrogel actuator. **b:** Photographs of a β CD-Fc gel(3,3,1) actuator in response to redox stimuli. After immersion into the buffer with an oxidant (CAN), the length of the hydrogel increased and the weight became down. Subsequent immersion into the buffer restored the weight to the original position. Scale bar indicates 1 cm. **c:** Plot of the relative position of the weight versus immersion time in the case of β CD-Fc gel(3,3,1) with a weight (291 mg).

This hydrogel actuator was immersed into the Tris/HCl buffer with CAN (50 mM) as an oxidation and subsequently immersed into the Tris/HCl buffer as a reduction. Figure 3-16b shows photographs of an experiment conducted on the hydrogel actuator composed of β CD-Fc gel (3,3,1) with a weight (291 mg). Oxidation expanded the hydrogel and the position of the weight became down. Reduced β CD-Fc gel contracted and restored the weight to the original position. Figure 3-16c plots the position of the weight against immersion time.

During the reduction step, the weight received mechanical work (W), which was determined by $W = (m - \rho V)gx$ (m : mass of the weight, ρ : density of the buffer, V : volume of the weight, g : acceleration of gravity, x : length of the weight that was lifted). In this case, the mechanical work was estimated to be ca. 2.0 μJ . Supplementary Figure 3-17 shows the same experiments conducted with βCD -Fc gels (1,1,1) and (2,2,1).

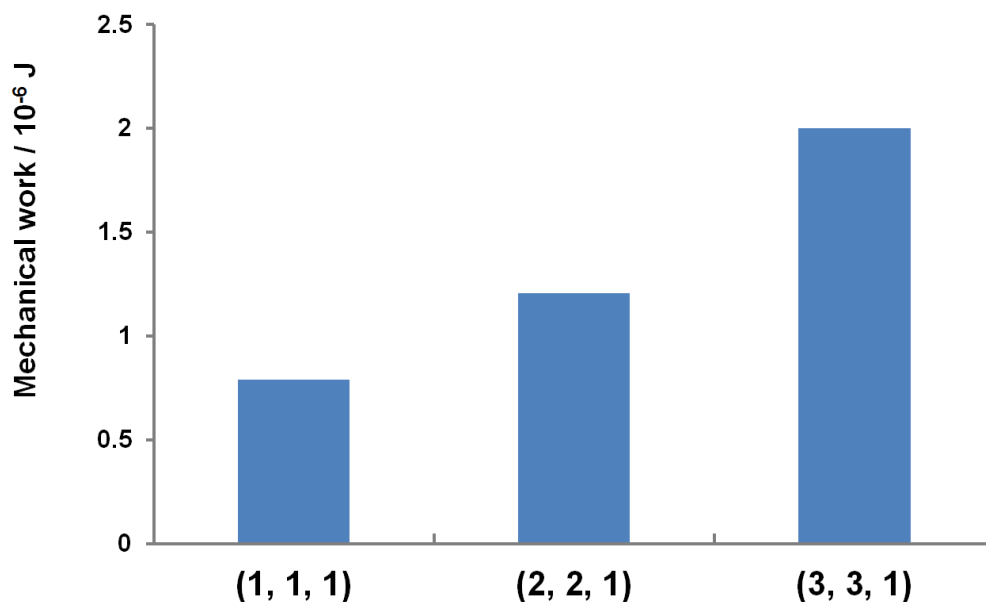


Figure 3-17. Mechanical work (W) done by the gel actuators composed of βCD -Fc gels (1,1,1), (2,2,1), and (3,3,1) with a weight (291 mg), respectively.

The mechanical work of the hydrogel actuator increased in accordance with the amount of host/guest units. These results demonstrate that this hydrogel actuator acts like muscles in response to redox stimuli even in an aqueous buffer solution with high ionic strength.

Conclusion

In conclusion, redox-responsive expansion and contraction of a hydrogel using inclusion complexes between βCD and Fc as “supramolecular crosslinks” is successfully achieved. βCD -Fc gel swells and shrinks by dissociating and re-forming supramolecular crosslinks using redox stimulus even at a high ionic strength comparable to a physiological saline solution. Moreover, this expansion and contraction of the hydrogel was visualized as a motion on a macroscale using a hydrogel actuator, and the mechanical work was evaluated. This type of hydrogel, which contains supramolecular crosslinks, can be applied to artificial muscles.

References

1. Kent, G. C., *Comparative anatomy of the vertebrates*. 6th ed.; Times Mirror/Mosby College Pub.: St. Louis, 1987.
2. Brough, B.; Northrop, B. H.; Schmidt, J. J.; Tseng, H.-R.; Houk, K. N.; Stoddart, J. F.; Ho, C.-M., *Proc. Natl. Acad. Sci. U.S.A.* **2006**, *103* (23), 8583-8588.
3. Coskun, A.; Banaszak, M.; Astumian, R. D.; Stoddart, J. F.; Grzybowski, B. A., *Chem. Soc. Rev.* **2012**, *41* (1), 19-30.
4. Gandhi, M. V.; Thompson, B. S., *Smart Materials and Structures*. Chapman & Hall: London, 1992.
5. (a) Urban, M. W., *Handbook of stimuli-responsive materials*. Wiley-VCH: Weinheim, Germany, 2011. (b) Minko, S., *Responsive Polymer Materials: Design and Applications*. Blackwell pub.: Oxford, 2006.
6. Ohm, C.; Brehmer, M.; Zentel, R., *Adv. Mater.* **2010**, *22* (31), 3366-3387.
7. (a) Mohsen, S.; Kwang, J. K., *Smart Mater. Struct.* **2005**, *14* (1), 197. (b) Otero, T. F.; Cortés, M. T., *Adv. Mater.* **2003**, *15* (4), 279-282. (c) Schneider, H.-J.; Kato, K.; Strongin, R., *Sensors* **2007**, *7* (8), 1578-1611. (d) Schneider, H.-J.; Strongin, R. M., *Acc. Chem. Res.* **2009**, *42* (10), 1489-1500. (e) Schneider, H.-J.; Kato, K., *J. Mater. Chem.* **2009**, *19* (5), 569-573.
8. (a) Bar-Cohen, Y., *Electroactive polymer (EAP) actuators as artificial muscles : reality, potential, and challenges*. 2nd ed.; SPIE Press: Bellingham, Wash., 2004. (b) Wallace, G. G.; Teasdale, P. R.; Spinks, G. M.; Kane-Maguire, L. A. P., *Conductive Electroactive Polymers: Intelligent Materials Systems, 2nd ed.*. CRC: Boca Raton, 2002.
9. (a) Osada, Y.; Okuzaki, H.; Hori, H., *Nature* **1992**, *355* (6357), 242-244. (b) Osada, Y.; Matsuda, A., *Nature* **1995**, *376* (6537), 219-219.
10. Beebe, D. J.; Moore, J. S.; Bauer, J. M.; Yu, Q.; Liu, R. H.; Devadoss, C.; Jo, B.-H., *Nature* **2000**, *404* (6778), 588-590.
11. Sidorenko, A.; Krupenkin, T.; Taylor, A.; Fratzl, P.; Aizenberg, J., *Science* **2007**, *315* (5811), 487-490.
12. Yoshida, R., *Adv. Mater.* **2010**, *22* (31), 3463-3483.
13. Stuart, M. A. C.; Huck, W. T. S.; Genzer, J.; Muller, M.; Ober, C.; Stamm, M.; Sukhorukov, G. B.; Szleifer, I.; Tsukruk, V. V.; Urban, M.; Winnik, F.; Zauscher, S.; Luzinov, I.; Minko, S., *Nat. Mater.* **2010**, *9* (2), 101-113.
14. Kobatake, S.; Takami, S.; Muto, H.; Ishikawa, T.; Irie, M., *Nature* **2007**, *446* (7137), 778-781.
15. Terao, F.; Morimoto, M.; Irie, M., *Angew. Chem. Int. Ed.* **2012**, *51* (4), 901-904.
16. Koshima, H.; Ojima, N.; Uchimoto, H., *J. Am. Chem. Soc.* **2009**, *131* (20), 6890-6891.
17. Kumar, G. S.; Neckers, D. C., *Chem. Rev.* **1989**, *89* (8), 1915-1925.
18. Küpfer, J.; Finkelmann, H., *Die Makromolekulare Chemie, Rapid Communications* **1991**, *12* (12), 717-726.
19. Ikeda, T.; Tsutsumi, O., *Science* **1995**, *268* (5219), 1873-1875.
20. Thomsen, D. L.; Keller, P.; Naciri, J.; Pink, R.; Jeon, H.; Shenoy, D.; Ratna, B. R., *Macromolecules* **2001**, *34* (17), 5868-5875.
21. Hugel, T.; Holland, N. B.; Cattani, A.; Moroder, L.; Seitz, M.; Gaub, H. E., *Science* **2002**, *296* (5570), 1103-1106.

22. Li, M. H.; Keller, P.; Li, B.; Wang, X.; Brunet, M., *Adv. Mater.* **2003**, *15* (7-8), 569-572.
23. Yu, Y.; Nakano, M.; Ikeda, T., *Nature* **2003**, *425* (6954), 145-145.
24. Camacho-Lopez, M.; Finkelmann, H.; Palffy-Muhoray, P.; Shelley, M., *Nat. Mater.* **2004**, *3* (5), 307-310.
25. Ikeda, T.; Mamiya, J.-i.; Yu, Y., *Angew. Chem. Int. Ed.* **2007**, *46* (4), 506-528.
26. van Oosten, C. L.; Bastiaansen, C. W. M.; Broer, D. J., *Nat. Mater.* **2009**, *8* (8), 677-682.
27. Lee, K. M.; Wang, D. H.; Koerner, H.; Vaia, R. A.; Tan, L.-S.; White, T. J., *Angew. Chem. Int. Ed.* **2012**, *51* (17), 4117-4121.
28. Hirokawa, Y.; Tanaka, T., *J. Chem. Phys.* **1984**, *81* (12), 6379-6380.
29. Luo, Q.; Mutlu, S.; Gianchandani, Y. B.; Svec, F.; Fréchet, J. M. J., *Electrophoresis* **2003**, *24* (21), 3694-3702.
30. (a) Kitano, S.; Koyama, Y.; Kataoka, K.; Okano, T.; Sakurai, Y., *J. Controlled Release* **1992**, *19* (1-3), 161-170. (b) Alexeev, V. L.; Sharma, A. C.; Goponenko, A. V.; Das, S.; Lednev, I. K.; Wilcox, C. S.; Finegold, D. N.; Asher, S. A., *Anal. Chem.* **2003**, *75* (10), 2316-2323. (c) Samoei, G. K.; Wang, W.; Escobedo, J. O.; Xu, X.; Schneider, H.-J.; Cook, R. L.; Strongin, R. M., *Angew. Chem. Int. Ed.* **2006**, *45* (32), 5319-5322.
31. Tanaka, T.; Fillmore, D.; Sun, S.-T.; Nishio, I.; Swislow, G.; Shah, A., *Phys. Rev. Lett.* **1980**, *45* (20), 1636-1639.
32. (a) Osada, Y., Conversion of chemical into mechanical energy by synthetic polymers (chemomechanical systems). In *Polymer Physics*, Springer Berlin Heidelberg: 1987; Vol. 82, pp 1-46. (b) Allcock, H. R.; Ambrosio, A. M. A., *Biomaterials* **1996**, *17* (23), 2295-2302.
33. Ohmine, I.; Tanaka, T., *J. Chem. Phys.* **1982**, *77* (11), 5725-5729.
34. Li, H.; Lai, F.; Luo, R., *Langmuir* **2009**, *25* (22), 13142-13150.
35. Tanaka, T.; Nishio, I.; Sun, S.-T.; Ueno-Nishio, S., *Science* **1982**, *218* (4571), 467-469.
36. Umezawa, K.; Osada, Y., *Chem. Lett.* **1987**, *16* (9), 1795-1798.
37. Katsumi, Y.; Kenji, N.; Shigenori, M.; Mitsuyoshi, O., *Jpn. J. Appl. Phys.* **1989**, *28* (11A), L2027.
38. Osada, Y.; Gong, J. P.; Sawahata, K., *J. Macromol. Sci., Chem.* **1991**, *28* (11-12), 1189-1205.
39. Ahn, S.-k.; Kasi, R. M.; Kim, S.-C.; Sharma, N.; Zhou, Y., *Soft Matter* **2008**, *4* (6), 1151-1157.
40. Takashima, Y.; Hatanaka, S.; Otsubo, M.; Nakahata, M.; Kakuta, T.; Hashidzume, A.; Yamaguchi, H.; Harada, A., *Nat. Commun.* **2012**, *3*, 1270.
41. Takada, K.; Tanaka, N.; Tatsuma, T., *J. Electroanal. Chem.* **2005**, *585* (1), 120-127.
42. Hempenius, M. A.; Cirmi, C.; Savio, F. L.; Song, J.; Vancso, G. J., *Macromol. Rapid Commun.* **2010**, *31* (9-10), 772-783.
43. Calvo-Marzal, P.; Delaney, M. P.; Auletta, J. T.; Pan, T.; Perri, N. M.; Weiland, L. M.; Waldeck, D. H.; Clark, W. W.; Meyer, T. Y., *ACS Macro Lett.* **2011**, *1* (1), 204-208.
44. Sui, X.; Hempenius, M. A.; Vancso, G. J., *J. Am. Chem. Soc.* **2012**, *134* (9), 4023-4025.
45. Nakahata, M.; Takashima, Y.; Yamaguchi, H.; Harada, A., *Nat Commun* **2011**, *2*, 511.
46. Ritter, H.; Mondrzik, B. E.; Rehahn, M.; Gallei, M., *Beilstein J. Org. Chem.* **2010**, *6*, 60.
47. To measure the volume change of the β CD-Fc gel more precisely, a digital inverted microscope (EVOS AME i2111, Advanced Microscopy Group) measured the size changes of gels. The digital inverted microscope

has a digital ruler, which measures diagonal lines up to 1 μm .

48. (a) Harada, A.; Takahashi, S., *J. Incl. Phenom.* **1984**, 2 (3-4), 791-798. (b) Wu, J.-S.; Toda, K.; Tanaka, A.; Sanemasa, I., *Bull. Chem. Soc. Jpn.* **1998**, 71 (7), 1615-1618.
49. Rekharsky, M. V.; Inoue, Y., *Chem. Rev.* **1998**, 98 (5), 1875-1918.
50. Moozyckine, A. U.; Bookham, J. L.; Deary, M. E.; Davies, D. M., *J. Chem. Soc., Perkin Trans. 2* **2001**, (9), 1858-1862.

Redox-Responsive Macroscopic Gel Assembly Based on Discrete Dual Interactions

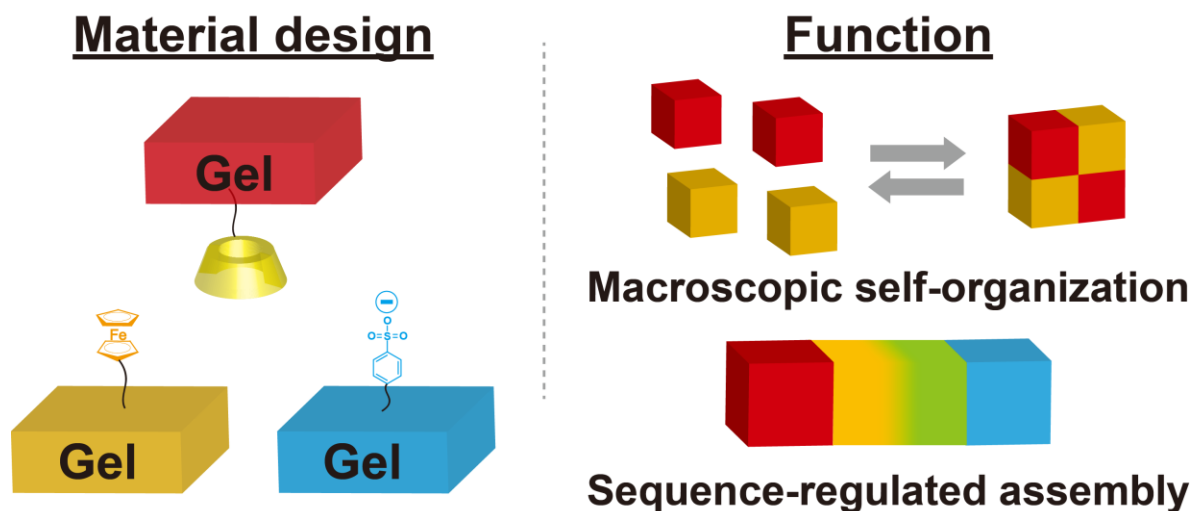


Figure 4-0. Conceptual illustration of chapter 4.

4-1. Introduction

In biological systems, there are various types of functional molecules and their assemblies which form macroscopic organizations based on selective molecular recognition. In artificial systems, macroscopic self-assemblies have been achieved mainly through macroscopic physical interactions¹⁻⁹. On the other hand, complementary complex formations should be more effective to construct multi-functional macroscopic self-assemblies, which have much potential for highly functional materials as represented by stimuli-responsive materials¹⁰⁻¹⁴, self-healing materials¹⁵⁻²⁰, artificial muscles²¹⁻²⁵, and so on²⁶. Various stimuli-responsive macroscopic assemblies based on polymeric hydrogels modified with cyclodextrins (CDs) and guest molecules were developed^{27a}. The A-B type gel assembly and dissociation can be controlled by various external stimuli, such as light^{27b}, chemical^{27c}, temperature^{27d}, pH^{27e}, and metal-ligand interactions^{27f}. Such macroscopic assemblies remind us of the selective formation of cell organization.

Ferrocene (Fc) is one of the most common redox-responsive compounds having a unique feature as a hydrophobic guest compound for CDs in its reduced state (Fc)²⁸ and as a hydrophilic cationic guest compound for calixarene derivatives in its oxidized state (Fc⁺)²⁹. To construct precisely controlled macroscopic self-assemblies, one stimulus should regulate multi-interactions. Previously, polymers modified with Fc produced redox-responsive materials, such as sol-gel phase transition materials³⁰⁻³², self-healing materials^{33a}, responsive gel actuator^{33b,34-36}, and others³⁷. It can be said that Fc is usable as a good probe molecule for observation of two or more discrete interactions on a macroscopic scale. Here, an A-B-C type redox-responsive gel assembly system based on host-guest interactions between CD and Fc / cation-anion interactions between Fc⁺ and sodium *p*-styrenesulfonate (SSNa) is reported. Each functional moiety is incorporated into the poly(acrylamide) (pAAm) gel network. Redox stimuli change the electronic state of the Fc and switch the discrete dual interactions between these gels to form different types of gel assemblies on a macroscopic scale.

4-2. Experimental section

Materials.

Acrylamide (AAm), 2,2'-azobis[2-(2-imidazolin-2-yl)-propane] dihydrochloride (VA-044), sodium *p*-styrenesulfonate (SSNa), calix[6]arene hexasulfonic acid sodium salt (CS6), CDCl_3 , and D_2O were purchased from Wako Pure Chemical Industries, Ltd. β -cyclodextrin (βCD) was obtained from Junsei Chemical Co., Ltd. Triethylamine (Et_3N), ethylenediamine, potassium hydroxide, sodium hydroxide, sodium chloride, hydrochloric acid, ammonium peroxodisulfate (APS), *N,N,N',N'*-tetramethylethylenediamine (TEMED), and *N,N'*-methylenebis(acrylamide) (MBAAm) were obtained from Nacalai Tesque Inc. Ferrocenecarboxylic acid (FcCOOH), oxalyl chloride, acryloyl chloride, and ceric ammonium nitrate (CAN) were purchased from Tokyo Chemical Industry Co., Ltd. Tetrahydrofuran (THF) was obtained from Kanto Chemical Co., Inc. $\text{DMSO}-d_6$ was obtained from Merck & Co., Inc. A highly porous synthetic resin (DIAION HP-20) used for column chromatography was purchased from Mitsubishi Chemical Co., Ltd. Water used for the preparation of the aqueous solutions was purified with a Millipore Elix 5 system. Other reagents were used without further purification. 6-Acrylamido- βCD ($\beta\text{CD-AAm}$) and Fc monomer (Fc-AAm) were prepared according to our previous report^{33a}.

Measurements.

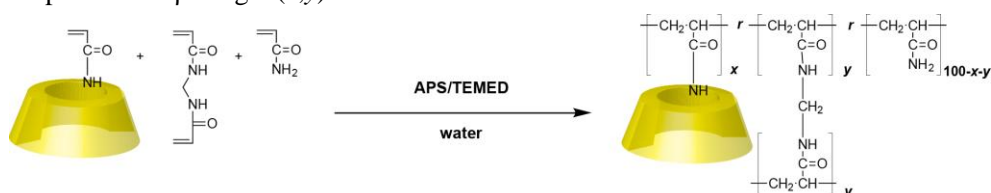
The ^1H NMR spectra were recorded at 500 MHz with a JEOL JNM-ECA 500 NMR spectrometer. The solid-state ^1H field gradient magic angle spinning (FGMAS) NMR spectra were recorded at 400 MHz with a JEOL JNM-ECA 400 NMR spectrometer. Sample spinning rate was 7 kHz. In all NMR measurements, chemical shifts were referenced to the solvent values ($\delta = 2.49$ ppm, 4.79 ppm, and 7.26 ppm for $\text{DMSO}-d_6$, D_2O , and CDCl_3 , respectively). The IR spectra were measured using a JASCO FT/IR-410 spectrometer. Positive-ion matrix-assisted laser desorption/ionization time-of-flight mass spectrometry (MALDI-TOF-MS) experiments were performed using a Bruker autoflex speed mass spectrometer using 2,5-dihydroxy-benzoic acid as a matrix. Mass number was calibrated by four peptides, i.e., angiotensin II ($[\text{M}+\text{H}]^+$ 1046.5418), angiotensin I ($[\text{M}+\text{H}]^+$ 1296.6848), substance P ($[\text{M}+\text{H}]^+$ 1347.7354), and bombesin ($[\text{M}+\text{H}]^+$ 1619.8223). Mechanical properties of the gels were measured by the mechanical tension testing system (Rheoner, RE-33005, Yamaden Ltd.).

Preparation of gels.

Preparation of βCD gel (x,y). (Scheme 4-1)

Typical procedure for βCD gel (3,2). $\beta\text{CD-AAm}$ (36 mg, 0.030 mmol), MBAAm (3.1 mg, 0.020 mmol), AAm (67.5 mg, 0.95 mmol), APS (2.3 mg, 0.01 mmol), and TEMED (1.5 μL , 0.01 mmol) were dissolved in water (1 mL). The solution turned into gel within a few minutes at room temperature. The gel was washed repeatedly with water.

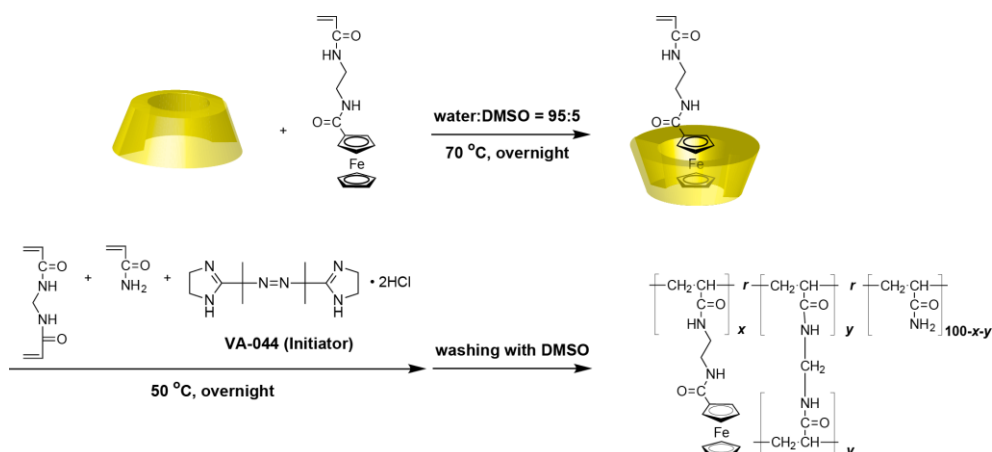
Scheme 4-1. Preparation of βCD gel (x,y).



Preparation of Fc gel (x,y). (Scheme 4-2)

Typical procedure for Fc gel (3,2). β CD (34 mg, 0.030 mmol) and Fc-AAm (9.8 mg, 0.030 mmol) were mixed in a mixed solvent of water/DMSO (95/5, v/v) (1 mL) and stirred at 70 °C for 3 h to give a transparent solution. MBAAm (3.1 mg, 0.020 mmol), AAm (67.5 mg, 0.95 mmol), and VA-044 (3.2 mg, 0.01 mmol) were added and dissolved. The solution was purged with argon gas for 1 h and was then heated at 50 °C overnight to form a gel. The gel was washed repeatedly with DMSO and water to remove β CD.

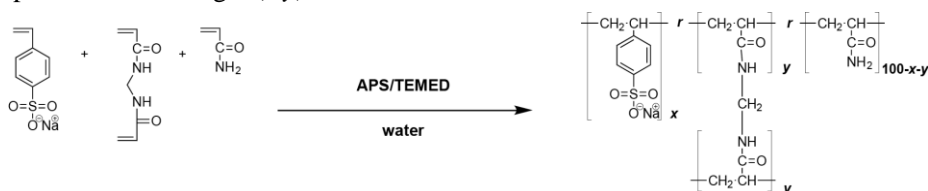
Scheme 4-2. Preparation of Fc gel (x,y).



Preparation of SSNa gel (x,y). (Scheme 4-3)

Typical procedure for SSNa gel (10,2). SSNa (21 mg, 0.10 mmol), MBAAm (3.1 mg, 0.020 mmol), AAm (62.6 mg, 0.88 mmol), APS (2.3 mg, 0.01 mmol), and TEMED (1.5 μ L, 0.01 mmol) were dissolved in water (1 mL). The solution turned into gel within a few minutes at room temperature. The gel was washed repeatedly with water.

Scheme 4-3. Preparation of SSNa gel (x,y).



Characterization of gels.

^1H FGMAS NMR spectra.

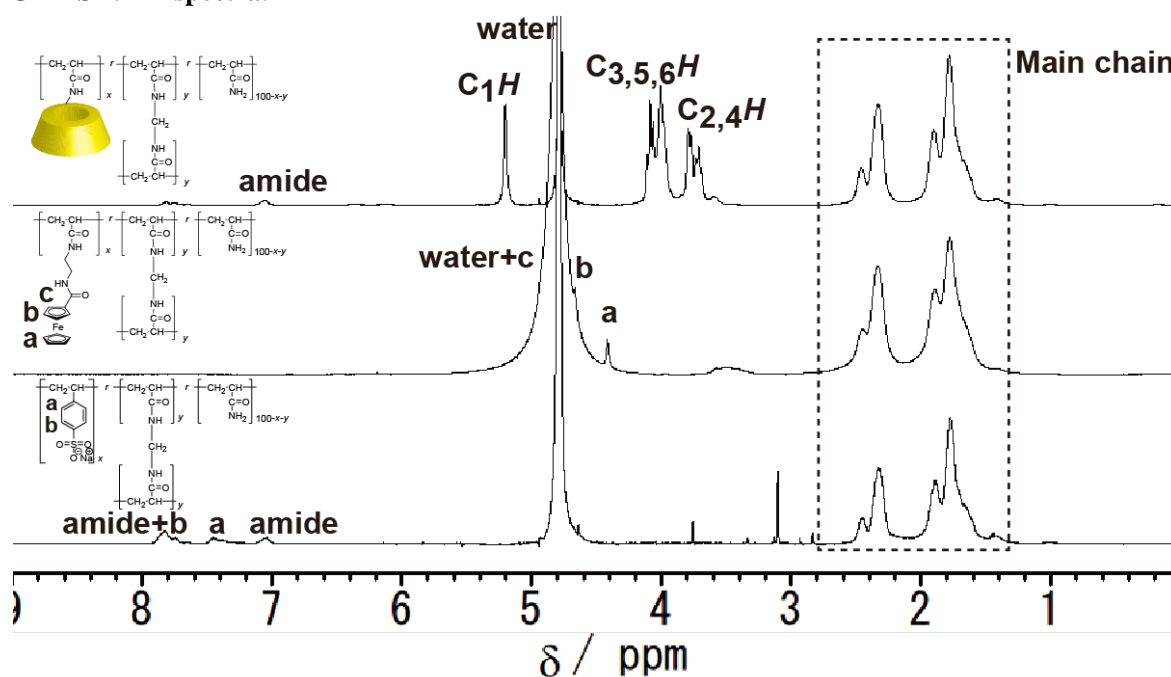


Figure 4-1. Solid-state ^1H FGMAS NMR spectra of βCD gel (5,2), Fc gel (5,2), and SSNa gel (5,2), respectively. (Immersed in D_2O (βCD gel and SSNa gel) or in 0.1 M NaOH in D_2O (Fc gel), 400 MHz, 30 $^\circ\text{C}$, rotation frequency = 7 kHz)

FT-IR spectra.

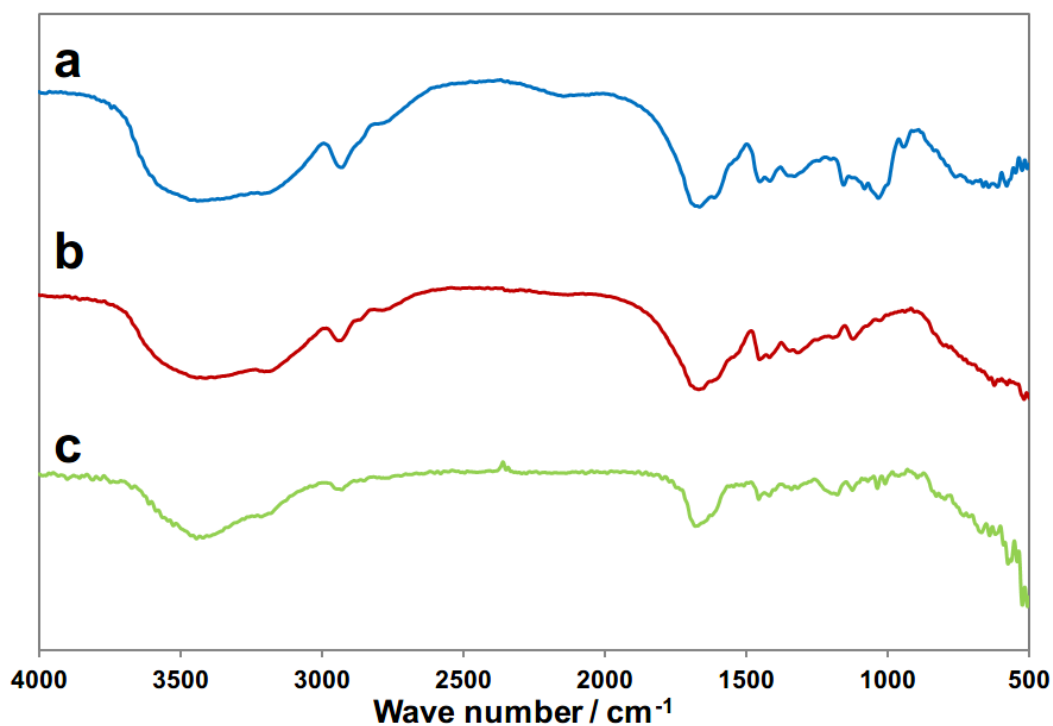


Figure 4-2. FT-IR spectra of (a) βCD gel (5,2), (b) Fc gel (5,2), and (c) SSNa gel (5,2), respectively. (KBr disc, r.t.)

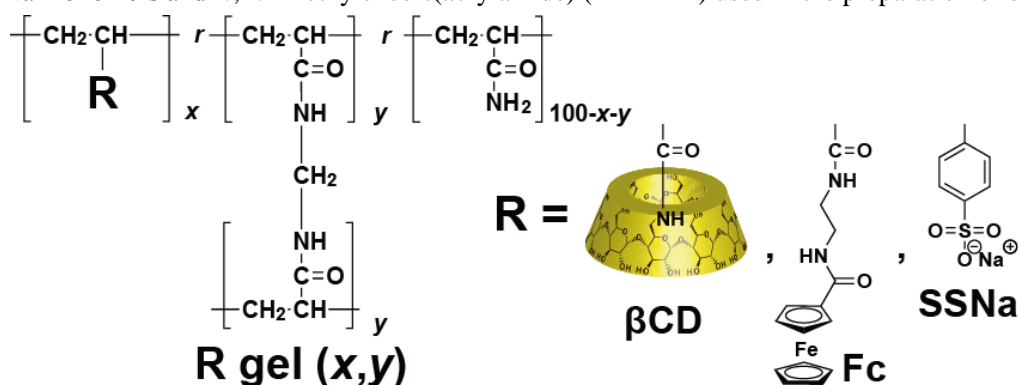
βCD gel (5,2): 3423, 3195 cm^{-1} (O–H stretching vibration, N–H asymmetric stretching vibration, and N–H symmetric stretching vibration), 2931 cm^{-1} (methylene C–H stretching vibration) 1664 cm^{-1} (C=O stretching vibration, N–H bending vibration).

Fc gel (5,2): 3379, 3176 cm^{-1} (N–H asymmetric stretching vibration, and N–H symmetric stretching vibration), 2941 cm^{-1} (methylene C–H stretching vibration) 1668 cm^{-1} (C=O stretching vibration, N–H bending vibration).

SSNa gel (5,2): 3421, 3184 cm^{-1} (N–H asymmetric stretching vibration, and N–H symmetric stretching vibration), 2929 cm^{-1} (methylene C–H stretching vibration) 1680 cm^{-1} (C=O stretching vibration, N–H bending vibration).

4-3. Preparation and characterization of gels

Scheme 4-4. Chemical structures of the gels used in this study. Here x and y represent the mol% of βCD/Fc/SSNa monomers and N, N' -methylenebis(acrylamide) (MBAAm) used in the preparation of each gel.



Scheme 4-4 shows chemical structures of β-cyclodextrin gel (βCD gel (x,y)), ferrocene gel (Fc gel (x,y)), and sodium p -styrenesulfonate gel (SSNa gel (x,y)), respectively. The βCD gel and the SSNa gel were prepared by homogeneous radical copolymerization of βCD or SSNa monomers, N, N' -methylenebis(acrylamide) (MBAAm), and acrylamide (AAm) initiated by a redox pair of ammonium peroxydisulfate (APS) and N,N,N',N' -tetramethylethylenediamine (TEMED) in water (See Schemes 4-1 and 4-3 in Supporting Information). The Fc gel was prepared by homogeneous radical copolymerization of the inclusion complex between Fc monomer (Fc–AAm) and βCD with MBAAm and AAm using 2,2'-azobis[2-(2-imidazolin-2-yl)-propane] dihydrochloride (VA-044) as a water-soluble radical initiator. βCD was washed out from the gel after the polymerization (Scheme 4-2). Here x and y represent the mol% of βCD/Fc/SSNa monomers and MBAAm unit. ^1H solid-state field-gradient magic-angle-spinning (FGMAS) NMR and fourier transform infrared (FT-IR) spectroscopies (Figures 4-1 and 4-2) suggested successful introduction of βCD/Fc/SSNa units into gels.

4-4. Adhesion test between β CD gel and Fc gel

First, the interaction between the β CD gel and the Fc gel was investigated. Figure 4-3a shows a typical experiment of the gel aggregation. Both gels were cut into cubes ($5 \times 5 \times 5 \text{ mm}^3$) and shaken together in water (See experimental section for detail). The β CD gel (clear and colorless) was stained with a red dye (rose bengal) for visibility. As shown in Figure 4-3a, the β CD gel (3,2) and the Fc gel (3,2) assembled together within a few minutes to form a large aggregate. On the other hand, this aggregate was not formed by adding competitive guest (sodium adamantanecarbonate (AdCANa)) or competitive host (β CD) molecules into the external solution (Figures 4-4a and 4-4b). β CD and Fc form an inclusion complex through host–guest interaction with relatively high association constant ($K_a = 17 \times 10^3 \text{ L mol}^{-1}$)²⁸. β CD has much higher association constant for the adamantane derivative ($K_a = 35 \times 10^3 \text{ L mol}^{-1}$)³⁸ than that for Fc. These results indicate that the β CD gel and the Fc gel adhered through the formation of inclusion complexes at the interfaces of the gels (Figure 4-3c).

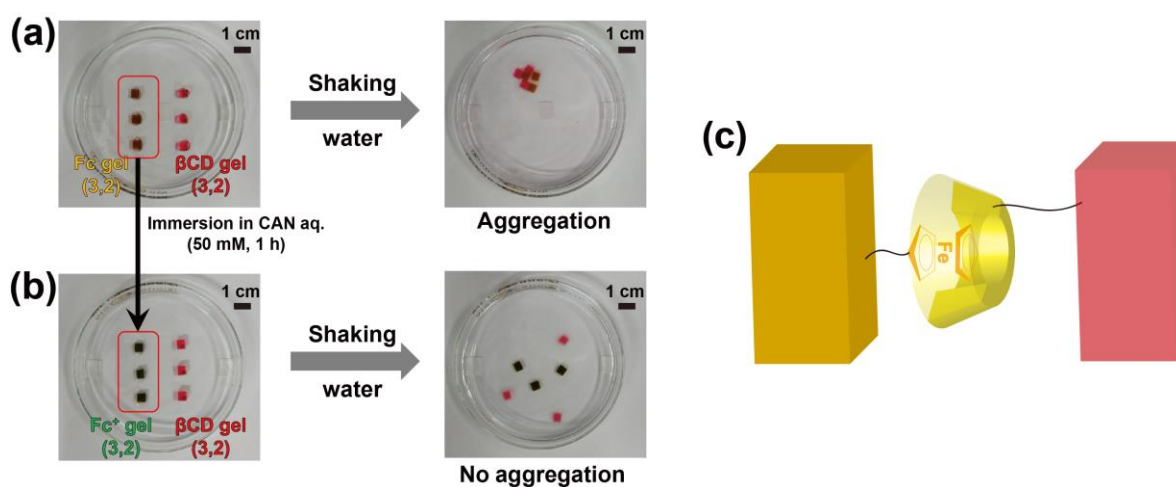


Figure 4-3. **a.** Photographs of the aggregation test between the Fc gel (3,2) and the β CD gel (3,2). **b.** Photographs of the aggregation test between the Fc^+ gel (3,2) and the β CD gel (3,2). **c.** Schematic illustration of the aggregate between the Fc gel and the β CD gel. The β CD gel was stained with a red dye (rose bengal) for visibility. Scale bar, 1 cm.

In the next step, the effect of redox stimuli on the aggregation between the β CD gel and the Fc gel (Figure 4-3b) was investigated. By immersing Fc gel into the aqueous solution of ceric ammonium nitrate (CAN) (50 mM), an oxidizing agent, the color of the gel changed from orange to green, which is a characteristic color of the ferrocenium cation (Fc^+). This indicates that the one-electron oxidation of Fc moiety took place inside the gel^{33b}. The oxidized gel did not adhere to the β CD gel at all by shaking together in water (Figure 4-3b). β CD shows a high affinity for the Fc in its reduced state owing to its hydrophobic nature, but the oxidized Fc^+ exhibits a low affinity for β CD due to its cationic nature³⁹.

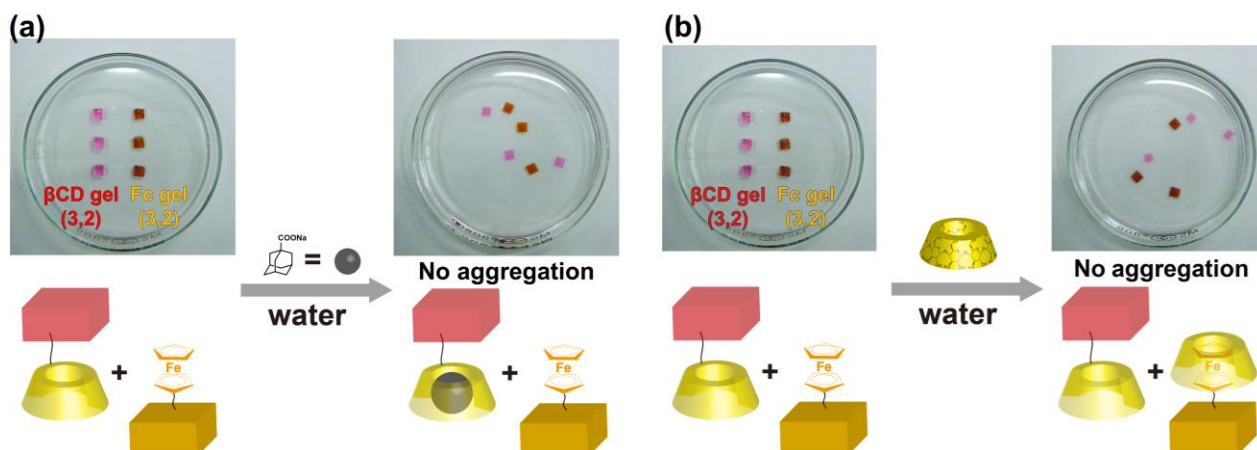


Figure 4-4. a. Photographs and schematic illustration of the competitive experiment in the case of β CD gel–Fc gel with competitive host (β CD). After adding β CD, no aggregation between β CD gel and Fc gel was observed. Scale bar, 1 cm.

4-5. Adhesion test between Fc gel and SSNa gel

Secondary, the interaction between Fc and SSNa gels was investigated. Figure 4-5a shows a typical procedure for the gel aggregation test. The Fc gel (3,2) and the SSNa gel (3,2) (with black beads embedded in the gel for visibility) formed no aggregate by shaking in water. On the other hand, immersing the Fc gel in CAN aq. (50 mM) for one hour caused the Fc⁺ gel to aggregate with the SSNa gel (Figure 4-5b).

By adding competitive host molecule (calix[6]arene hexasulfonic acid sodium salt (CS6)), no aggregate was formed (Figure 4-6). CS6 has a relatively high association constant ($K_a = 24 \times 10^3 \text{ L mol}^{-1}$) for the Fc⁺ derivative²⁹. CS6 served as a competitive host molecule for Fc⁺ moieties to inhibit the aggregation between the Fc⁺ gel and the SSNa gel. These results indicate that the Fc⁺ gel and the SSNa gel adhered through the cation-anion interaction at the interfaces of the gels (Figure 4-5c).

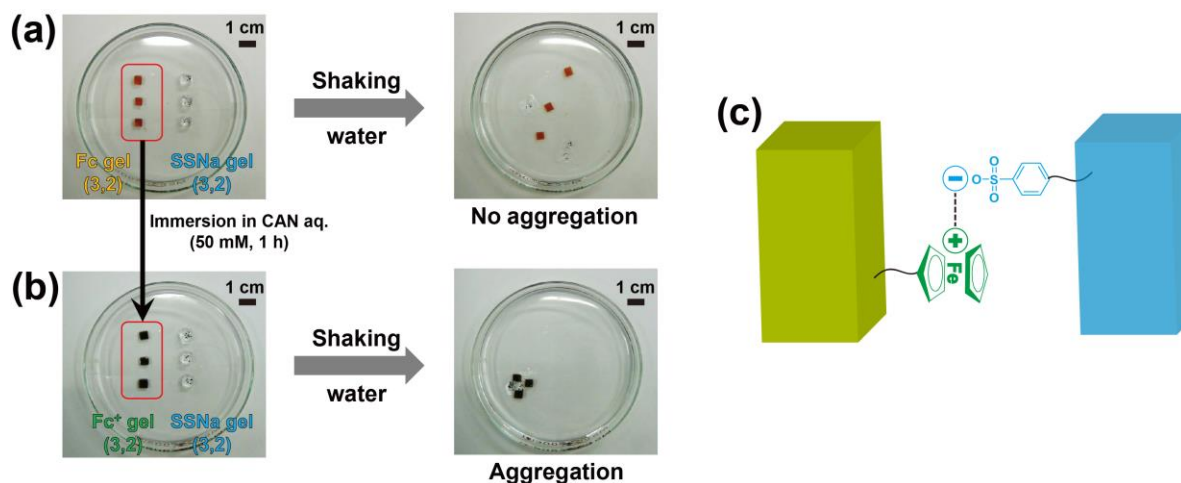


Figure 4-5. a. Photographs of the aggregation test between the Fc gel (3,2) and the SSNa gel (3,2). b. Photographs of the aggregation test between the Fc⁺ gel (3,2) and the SSNa gel (3,2). c. Schematic illustration of the aggregate between the Fc⁺ gel and the SSNa gel. The β CD gel was stained with a red dye (rose bengal), and black beads are embedded in the SSNa gel for visibility, respectively. Scale bar, 1 cm.

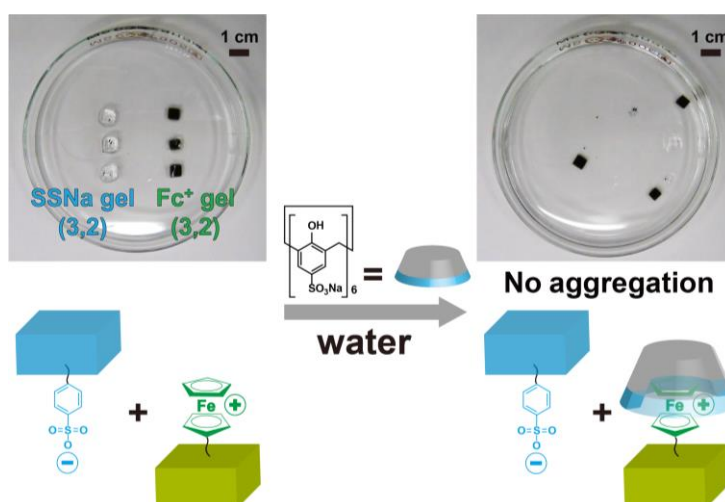
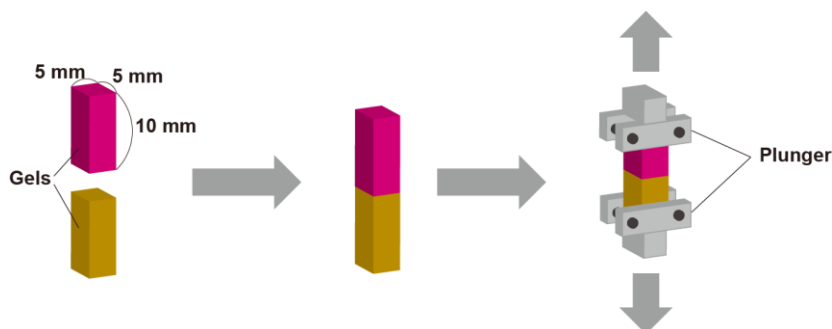


Figure 4-6. Photographs and schematic illustration of the competitive experiment in the case of Fc⁺ gel–SSNa gel with competitive host (CS6). Adding CS6 resulted in no aggregation between Fc⁺ gel and SSNa gel. Scale bar, 1 cm.

Scheme 4-5. Typical procedure for stress-strain measurements.

4-6. Stress-strain measurements

The adhesion strength between the β CD gel and the Fc gel was measured using creepmeter (Scheme 4-5). The combined gel pieces were pulled toward the opposite side and the rupture stress was estimated from the obtained



stress-strain curves (Figures 4-7a and 4-7c) as a maximal force divided by surface-to-surface area. The values of rupture stresses between Fc gel ($x,2$)- β CD gel ($x,2$) ($x = 1, 2, 3, 4$, and 5) are shown in Figure 4-7b. As shown in the Figure 4-7b, the rupture stress increased as a function of the contents (x) of β CD and Fc moieties. This result indicates that the amount of host and guest moieties directly affect the adhesion strength. The adhesion strength between the Fc^+ gel ($x,2$) and the SSNa gel ($x,2$) was also measured in the same way (Figure 4-7d). The adhesion stress between the Fc^+ gel ($x,2$) and the SSNa gel ($x,2$) increased as the mol% of the Fc and the SSNa units increased, as shown in Figure 4-7d. These results clearly show that the number of Fc^+ and styrenesulfonate anion moieties has a direct influence on the adhesion strength.

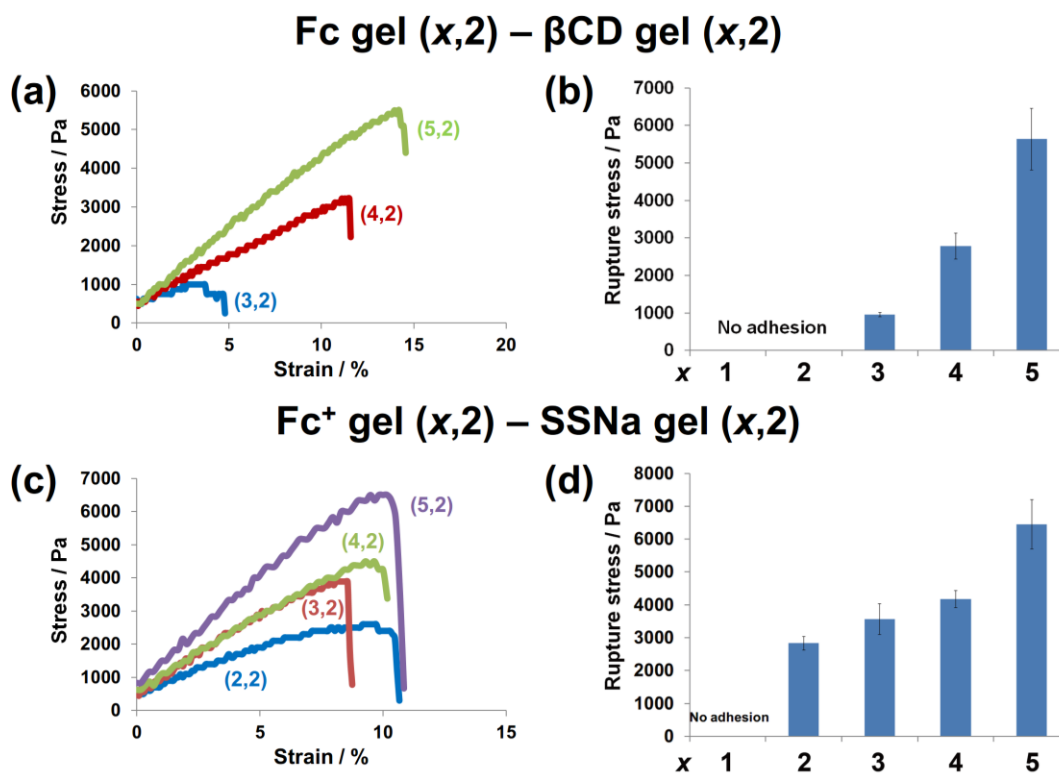


Figure 4-7. **a.** Stress-strain curves of the joined surface between β CD gel ($x,2$) and Fc gel ($x,2$) ($x = 3$ (blue), 4 (red) and 5 (green)), respectively. **b.** Rupture stress between Fc gel ($x,2$) and β CD gel ($x,2$) ($x = 1, 2, 3, 4$, and 5). **c.** Stress-strain curves of the joined surface between Fc^+ gel ($x,2$) and SSNa gel ($x,2$) ($x = 2$ (blue), 3 (red), 4 (green) and 5 (purple)), respectively. **d.** Rupture stress between Fc^+ gel ($x,2$) and SSNa gel ($x,2$) ($x = 1, 2, 3, 4$, and 5). The rupture stress was estimated from the obtained stress-strain curves as a maximal force divided by surface-to-surface area. $n=3$, error bars are standard deviation.

4-7. Adhesion partner switching experiment

Finally, an adhering partner switching experiment was demonstrated using three gels together. Figure 4-8a shows photographs of the experimental procedure. First, two pieces of the Fc gel (3,2) are prepared and one of them was immersed in water and the other in CAN aq. (50 mM) to obtain Fc gel and Fc⁺ gel. After one hour, β CD gels (3,2) and SSNa gels (3,2) were put on the left and right sides of the Fc gel or Fc⁺ gel, respectively. By picking up the Fc gel and Fc⁺ gel located in the middle position of the three gels, the Fc gel adhered with only the β CD gel, whereas the Fc⁺ gel stuck to only the SSNa gel (Figure 4-8b). This is a switching of adhering partner with all-or-nothing selectivity on a macroscale (Figure 4-8c).

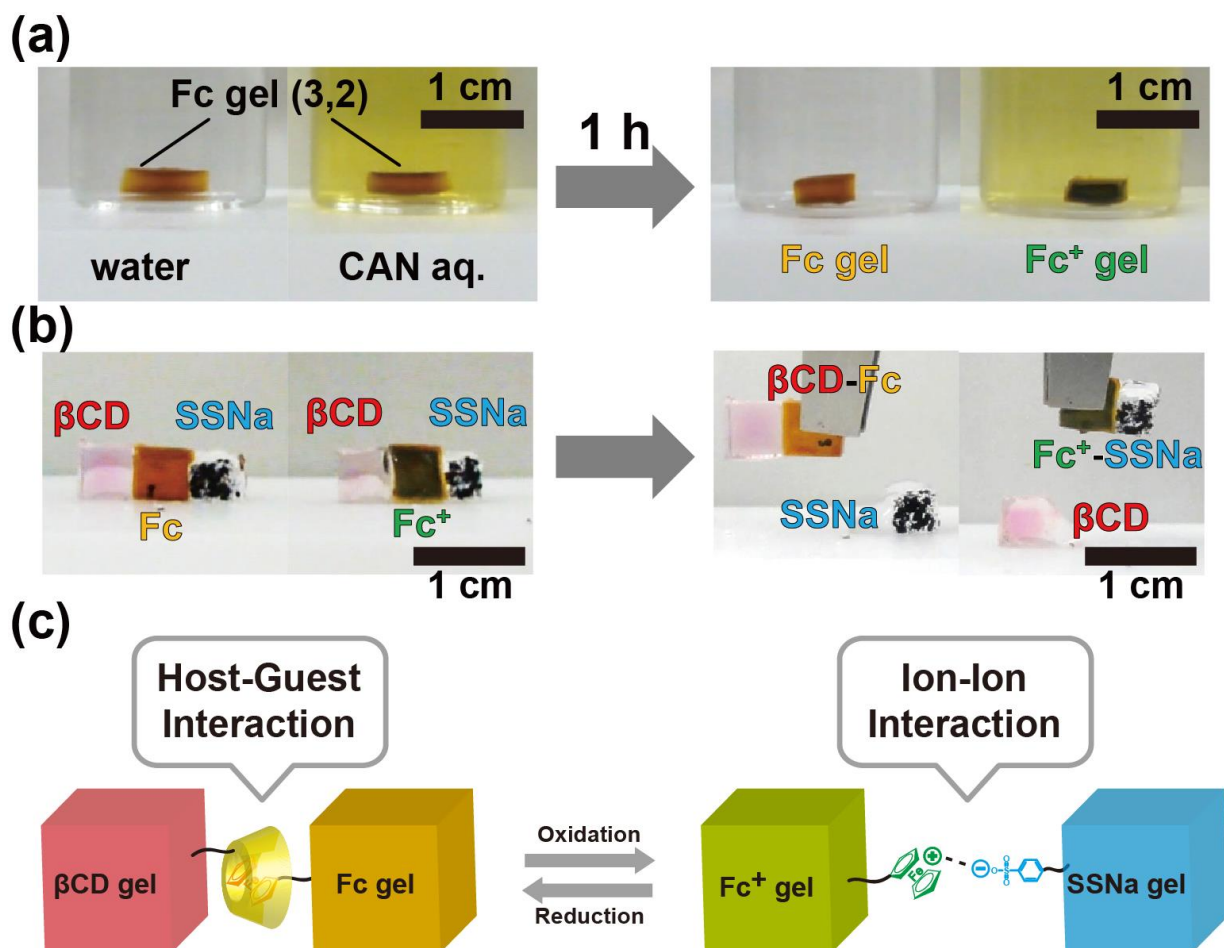


Figure 4-8. **a.** Photographs of the oxidation of the Fc gel. Fc gel (3,2) immersed in CAN aq. (50 mM) changed its color from orange to green. **b.** Photographs of the adhering partner switching experiment using Fc gel (3,2) and Fc⁺ gel (3,2). Scale bar, 1 cm. **c.** Schematic illustration of redox-responsive adhering partner switching system.

4-8. Formation of an ABC-type assembly

Also, an experiment to control a sequence of the assembly was demonstrated. Figure 4-9a shows the experimental procedure. First, the half volume of the Fc gel (4,2) ($10 \times 5 \times 5 \text{ mm}^3$) was immersed in the CAN aq. (50 mM), whereas the opposite half volume of the gel was exposed to air. After 10 minutes, an Fc/Fc⁺ gel having oxidized surface on the one side and reduced surface on the opposite side was obtained. When this Fc/Fc⁺ gel was shaken together with β CD gel (5,2) and SSNa gel (5,2) in water, three gels formed an ABC-type assembly composed of β CD gel–Fc/Fc⁺ gel–SSNa gel in the order (Figure 4-9b). This is because Fc or Fc⁺ moieties were associated with β CD or SSNa moieties through different types of interactions (Figure 4-9c). From these experiments, it was found that Fc gel can discriminate the β CD gel and the SSNa gel through discrete two types of non-covalent interactions (host–guest and ion–ion interactions), by simply changing redox state of the Fc moieties.

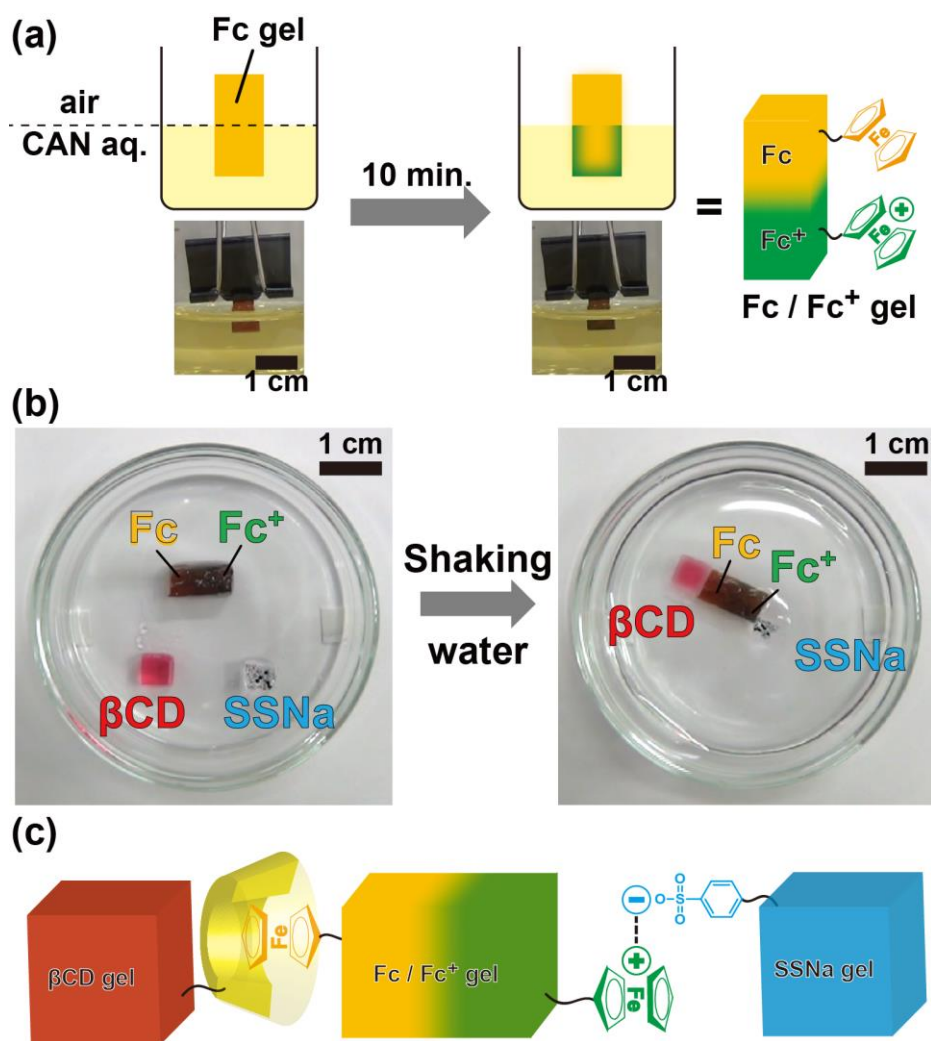


Figure 4-9. **a.** Photographs and schematic illustration of the procedure to make an Fc/Fc⁺ gel. First, the half volume of the Fc gel (4,2) ($10 \times 5 \times 5 \text{ mm}^3$) was immersed in the CAN aq. (50 mM), whereas the opposite half volume of the gel was exposed to air. After 10 minutes, an Fc/Fc⁺ gel having oxidized surface on the one side and reduced surface on the opposite side was obtained. **b.** Photographs of the experimental procedure to make an ABC-type assembly. **c.** Schematic illustration of the ABC-type assembly composed of β CD gel–Fc/Fc⁺ gel–SSNa gel. Scale bar, 1 cm.

Conclusion

In conclusion, a redox-responsive gel assembly system using Fc gel as an intelligent recognizer of suitable adhering partner on a macroscopic scale was successfully developed. In the previous works, only single non-covalent interaction have been utilized to form simple A-B type assemblies. The Fc/Fc⁺ gel can form a sequentially-controlled an A-B-C type macroscopic assembly using two discrete non-covalent interactions. This intelligent macroscopic self-assembly system has much potential for use not only in medical applications (for example; stimuli-responsive drug delivery system), but also in material science (for example; selective adhesive). To investigate the surface density of the functional group and the surface property (the effective depth and roughness) should be the next issue.

References

1. Grzybowski, B.; Jiang, X.; Stone, H.; Whitesides, G., *Physical Review E* **2001**, *64* (1), 011603.
2. Whitesides, G. M.; Grzybowski, B., *Science* **2002**, *295* (5564), 2418-2421.
3. Boncheva, M.; Andreev, S. A.; Mahadevan, L.; Winkleman, A.; Reichman, D. R.; Prentiss, M. G.; Whitesides, S.; Whitesides, G. M., *Proc. Natl. Acad. Sci. U.S.A.* **2005**, *102* (11), 3924-3929.
4. Mirica, K. A.; Ilievski, F.; Ellerbee, A. K.; Shevkoplyas, S. S.; Whitesides, G. M., *Adv. Mater.* **2011**, *23* (36), 4134-4140.
5. Grzybowski, B. A.; Winkleman, A.; Wiles, J. A.; Brumer, Y.; Whitesides, G. M., *Nat. Mater.* **2003**, *2* (4), 241-245.
6. McCarty, L. S.; Winkleman, A.; Whitesides, G. M., *Angew. Chem. Int. Ed.* **2007**, *46* (1-2), 206-209.
7. Bowden, N.; Terfort, A.; Carbeck, J.; Whitesides, G. M., *Science* **1997**, *276* (5310), 233-235.
8. Kim, E.; Whitesides, G. M., *J. Phys. Chem. B* **1997**, *101* (6), 855-863.
9. Bowden, N. B.; Weck, M.; Choi, I. S.; Whitesides, G. M., *Acc. Chem. Res.* **2000**, *34* (3), 231-238.
10. Feringa, B. L.; Browne, W. R., *Molecular switches*. 2nd, completely rev. and enl. ed.; Wiley-VCH: Weinheim, Germany, 2011.
11. Urban, M. W., *Handbook of stimuli-responsive materials*. Wiley-VCH: Weinheim, Germany, 2011.
12. Minko, S., *Responsive polymer materials : design and applications*. 1st ed.; Blackwell Pub.: Ames, Iowa, 2006.
13. Harada, A., *Supramolecular polymer chemistry*. Wiley-VCH: Weinheim, Germany, 2012.
14. (a) Tamagawa, H.; Nogata, F.; Umemoto, S.; Okui, N.; Popovic, S.; Taya, M., *Bull. Chem. Soc. Jpn.* **2002**, *75* (2), 383-388. (b) Asoh, T.-A.; Kikuchi, A., *Chem. Commun.* **2010**, *46* (41), 7793-7795.
15. Binder, W. H., *Self-Healing Polymers: From Principles to Applications*. Wiley-VCH: Weinheim, 2013.
16. Cordier, P.; Tournilhac, F.; Soulie-Ziakovic, C.; Leibler, L., *Nature* **2008**, *451* (7181), 977-980.
17. Burnworth, M.; Tang, L.; Kumpfer, J. R.; Duncan, A. J.; Beyer, F. L.; Fiore, G. L.; Rowan, S. J.; Weder, C., *Nature* **2011**, *472* (7343), 334-337.
18. Wang, Q.; Mynar, J. L.; Yoshida, M.; Lee, E.; Lee, M.; Okuro, K.; Kinbara, K.; Aida, T., *Nature* **2010**, *463* (7279), 339-343.
19. Sun, T. L.; Kurokawa, T.; Kuroda, S.; Ihsan, A. B.; Akasaki, T.; Sato, K.; Haque, M. A.; Nakajima, T.; Gong, J. P., *Nat. Mater.* **2013**, *12* (10), 932-937.
20. Kakuta, T.; Takashima, Y.; Nakahata, M.; Otsubo, M.; Yamaguchi, H.; Harada, A., *Adv. Mater.* **2013**, *25* (20), 2849-2853.
21. Gandhi, M. V.; Thompson, B. S., *Smart Materials and Structures*. Chapman & Hall: London, 1992.
22. Ohm, C.; Brehmer, M.; Zentel, R., *Adv. Mater.* **2010**, *22* (31), 3366-3387.
23. (a) Bar-Cohen, Y., *Electroactive polymer (EAP) actuators as artificial muscles : reality, potential, and challenges*. 2nd ed.; SPIE Press: Bellingham, Wash., 2004. (b) Wallace, G. G.; Teasdale, P. R.; Spinks, G. M.; Kane-Maguire, L. A. P., *Conductive Electroactive Polymers: Intelligent Materials Systems, 2nd ed.*. CRC: Boca Raton, 2002.
24. (a) Mohsen, S.; Kwang, J. K., *Smart Mater. Struct.* **2005**, *14* (1), 197. (b) Otero, T. F.; Cortés, M. T., *Adv. Mater.* **2003**, *15* (4), 279-282. (c) Schneider, H.-J.; Kato, K., *J. Mater. Chem.* **2009**, *19* (5), 569-573. (d)

- Schneider, H.-J.; Kato, K.; Strongin, R., *Sensors* **2007**, 7 (8), 1578-1611. (e) Schneider, H.-J.; Strongin, R. M., *Acc. Chem. Res.* **2009**, 42 (10), 1489-1500.
25. Takashima, Y.; Hatanaka, S.; Otsubo, M.; Nakahata, M.; Kakuta, T.; Hashidzume, A.; Yamaguchi, H.; Harada, A., *Nat. Commun.* **2012**, 3, 1270.
26. Schneider, H. J.; Tianjun, L.; Lomadze, N.; Palm, B., *Adv. Mater.* **2004**, 16 (7), 613-615.
27. (a) Harada, A.; Kobayashi, R.; Takashima, Y.; Hashidzume, A.; Yamaguchi, H., *Nat. Chem.* **2011**, 3 (1), 34-37. (b) Yamaguchi, H.; Kobayashi, Y.; Kobayashi, R.; Takashima, Y.; Hashidzume, A.; Harada, A., *Nat. Commun.* **2012**, 3, 603. (c) Zheng, Y.; Hashidzume, A.; Takashima, Y.; Yamaguchi, H.; Harada, A., *Nat. Commun.* **2012**, 3, 831. (d) Zheng, Y.; Hashidzume, A.; Takashima, Y.; Yamaguchi, H.; Harada, A., *ACS Macro Lett.* **2012**, 1 (8), 1083-1085. (e) Zheng, Y.; Hashidzume, A.; Harada, A., *Macromol. Rapid Commun.* **2013**, 34 (13), 1062-1066. (f) Kobayashi, Y.; Takashima, Y.; Hashidzume, A.; Yamaguchi, H.; Harada, A., *Sci. Rep.* **2013**, 3, 1243.
28. (a) Harada, A.; Takahashi, S., *J Incl. Phenom.* **1984**, 2 (3-4), 791-798. (b) Wu, J.-S.; Toda, K.; Tanaka, A.; Sanemasa, I., *Bull. Chem. Soc. Jpn.* **1998**, 71 (7), 1615-1618.
29. Komura, T.; Yamaguchi, T.; Kura, K.; Tanabe, J., *J. Electroanal. Chem.* **2002**, 523 (1-2), 126-135.
30. Tsuchiya, K.; Orihara, Y.; Kondo, Y.; Yoshino, N.; Ohkubo, T.; Sakai, H.; Abe, M., *J. Am. Chem. Soc.* **2004**, 126 (39), 12282-12283.
31. Tomatsu, I.; Hashidzume, A.; Harada, A., *Macromol. Rapid Commun.* **2006**, 27 (4), 238-241.
32. Zuo, F.; Luo, C.; Ding, X.; Zheng, Z.; Cheng, X.; Peng, Y., *Supramol. Chem.* **2008**, 20 (6), 559-564.
33. (a) Nakahata, M.; Takashima, Y.; Yamaguchi, H.; Harada, A., *Nat. Commun.* **2011**, 2, 511. (b) Nakahata, M.; Takashima, Y.; Hashidzume, A.; Harada, A., *Angew. Chem. Int. Ed.* **2013**, 52 (22), 5731-5735.
34. Calvo-Marzal, P.; Delaney, M. P.; Auletta, J. T.; Pan, T.; Perri, N. M.; Weiland, L. M.; Waldeck, D. H.; Clark, W. W.; Meyer, T. Y., *ACS Macro Lett.* **2011**, 1 (1), 204-208.
35. Hempenius, M. A.; Cirmi, C.; Savio, F. L.; Song, J.; Vancso, G. J., *Macromol. Rapid Commun.* **2010**, 31 (9-10), 772-783.
36. Sui, X.; Hempenius, M. A.; Vancso, G. J., *J. Am. Chem. Soc.* **2012**, 134 (9), 4023-4025.
37. Ahn, Y.; Jang, Y.; Selvapalam, N.; Yun, G.; Kim, K., *Angew. Chem. Int. Ed.* **2013**, 52 (11), 3140-3144.
38. Ritter, H.; Mondrzik, B. E.; Rehahn, M.; Gallei, M., *Beilstein J. Org. Chem.* **2010**, 6, 60.
39. Rekharsky, M. V.; Inoue, Y., *Chem. Rev.* **1998**, 98 (5), 1875-1918.
40. Moozyckine, A. U.; Bookham, J. L.; Deary, M. E.; Davies, D. M., *J Chem. Soc., Perkin Trans. 2* **2001**, (9), 1858-1862.

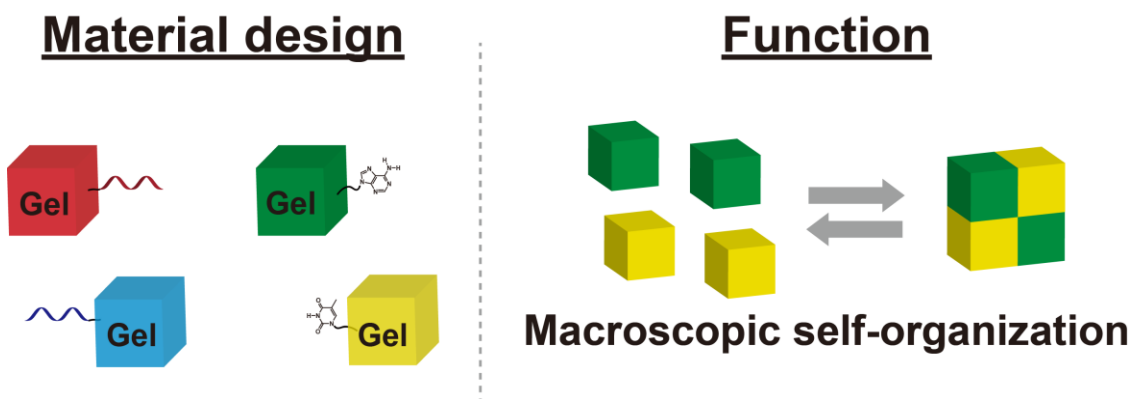


Figure 5-0. Conceptual illustration of chapter 5.

5-1. Introduction

All parts of biological systems, for example, cells, organs, and the living organisms themselves, are complicated, highly ordered structures self-organized through selective molecular recognition. These high-order structures maintain their structure and functions, communicate with each other, and repair themselves to sustain our lives. One of the most representative sequence-specific biomolecules is DNA, which has key roles to produce, store, and transfer genetic information for the next generation¹. In DNA transcription, the sequence of the template DNA chain—consisting of four kinds of nucleobases, adenine (A), thymine (T), guanine (G), and cytosine (C)—is read and transcribed into complementary RNA with almost no misreading²⁻⁶. This is an attractive recognition motif that has been used to construct highly intelligent materials. Many researchers in chemistry and materials science have developed intelligent self-assembly systems on a molecular scale, for example, DNA origami⁷⁻⁹, 3D nanostructures¹⁰⁻¹², metal arrays¹³⁻¹⁵, and stimuli-responsive DNA¹⁶. However, how to construct well-defined self-assemblies on the macroscopic scale is still a big issue for scientists¹⁷⁻²¹. DNA oligonucleotides with ten or more nucleobases form stable duplexes through complementary nucleobase pairing in aqueous media. On the other hand, it is difficult to achieve the formation of self-assemblies by using only a few base pairs²². Therefore, it is of interest to construct macroscopic self-assemblies by using the base pairs themselves in organic media²³. Attaching base pairs onto a polymer backbone induces multivalent interactions between side chains, which leads to an increase in the apparent association constant (K_a). This is the key for the formation of macroscopic assemblies.

Previously, the formation of self-assembly systems by using macroscopic objects (e.g., gels) through host–guest interactions²⁴⁻²⁸ and metal–ligand interactions²⁹ were reported. More recently, there have been some reports on macroscopic adhesion systems based on various noncovalent interactions, as represented by dynamic covalent bonds^{30,31}, ion–ion interactions^{32,33}, hydrogen bonds³⁴, and so on³⁵. Most recently, a DNA-based gel assembly system was developed by using a DNA polymerase-mediated rolling circle amplification (RCA) method on the surface of a gel³⁶; alternatively, we have been studying gel assembly by using oligonucleotides. As just described, macroscopic self-assembly through molecular recognition has attracted much attention owing to the various applications for functional materials. Herein, macroscopic gel assembly systems based on the hydrogen bonds between nucleobase pairs are reported. Two approaches are employed for selective assembly formation in

different media. One is the interaction between hydrogels modified with complementary oligonucleotides in aqueous media. The other is the interaction between organogels modified with nucleobases (A, T, G, and C) in organic media.

5-2. Experimental section

Materials.

Acrylamide (AAm), CDCl_3 , and D_2O were purchased from Wako Pure Chemical Industries, Ltd. Styrene (St), 2,2'-azobis(isobutyronitrile) (AIBN), *N,N*-dimethylformamide (DMF), toluene, chloroform, sodium chloride, magnesium chloride, ethidium bromide (EtBr), tris(hydroxymethyl)aminomethane, hydrochloric acid, ammonium peroxodisulfate (APS), *N,N,N',N'*-tetramethylethylenediamine (TEMED), and *N,N'*-methylenebis(acrylamide) (MBAAm) were obtained from Nacalai Tesque Inc. *p*-Divinylbenzene (DVB) was purchased from Tokyo Chemical Industry Co., Ltd. Deuterated dimethyl sulfoxide ($\text{DMSO-}d_6$) was obtained from Merck & Co., Inc. Water used for the preparation of the aqueous solutions was purified with a Millipore Milli-Q system. Oligonucleotide monomers (**1**: 5'-acrydite-TTTTTCACAGATGAGT-3' (16mer), **1'**: 5'-acrydite-TTTTACTCATCTGTGA-3' (16mer), and **2**: 5'-acrydite-TTTTTTTTTTTTTTTT-3' (16mer)) were purchased from Nihon Gene Research Laboratories, Inc. Here, "acrydite" is a trivial name for phosphoramidite which allows modification of oligonucleotides with a methacryl group at the 5' end (see also Scheme 5-2). Nucleobase monomers (St-A/St-T/St-G/St-C) were prepared according to previous reports.^{1,2} Other reagents were used without further purification.

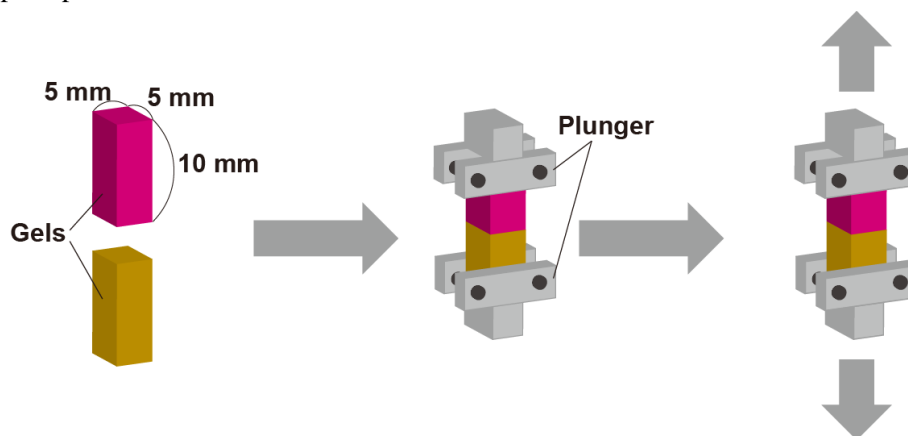
Measurements.

^1H and DOSY NMR spectra were recorded at 500 MHz with a JEOL JNM-ECA 500 NMR spectrometer. Solid-state ^1H field gradient magic angle spinning (FGMAS) NMR spectra were recorded at 400 MHz with a JEOL JNM-ECA 400 NMR spectrometer. Sample spinning rate was 7 kHz. In all NMR measurements, chemical shifts were referenced to the solvent values ($\delta = 2.49$ ppm, 4.79 ppm, and 7.26 ppm for $\text{DMSO-}d_6$, D_2O , and CDCl_3 , respectively). The IR spectra were measured using a JASCO FT/IR-410 spectrometer. Positive-ion matrix-assisted laser desorption/ionization time-of-flight mass spectrometry (MALDI-TOF-MS) experiments were performed using a Bruker autoflex speed mass spectrometer using 2,5-dihydroxybenzoic acid as a matrix. Mass number was calibrated by four peptides, i.e., angiotensin II ($[\text{M}+\text{H}]^+$ 1046.5418), angiotensin I ($[\text{M}+\text{H}]^+$ 1296.6848), substance P ($[\text{M}+\text{H}]^+$ 1347.7354), and bombesin ($[\text{M}+\text{H}]^+$ 1619.8223). Mechanical properties of the gels were measured by the mechanical tension testing system (Rheoner, RE-33005, Yamaden Ltd.). The size of gel was measured using a digital inverted microscope (EVOS AME i2111, Advanced Microscopy Group).

Stress-strain measurements.

Mechanical properties of the gels were measured by the mechanical tension testing system (Rheoner, RE-33005, Yamaden Ltd.) (Scheme 5-1) using either one of the following two methods. (1) (For oligonucleotide gels): Two pieces of gels fixed on plungers were contacted to each other. The gel pieces were separated from one another by pulling the gels from both sides. The rupture stress was estimated from the obtained stress-strain curves. (2) (For nucleobase gels): A piece of bound gels was pulled from both sides. The rupture stress was estimated from the stress-strain curves obtained.

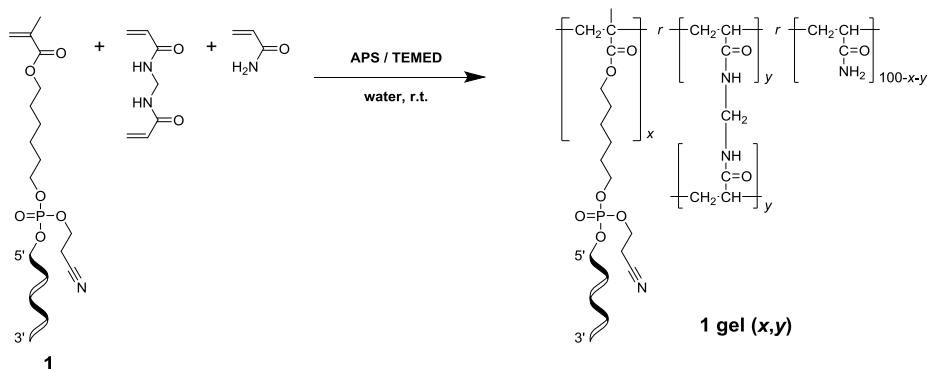
Scheme 5-1. Typical procedure for stress-strain measurements.



Preparation of DNA gels. (Scheme 5-2)

A typical procedure for **1** gel (0.002,0.5) is described below. **1** monomer (2.0×10^{-5} mol), MBAAm (0.8 mg, 5.0×10^{-3} mol), AAm (71 mg, 1.0×10^{-3} mol), APS (2.3 mg, 0.010 mmol), and TEMED (1.5 μ L, 0.010 mmol) were dissolved in Milli-Q water (1.0 mL). The solution turned into gel within a few minutes at room temperature. The gel was washed repeatedly with Milli-Q water to remove unreacted compounds.

Scheme 5-2. Preparation of DNA gels (*x,y*).

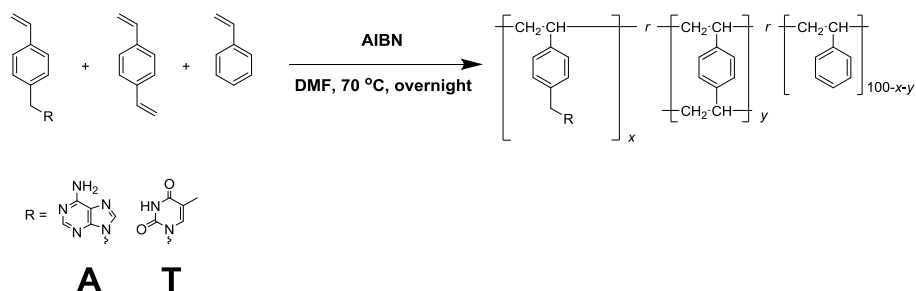


Preparation of A and T gels. (Scheme 5-3)

A typical procedure for **A** gel (4,15) is described below. St-A monomer (20 mg, 0.080 mmol), DVB (43 μ L, 0.30 mmol), St (186 μ L, 1.6 mmol), and AIBN (3.3 mg, 0.020 mmol) were dissolved in DMF (1.0 mL). The solution was purged with argon gas for 1 h and was then heated at 70 °C overnight to form a gel. The gel was washed repeatedly with DMF to remove unreacted compounds.

Also, the model A and T polymers (*x*) were prepared without chemical crosslinker (DVB) in the same procedures.

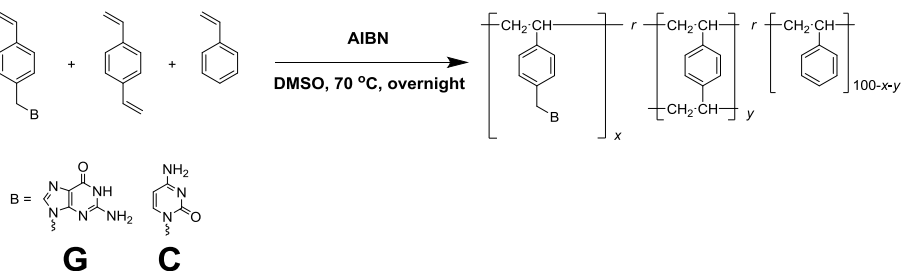
Scheme 5-3. Preparation of **A**, **T** gels (*x,y*).



Preparation of G and C gels. (Scheme 5-4)

G gel and C gel were prepared using the same procedure as those of A gel and T gel in DMSO.

Scheme 5-4. Preparation of **G**, **C** gels (*x,y*).



Characterization of gels.

Fluorescence experiment on the DNA gels.

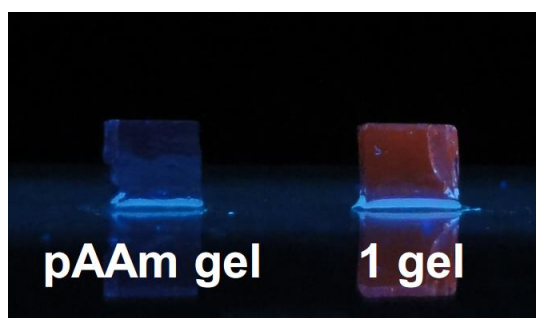


Figure 5-1. Photograph of the cubes of pAAm gel (0.5) and **1** gel (0.002,0.5) immersed in the ethidium bromide (EB) solution (1 μM , in a Tris/HCl buffer (10 mM, pH 8) containing 50 mM NaCl and 10 mM MgCl_2) on a glass plate under UV light ($\lambda = 365 \text{ nm}$). The lower half of the image is the reflection from the glass plate.

^1H FGMAS NMR spectra of A gel (5,10) and T gel (5,10).

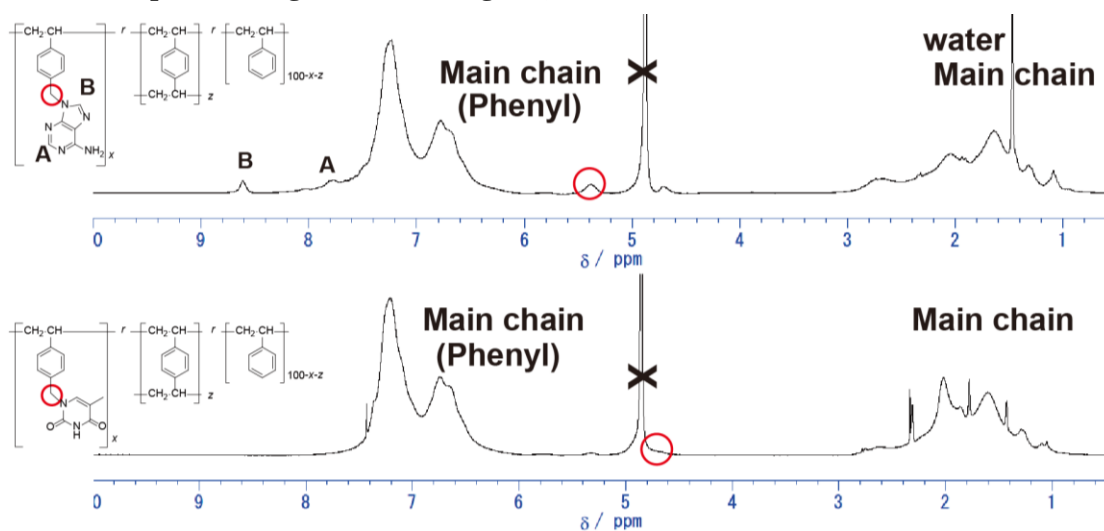


Figure 5-2. Solid-state ^1H FGMAS NMR spectra of A gel (5,10) and T gel (5,10). (Immersed in CDCl_3 , 400 MHz, 30 $^\circ\text{C}$, rotation frequency = 7 kHz. X: Solvent residual signal)

FT-IR spectra of the nucleobase gels.

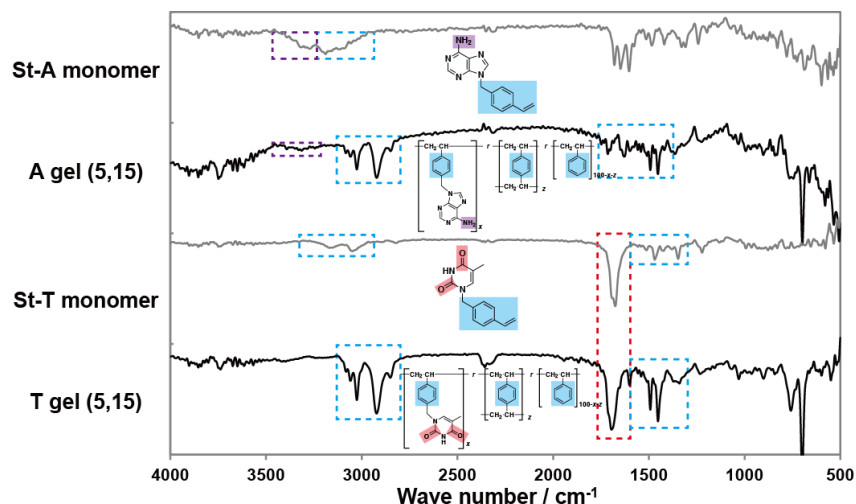
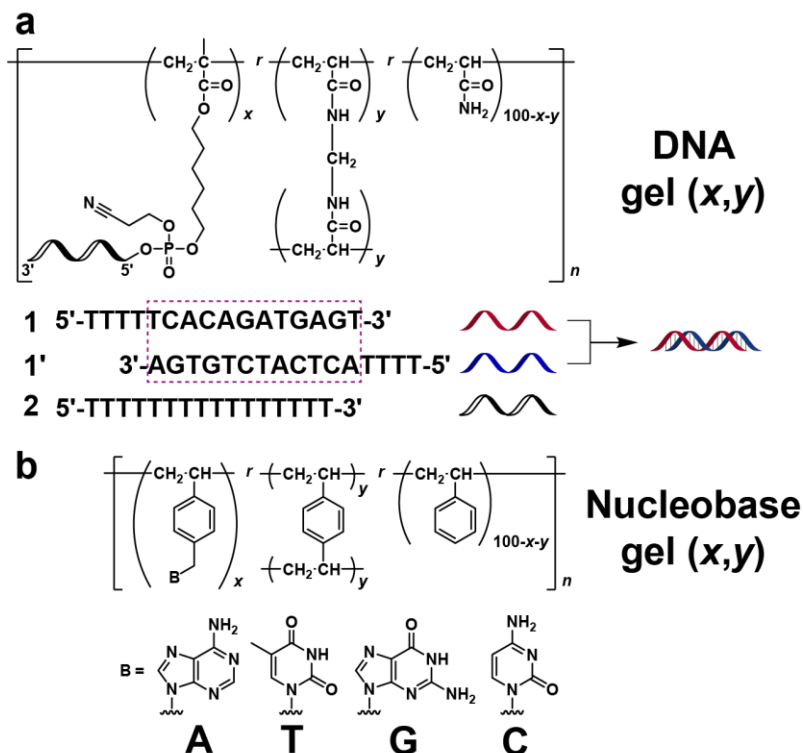


Figure 5-3. FT-IR spectra of St-A monomer, A gel (5,15), St-T monomer, and T gel (5,15), respectively. (KBr disc, r.t.)

5-3. Preparation and characterization of gels

Scheme 5-5 shows the chemical structures of the oligonucleotide gels (DNA gels) and the nucleobase gels used in this study. The DNA gels (Scheme 5-5a) were prepared by using DNA monomers **1** (5'-TTTTTCACAGATGAGT-3' (16 mer)) / **1'** (5'-TTTTACTCATCTGTGA-3' (16 mer)) / **2** (5'-TTTTTTTTTTTTTTTTT-3' (16 mer)), methylenebis(acrylamide) (MBAAm), and acrylamide (AAm). The reaction was initiated by a redox pair of ammonium peroxodisulfate (APS) and *N,N,N',N'*-tetramethylethylenediamine (TEMED) in water (see Scheme 5-2). Oligonucleotides **1** and **1'** have complementary sequences, which complex each other with $K_a \sim 10^9 \text{ L mol}^{-1}$, estimated by the nearest base pair method²². Herein, the resultant gel samples are named **z** gel (*x*,*y*), where **z** represents the oligonucleotide or nucleobase used and *x* and *y* represent the mol% content of functional monomers and chemical crosslinking units, respectively. After immersion of **1**gel (0.002,0.5) in an ethidium bromide (EB) solution (1 mM) in a Tris/HCl buffer (10 mM, pH8) containing 50 mM NaCl and 10 mM MgCl₂, the **1** gel emitted orange light under UV irradiation ($\lambda=365 \text{ nm}$), unlike the pAAm gel (*y*=0.5) used as a control sample (Figure 5-1). As EB becomes fluorescent when bound to DNA⁴⁰, the observed fluorescence indicates successful introduction of the oligonucleotides into DNA gels. The nucleobase gels (Scheme 5-5b) were prepared by homogeneous radical terpolymerization of styrene (St), styrene-based St-A/St-T/St-G/St-C monomers (see also Table 5-1)³⁷⁻³⁹, and *p*-divinylbenzene (DVB), a process that was initiated by 2,2'-azobis(isobutyronitrile) (AIBN) in *N,N*-dimethylformamide (DMF) or dimethyl sulfoxide (DMSO) (Schemes 5-3 and 5-4). ¹H solid-state field-gradient magic-angle-spinning (FGMAS) NMR and Fourier transform infrared (FT-IR) spectroscopies (Figures 5-2 and 5-3) indicated successful introduction of the nucleobases into the nucleobase gels.

Scheme 5-5. Chemical structures of the gels used in this study. **a.** Poly(acrylamide) gels are modified with oligonucleotides **1** (16mer), **1'** (16mer), or **2** (16mer). **1** and **1'** can form complementary duplex in aqueous media. **b.** Poly(styrene) gels are modified with adenine (**A** gel), thymine (**T** gel), guanine (**G** gel), or cytosine (**C** gel) respectively. Here x and y represent the mol % contents of the functional moieties and chemical crosslinking units, respectively.



5-4. Adhesion test between oligonucleotide gels

First, the adhesion test between DNA gels was carried out. **1** gel (0.002,0.5), **1'** gel (0.002,0.5), and **2** gel (0.002,0.5) were cut into cubes with 5 mm edges. All gel cubes were immersed in a Tris/HCl buffer (10 mM, pH 8, containing 50 mM NaCl and 10 mM MgCl₂) at 4 °C and were placed in contact with another cube in the combinations **1–1'**, **1–2**, and **1'–2**. Figure 5-4a shows that only **1–1'** gel cubes adhered to each other. The adhesion strength between the gel pieces was estimated quantitatively by using a creepmeter. Two gel cubes, each fixed on plungers, were brought into contact with each other. The gel pieces were separated by pulling the gels in opposite directions. The rupture stress was estimated from the stress–strain curves. Figure 5-4c shows the rupture stress between **1** gel (0.002,0.5)–**1'** gel (0.002,0.5), **1**gel (0.002,0.5)–**2** gel (0.002,0.5), and **1'** gel (0.002,0.5)–**2**gel (0.002,0.5) pieces estimated from the stress–strain curves (Figure 5-5). The adhesion strength between the **1** and **1'** gel pieces is much larger than those of the control samples, owing to the complementarity between the **1** gel and **1'** gel (Figure 5-4 b).

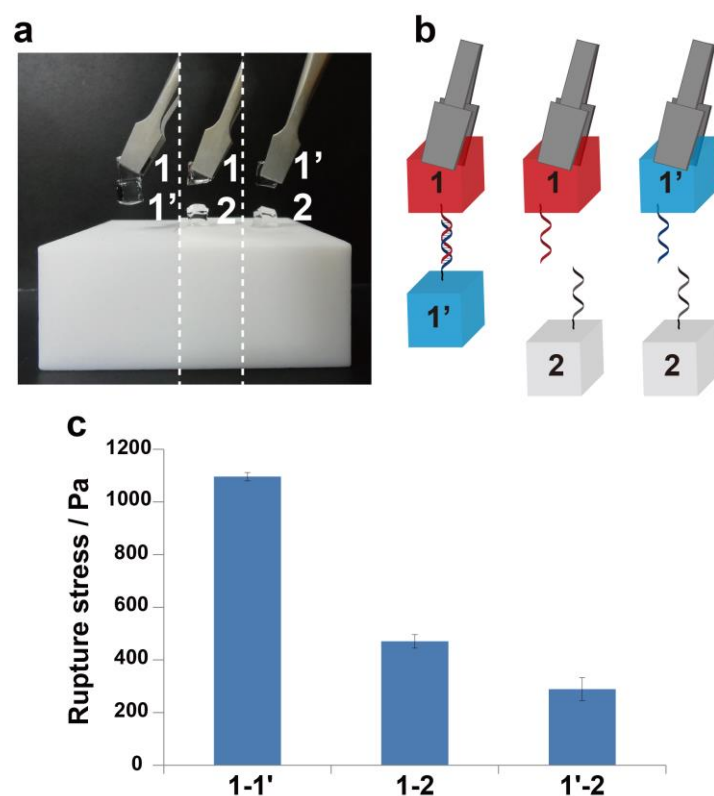


Figure 5-4. Adhesion between oligonucleotide gels. **a.** Photographs of **1** gel-**1'** gel, **1** gel-**2** gel, and **1'** gel-**2** gel, from left to right, respectively. Only **1** gel-**1'** gel adhered after contacted to each other. **b.** Schematic illustration of the interactions between oligonucleotide gels. Oligonucleotide gels with complementary sequences adhered to each other, whereas no interaction occurred between control gels. **c.** Stress-strain measurements between **1** gel-**1'** gel, **1** gel-**2** gel, and **1'** gel-**2** gel, respectively. The rupture stress between **1** gel-**1'** gel is significantly bigger than those of control samples.

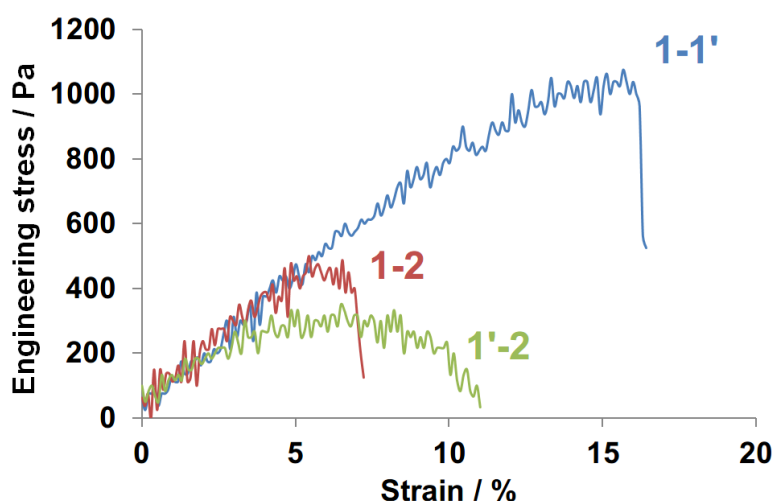


Figure 5-5. Stress-strain curves of the joined surface between pieces of **1** gel (0.002,0.5)-**1'** gel (0.002,0.5) (blue line), **1** gel (0.002,0.5)-**2** gel (0.002,0.5) (red line), and **1'** gel (0.002,0.5)-**2** gel (0.002,0.5) (green line), respectively.

To confirm the complementarity of the adhesion between oligonucleotide gels, a competition experiment was performed. Two competitive nucleotides **C1** and **C1'**, which have complementary sequences for **1** and **1'**, were used (Figure 5-6a). When the surface of the **1'** gel (0.002,0.5) cube was coated with a Tris/HCl buffer containing NaCl and MgCl₂, adhesion between the gel cubes was observed after putting a cube of **1** gel (0.002,0.5) on top and allowing them to stand for 10 min at 4 °C. Conversely, when the surface of the **1'** gel (0.002,0.5) cube was coated with aqueous buffer solutions of the oligonucleotides **C1** or **C1'** (100 μM), no adhesion to the **1** gel (0.002,0.5) cube was observed under the same conditions (Figure 5-6c). **1** and **1'** gels have full-match DNA sequences, which are able to form a complementary double helix (Figure 5-6b). This result indicates that the hybridization of the complementary oligonucleotides on the surfaces of the gels plays an important role for their adhesion.

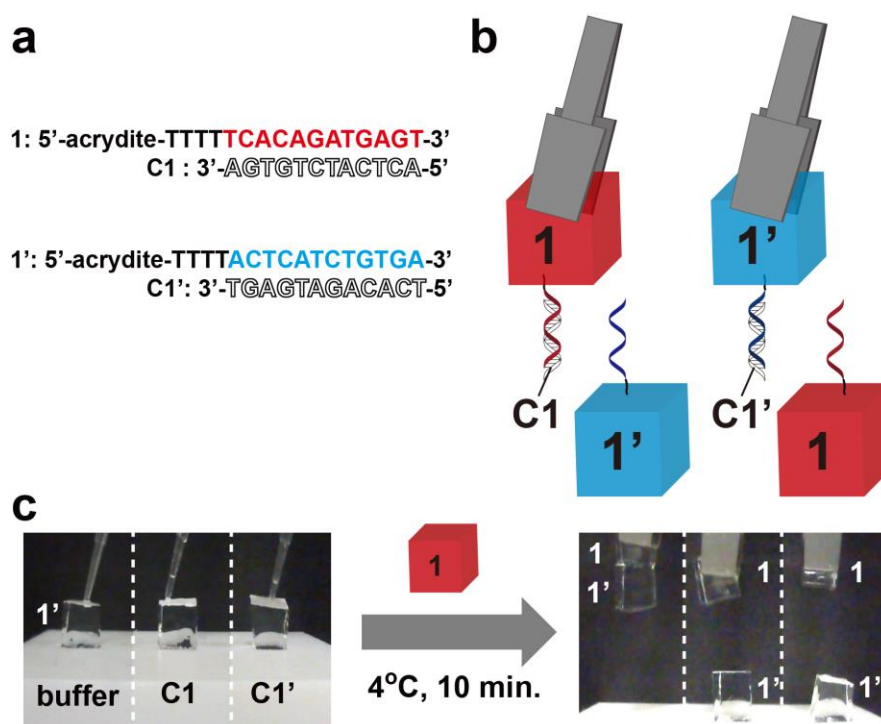


Figure 5-6. A Competitive experiment between oligonucleotide gels. **a.** Sequences of the competitive oligonucleotides **C1** and **C1'**. **C1** and **C1'** have complementary sequences for **1** and **1'**, respectively. **b.** Schematic illustration of inhibition of the adhesion by competitive nucleotides. **c.** Experimental procedure and results of competitive test. First, the surface of the **1'** gel (0.002,0.5) cube was coated with buffer (1 μL), buffer solution of **C1** (1 μL), or buffer solution of **C1'** (1 μL). After putting **1** gel (0.002, 0.5) cube from above, the **1** gel was picked up after 10 min at 4 °C. Competitive oligonucleotides inhibited adhesion between the gels, whereas the control gels with buffer adhered to each other.

5-5. Adhesion test between base pair gels

5-5-1. Interaction between St-A and St-T monomers in the solution.

^1H NMR spectra of the mixture of St-A monomer and St-T monomer.

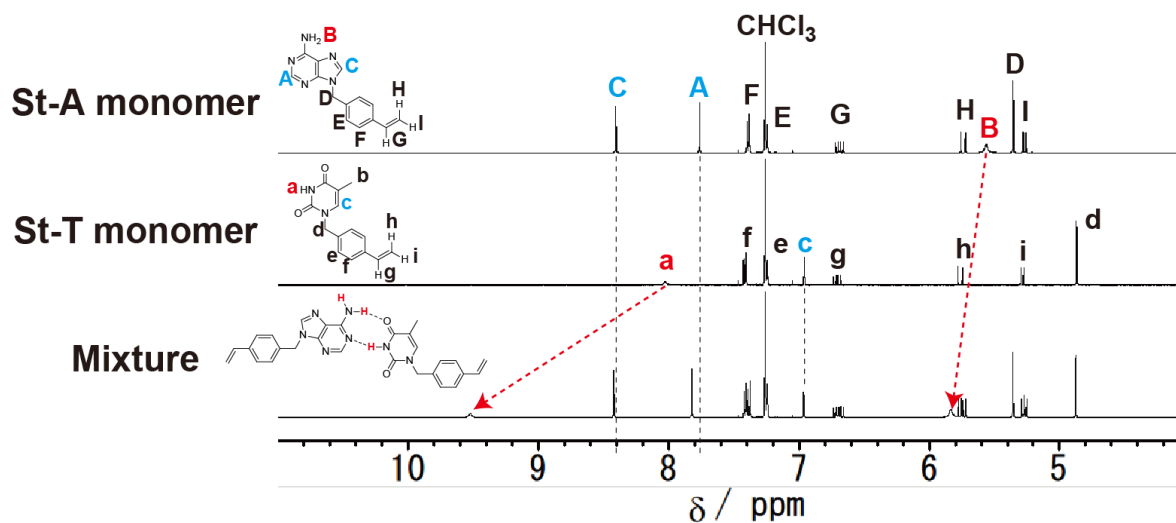


Figure 5-7. ^1H NMR spectra of the St-A monomer (5 mM, upper), St-T monomer (5 mM, middle), and mixture of the St-A monomer and the St-T monomer (5 mM + 5 mM, lower), respectively. (CDCl_3 , 500 MHz, 30 °C) The B and a protons shifted downfield, indicating the complementary hydrogen bonding between St-A and St-T monomers.

Determination of association constant between St-A and St-T monomers.

An association constant (K_a) between St-A monomer and St-T monomer in chloroform-*d* was determined using the same way as Chapter 3. Figure 5-8 shows a typical example of the ^1H NMR spectra for St-A monomer in the presence of varying concentrations of St-T monomer (C_T). As C_T is increased, the peak which is attributed to the a proton of the St-A monomer clearly shifted to a lower field, indicating the interaction of A with the T group. The peak shift ($\Delta\delta$) are plotted against C_T . As can be seen in Figure 5-9, the curve using eq. (1) fitted the plots, indicating that the interaction of A with the T group can be analyzed based on the formation of one-to-one complexes. The apparent association constant K_a value was determined to be $53 \pm 2 \text{ M}^{-1}$ in chloroform-*d*.

$$\Delta\delta_{obs} = \frac{\Delta\delta}{2K_a[A]_0} \left[1 + K_a[T]_0 + K_a[A]_0 - \left\{ (1 + K_a[T]_0 + K_a[A]_0)^2 - 4K_a^2[T]_0[A]_0 \right\}^{\frac{1}{2}} \right] \quad (1)$$

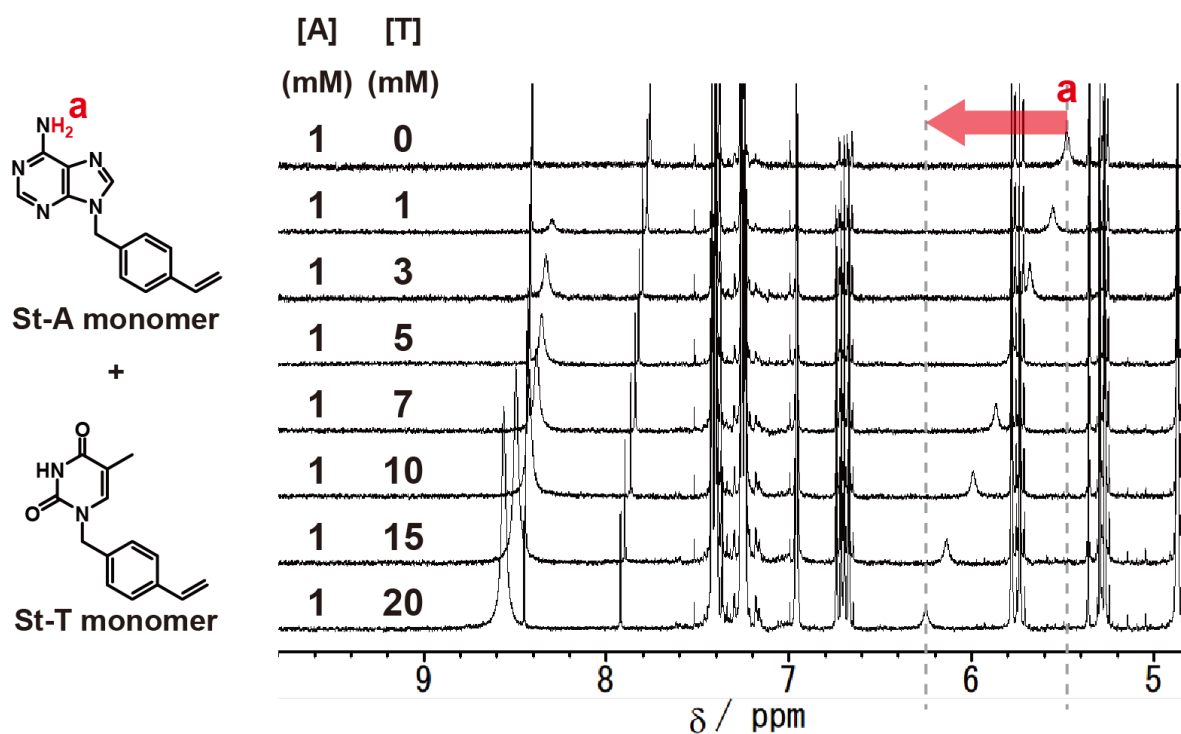


Figure 5-8. Partial ^1H NMR spectra of St-A monomer (1 mM) in the presence of varying concentrations ($C_T = 0, 1, 3, 5, 7, 10, 15$, and 20 mM) of St-T monomer. (CDCl_3 , 400 MHz, 30°C).

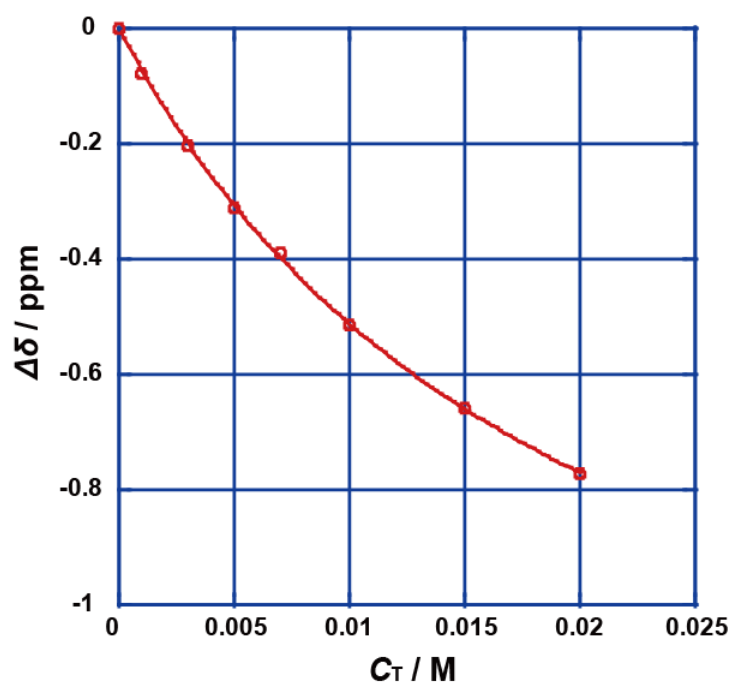


Figure 5-9. The peak shift ($\Delta\delta$) for the signal due to the **a** proton of the St-A monomer as a function of C_T . The best fitted curve using eq. S1 is also drawn.

5-5-2. Interaction between nucleobase gels.

As described above, the DNA gels achieved adhesion in accordance with the hybridization of complementary oligonucleotides with 12 nucleobases. On the basis of these results, it was hypothesized that synthetic polymers modified with nucleobases on the polymer side chain could realize selective adhesion in accordance with the complementary base pairs. Figure 5-10a shows a typical experiment with the gel assembly that uses **A** gel (4,15) and **T** gel (4,15) immersed in toluene. **A** gel and **T** gel were cut into triangle- and square-shaped pieces with 4 mm edges, respectively, and shaken together in toluene. As shown in Figure 5-7a, pieces of **A** gel (4,15) and **T** gel (4,15) formed an assembly within a few minutes. Gels of the same type did not adhere to each other at all, whereas the **A** gel and **T** gel pieces formed an assembly in an alternating manner, indicating the complementarity of the assembly (Figure 5-11).

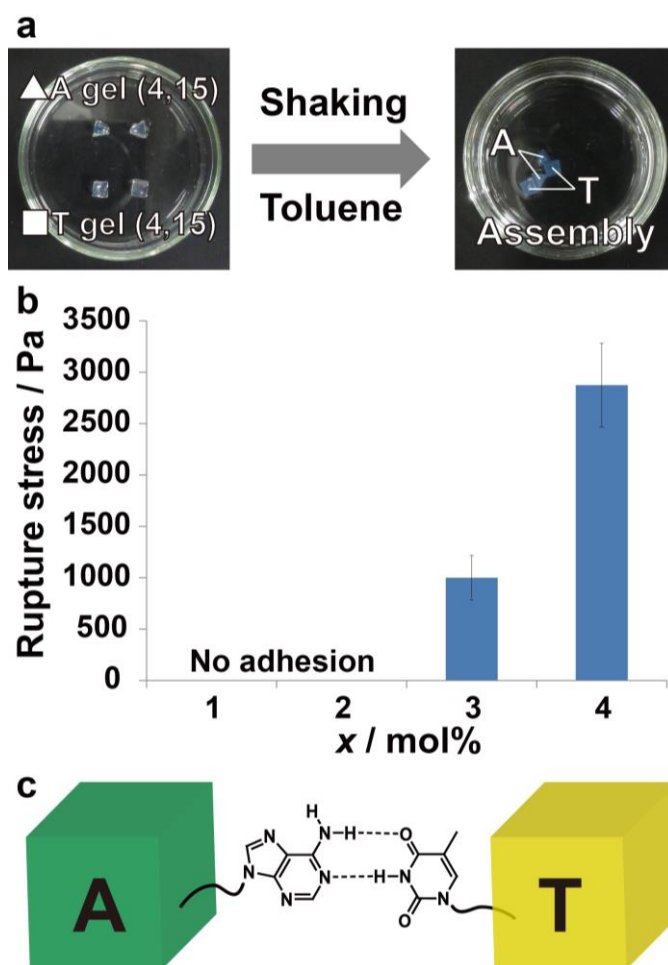


Figure 5-10. Adhesion between the nucleobase gels. **a.** Photographs of pieces of **A** gel (4,15) (triangle) and **T** gel (4,15) (square) shaken in toluene. Four pieces of gels adhered to form an assembly after the agitation in toluene. **b.** Stress-strain measurements between pieces of **A** gel (x,15) and **T** gel (x,15). The rupture stress increased as a function of the contents of **A** and **T** moieties. **c.** Schematic illustration of the adhesion between **A** gel and **T** gel.

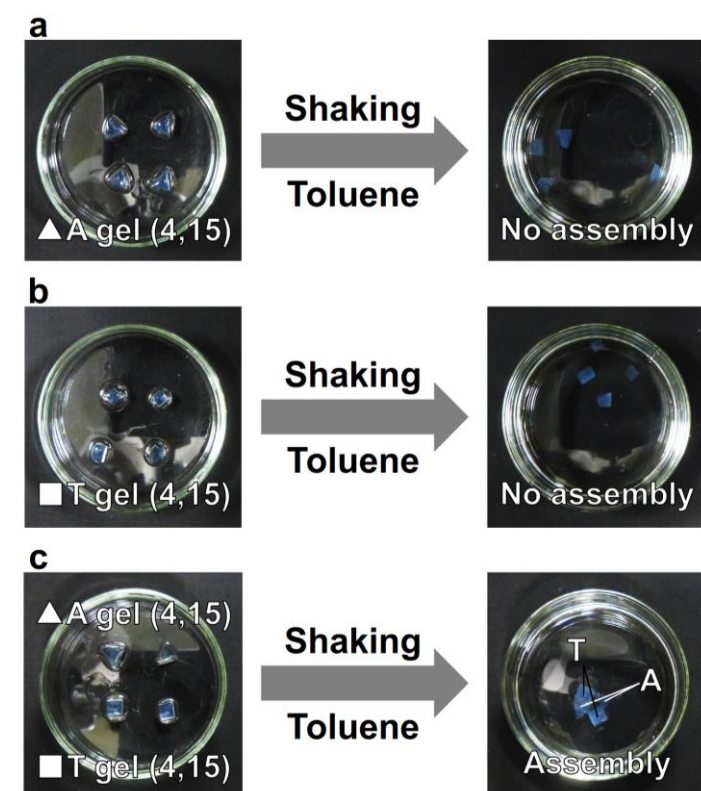


Figure 5-11. Aggregation between same type of gels did not occur at all (a, b), whereas the mixture of pieces of A gel and T gel formed an alternate assembly (c).

The adhesion strength between the A gel and T gel pieces was estimated semi-quantitatively by using stress–strain measurements (Scheme 5-1). Figure 5-10b shows the rupture stress between A gel ($x,15$) and T gel ($x,15$) ($x = 1, 2, 3$, or 4) determined from the stress–strain curves (Figure 5-12). The rupture stress increases as the content of the A and T moieties (x) increases.

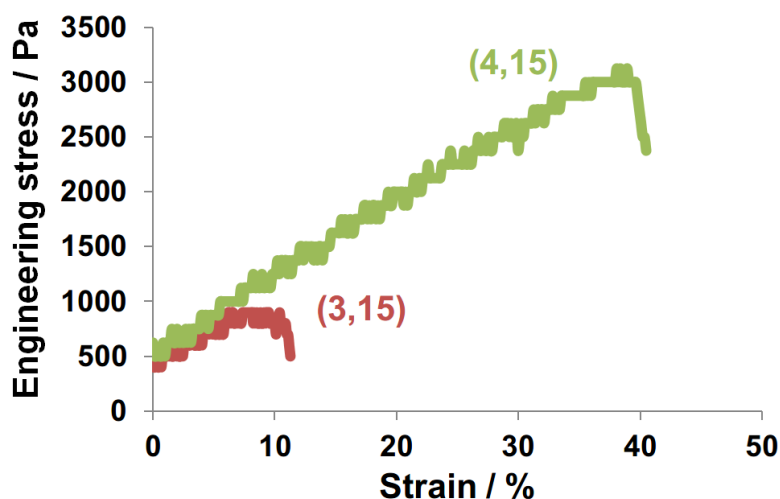


Figure 5-12. Stress-strain curves of the joined surface between pieces of A gel ($x,15$) and T gel ($x,15$) ($x = 3, 4$), respectively.

To confirm the adhesion is based on the complementary interaction between the nucleobase pairs, the effect of solvent and competitive molecules on the gel assembly was investigated. As shown in Figure 5-13, pieces of **A** gel (4,15) and **T** gel (4,15) formed partial assemblies when they were agitated in chloroform. No assemblies were formed in DMF, a highly polar solvent. These observations show that the formation of the gel assembly depends on the polarity of the solvent, indicating that the adhesion between **A** gel and **T**gel pieces is due to hydrogen bonding between the **A** and **T** moieties (Figure 5-10c).

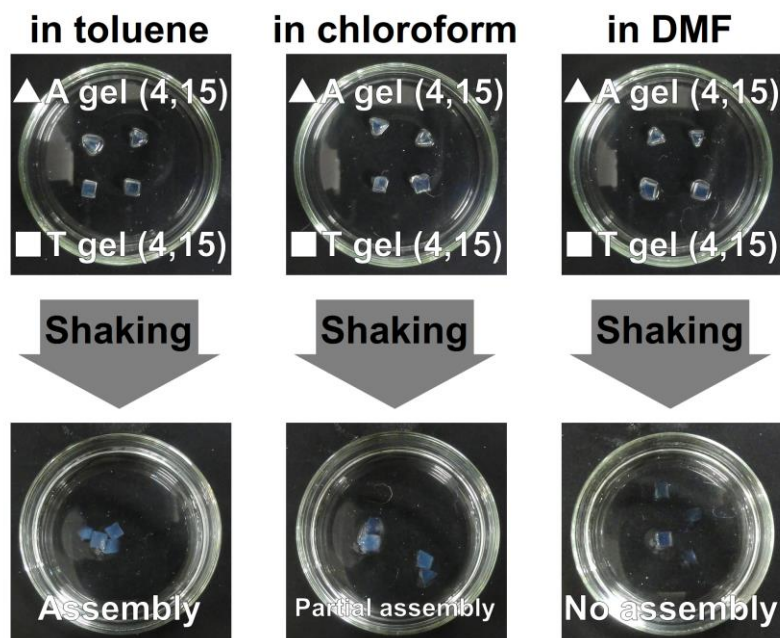


Figure 5-13. Photographs of pieces of **A** gel (4,15) (triangle) and **T** gel (4,15) (square) shaken in toluene (left), chloroform (middle), and DMF (right), respectively.

Furthermore, the competitive polymers (**A** polymer (x) and **T** polymer (x)) were prepared by the same procedure as for the preparation of the gels but without DVB (Figure 5-14a and Scheme 5-3). As shown in Figure 5-14b, pieces of **A** gel (4,15) and **T** gel (4,15) formed no assemblies when they were shaken in the presence of **A** polymer (5) or **T** polymer (5) (both at 10 mg mL⁻¹). These results indicate that competitive polymer inhibits the formation of assemblies of **A** gel and **T** gel (Figure 5-14c). ¹H NMR studies of the **A** monomer and **T** monomer in CDCl₃ solutions provided further evidence for the interaction between **A–T** units at each hydrogen-bonding site (Figures 5-7, 5-8, and 5-9). These results indicate that the **A–T** gels adhere through hydrogen bonding of the complementary base pairs on the surfaces of the gels.

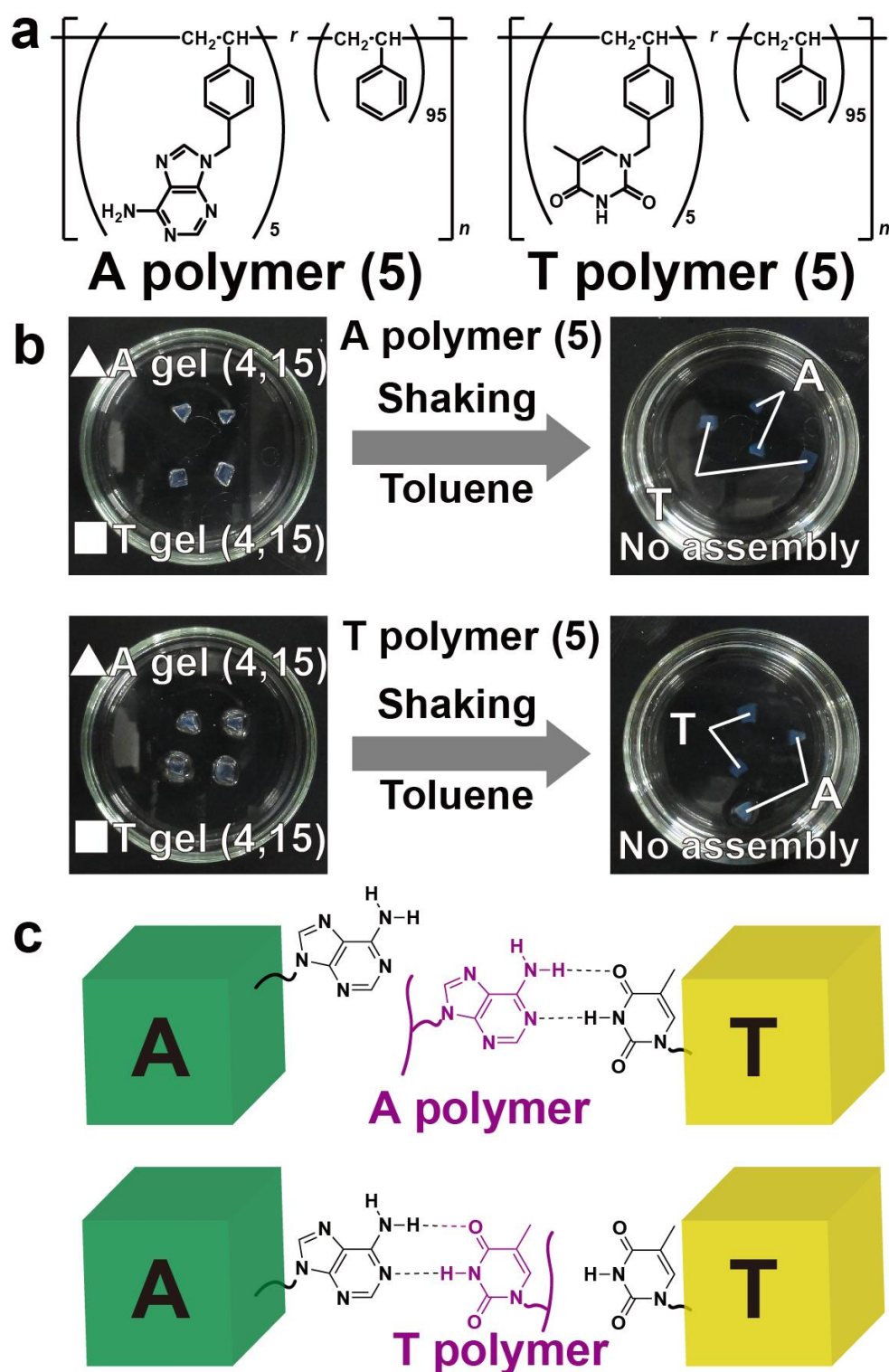


Figure 5-14. Competitive experiment between nucleobase gels. **a.** Chemical structures of competitive polymers (A polymer (5) and T polymer (5)). **b.** When pieces of A gel (4,15) (triangle) and T gel (4,15) (square) were shaken in toluene with competitive polymers (10 mg/mL), no assembly was formed. **c.** Schematic illustration for the inhibition of adhesion between A gel and T gel by competitive polymers.

The **A–T** gel assembly forms with very high selectivity. Figure 5-15 shows an adhesion experiment with **A** gel (4,15), **T** gel (4,15), **G** gel (5,10), and **C** gel (5,10) together in the same petri dish. Pieces of **A** gel and **T** gel formed a selective assembly out of the four nucleobase gels without any mismatch. Although it is well known that **G** and **C** form a more stable base pair than the **A–T** base pair, these gels did not form any assembly at all (see also Figure 5-16). Previous studies have also shown that **G** moieties easily form self-oligomeric structures in nonpolar solvents⁴¹. Thus, the interaction between **G** moieties themselves would inhibit the adhesion between **G** gel and **C** gel (Table 5-1 and Figure 5-17). Further improvements may be required for the formation of discrete assemblies (**A** gel–**T** gel and **G** gel–**C** gel) or artificial transcription systems using gels, which are the subjects of our next research project.

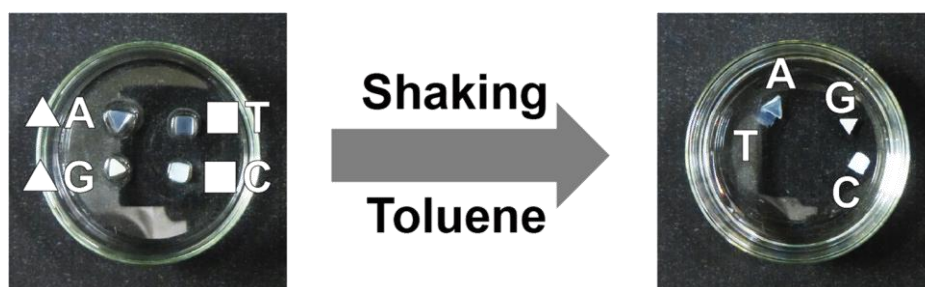


Figure 5-15. Adhesion experiment using four kinds of nucleobase gels. Each piece of **A** gel (4,15) (triangle), **T** gel (4,15) (square), **G** gel (5,10) (triangle), and **C** gel (5,10) (square) are shaken in toluene. Only **A** gel and **T** gel formed an assembly out of four gel pieces without any mismatch after the agitation in toluene.

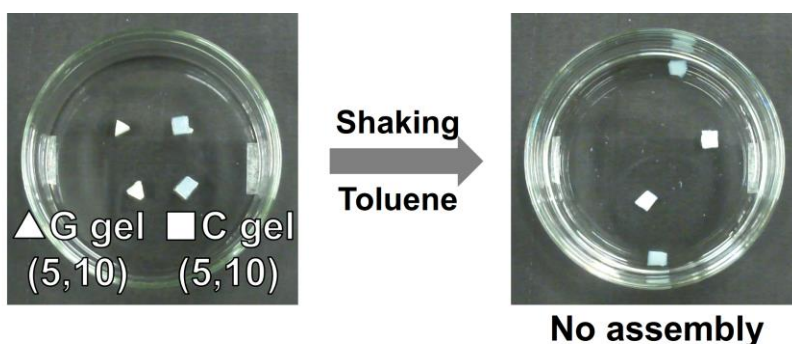
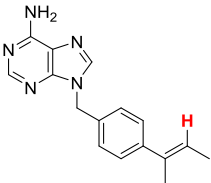
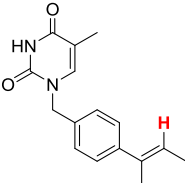
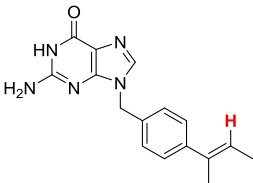
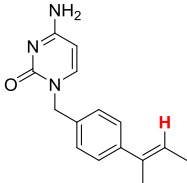
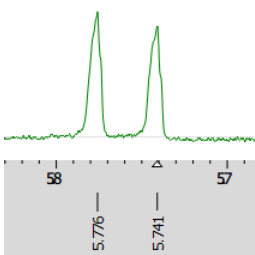
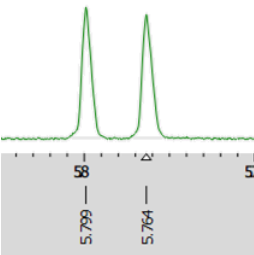
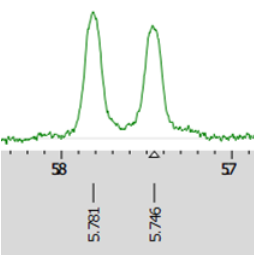
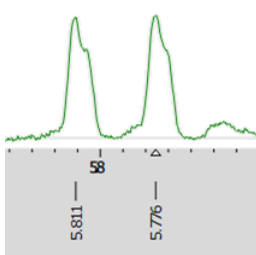


Figure 5-16. Photographs of **G** gel (5,10) (triangle) and **C** gel (5,10) (square) before and after shaking in toluene, respectively.

Formation of self-oligomeric structure between St-G monomers.

Above all other monomers, St-G monomer has the lowest solubility in common organic solvents, suggesting the aggregation of G moieties themselves. Only dimethyl sulfoxide (DMSO) can dissolve St-G monomer. 2D DOSY NMR spectra of St-A, St-T, St-G, and St-C monomers in DMSO-*d*₆ were measured to determine the diffusion coefficient (*D*) of each monomer. Table 5-1 shows the *D* value of each monomer in 20 mM solutions. As shown in Table 5-1, St-G monomer has the lowest *D* value among all nucleobase monomers, indicating the aggregation tendency of St-G monomers themselves even in highly polar solvent.

Table 5-1. Chemical structures, ¹H NMR peaks of vinyl protons (red H in chemical structures), and diffusion coefficient (*D*) values of A, T, G, and C monomers in 20 mM DMSO-*d*₆ solutions.

Chemical structure	 A monomer	 T monomer	 G monomer	 C monomer
Vinyl proton				
<i>D</i> / m ² s ⁻¹	3.0×10^{-9}	2.6×10^{-9}	2.1×10^{-9}	2.7×10^{-9}

Length change of the G gels in the solution of St-G monomer.

Length change of the G gel immersed in the solution of St-G monomer in DMSO was measured. Cubes of G gels (5,10) (size: $1 \times 1 \times 1 \text{ mm}^3$) were immersed in 3 mL of DMSO solutions of St-G monomer (10 mM) for three hours. A digital microscope measured the size changes of gels. The ratio of the lengths was determined as $L_f / L_i \times 100 (\%)$ (L_f : length of the gel after equilibrium swelling, L_i : length of the gel before). Figure 5-17a shows photographs of the G gel (5,10) before and after immersion in 10 mM DMSO solution of St-G monomer. Immersing the G gel (5,10) in 10 mM St-G monomer solution increased the length to $103 \pm 0.8\%$ of the original length (Figure 5-17b). These results indicate that self-oligomeric structures between G moieties function as crosslinker inside the gel even in highly polar solvent (DMSO). After immersing, competitive St-G monomers decompose the oligomeric structures to swell G gel.

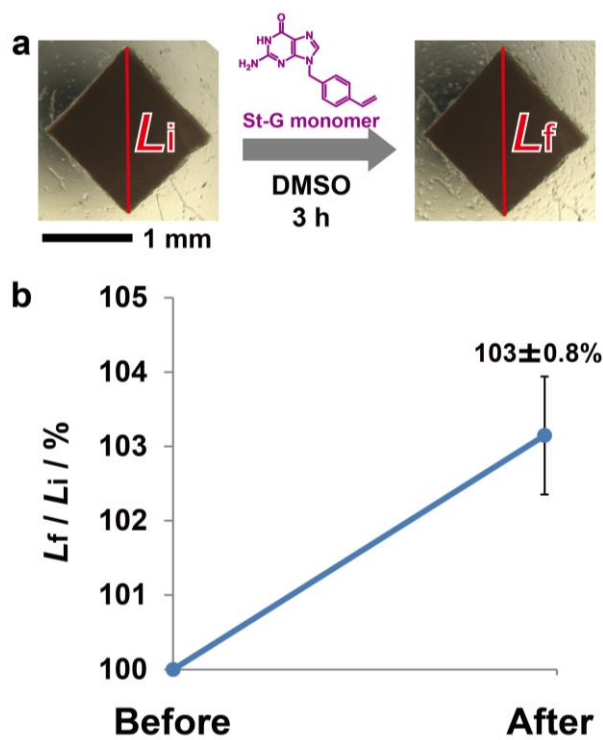


Figure 5-17. (a) Photographs of the G gel before and after immersed in the DMSO solution of St-G monomer. (b) Size change of the G gel immersed in the solution of St-G monomer.

Conclusion

In conclusion, macroscopic self-assembly systems based on the complementary hydrogen bonds between nucleobase pairs were successfully achieved. In the oligonucleotide-modified hydrogel system, the duplex formation between oligonucleotide chains was visualized on a macroscopic scale. In the nucleobase-modified organogel system, the **A** gels and **T** gels selectively adhered to each other by simple agitation in a nonpolar organic solvent. Although the association constant between nucleobases is not very high, the multivalent interaction at the side chain of polymer increases the bonding strength between gels. Macroscopic self-assembly through hydrogen bonding is a versatile concept that can be applied in various media (aqueous and organic), including in the bulk state without any solvent. Direct adhesion between macroscopic objects by hydrogen bonding will provide a technology to bind many kinds of heterogeneous materials (from inorganic to organic) without adhesives, which is highly desired in materials science, medicine, biology, and so on.

References

1. Bloomfield, V. A.; Crothers, D. M.; Tinoco, I., *Nucleic acids : structures, properties, and functions*. University Science Books: Sausalito, Calif., 2000.
2. Budisa, N., *Engineering the genetic code : expanding the amino acid repertoire for the design of novel proteins*. Wiley-VCH: Weinheim, 2006.
3. Blackburn, G. M., *Nucleic acids in chemistry and biology*. 3rd ed.; RSC Pub.: Cambridge, UK, 2006.
4. Herdewijn, P., *Modified nucleosides : in biochemistry, biotechnology, and medicine*. Wiley-VCH: Weinheim, 2008.
5. Mayer, G. n., *The chemical biology of nucleic acids*. Wiley: Chichester, UK, 2010.
6. Egli, M.; Herdewijn, P.; Matsuda, A.; Sanghvi, Y. S., *Current Protocols in Nucleic Acid Chemistry*. John Wiley & Sons, Inc.: Chichester, UK, 2001.
7. Rothmund, P. W. K., *Nature* **2006**, *440* (7082), 297-302.
8. Lund, K.; Manzo, A. J.; Dabby, N.; Michelotti, N.; Johnson-Buck, A.; Nangreave, J.; Taylor, S.; Pei, R.; Stojanovic, M. N.; Walter, N. G.; Winfree, E.; Yan, H., *Nature* **2010**, *465* (7295), 206-210.
9. Pal, S.; Deng, Z.; Ding, B.; Yan, H.; Liu, Y., *Angew. Chem. Int. Ed.* **2010**, *49* (15), 2700-2704.
10. Aldaye, F. A.; Palmer, A. L.; Sleiman, H. F., *Science* **2008**, *321* (5897), 1795-1799.
11. Lo, P. K.; Mettera, K. L.; Sleiman, H. F., *Curr. Opin. Chem. Biol.* **2010**, *14* (5), 597-607.
12. Lo, P. K.; Karam, P.; Aldaye, F. A.; McLaughlin, C. K.; Hamblin, G. D.; Cosa, G.; Sleiman, H. F., *Nat. Chem.* **2010**, *2* (4), 319-328.
13. Yang, H.; McLaughlin, C. K.; Aldaye, F. A.; Hamblin, G. D.; Rys, A. Z.; Rouiller, I.; Sleiman, H. F., *Nat. Chem.* **2009**, *1* (5), 390-396.
14. Osuga, T.; Murase, T.; Fujita, M., *Angew. Chem. Int. Ed.* **2012**, *51* (49), 12199-12201.
15. Tanaka, K.; Tengeji, A.; Kato, T.; Toyama, N.; Shionoya, M., *Science* **2003**, *299* (5610), 1212-1213.
16. Asanuma, H.; Ito, T.; Yoshida, T.; Liang, X.; Komiyama, M., *Angew. Chem. Int. Ed.* **1999**, *38* (16), 2393-2395.
17. (a) Whitesides, G. M.; Grzybowski, B., *Science* **2002**, *295* (5564), 2418-2421. (b) Grzybowski, B. A.; Winkleman, A.; Wiles, J. A.; Brumer, Y.; Whitesides, G. M., *Nat. Mater.* **2003**, *2* (4), 241-245. (c) Bowden, N.; Terfort, A.; Carbeck, J.; Whitesides, G. M., *Science* **1997**, *276* (5310), 233-235.
18. (a) Appel, E. A.; Loh, X. J.; Jones, S. T.; Biedermann, F.; Dreiss, C. A.; Scherman, O. A., *J. Am. Chem. Soc.* **2012**, *134* (28), 11767-11773. (b) Zhang, J.; Coulston, R. J.; Jones, S. T.; Geng, J.; Scherman, O. A.; Abell, C., *Science* **2012**, *335* (6069), 690-694.
19. Gao, B.; Arya, G.; Tao, A. R., *Nat. Nanotech.* **2012**, *7* (7), 433-437.
20. Fang, S.; Fueangfung, S.; Lin, X.; Zhang, X.; Mai, W.; Bi, L.; Green, S. A., *Chem. Commun.* **2011**, *47* (4), 1345-1347.
21. Peng, L.; You, M.; Yuan, Q.; Wu, C.; Han, D.; Chen, Y.; Zhong, Z.; Xue, J.; Tan, W., *J. Am. Chem. Soc.* **2012**, *134* (29), 12302-12307.
22. SantaLucia, J., *Proc. Natl Acad. Sci. U.S.A.* **1998**, *95* (4), 1460-1465.
23. Brunsveld, L.; Folmer, B. J. B.; Meijer, E. W.; Sijbesma, R. P., *Chem. Rev.* **2001**, *101* (12), 4071-4098.
24. Harada, A.; Kobayashi, R.; Takashima, Y.; Hashidzume, A.; Yamaguchi, H., *Nat. Chem.* **2011**, *3* (1),

34-37.

25. Yamaguchi, H.; Kobayashi, Y.; Kobayashi, R.; Takashima, Y.; Hashidzume, A.; Harada, A., *Nat. Commun.* **2012**, *3*, 603.
26. Zheng, Y.; Hashidzume, A.; Takashima, Y.; Yamaguchi, H.; Harada, A., *Nat. Commun.* **2012**, *3*, 831.
27. Zheng, Y.; Hashidzume, A.; Takashima, Y.; Yamaguchi, H.; Harada, A., *ACS Macro Lett.* **2012**, *1* (8), 1083-1085.
28. Zheng, Y.; Hashidzume, A.; Harada, A., *Macromol. Rapid Commun.* **2013**, *34* (13), 1062-1066.
29. Kobayashi, Y.; Takashima, Y.; Hashidzume, A.; Yamaguchi, H.; Harada, A., *Sci. Rep.* **2013**, *3*.
30. Liang, E.; Zhou, H.; Ding, X.; Zheng, Z.; Peng, Y., *Chem. Commun.* **2013**, *49* (47), 5384-5386.
31. Nakahata, M.; Mori, S.; Takashima, Y.; Hashidzume, A.; Yamaguchi, H.; Harada, A., *ACS Macro Lett.* **2014**, *3* (4), 337-340.
32. Asoh, T.-A.; Kikuchi, A., *Chem. Commun.* **2010**, *46* (41), 7793-7795.
33. Nakahata, M.; Takashima, Y.; Harada, A., *Angew. Chem. Int. Ed.* **2014**, *53* (14), 3617-3621.
34. Anderson, C. A.; Jones, A. R.; Briggs, E. M.; Novitsky, E. J.; Kuykendall, D. W.; Sottos, N. R.; Zimmerman, S. C., *J. Am. Chem. Soc.* **2013**, *135* (19), 7288-7295.
35. Ahn, Y.; Jang, Y.; Selvapalam, N.; Yun, G.; Kim, K., *Angew. Chem. Int. Ed.* **2013**, *52* (11), 3140-3144.
36. Qi, H.; Ghodousi, M.; Du, Y.; Grun, C.; Bae, H.; Yin, P.; Khademhosseini, A., *Nat. Commun.* **2013**, *4*.
37. McHale, R.; O'Reilly, R. K., *Macromolecules* **2012**, *45* (19), 7665-7675.
38. Sedlák, M.; Šimůnek, P.; Antonietti, M., *J. Heterocycl. Chem.* **2003**, *40* (4), 671-675.
39. Purohit, C. S.; Parvez, M.; Verma, S., *Applied Catalysis A: General* **2007**, *316* (1), 100-106.
40. Lepecq, J. B.; Paoletti, C., *J. Mol. Biol.* **1967**, *27* (1), 87-106.
41. Fathalla, M.; Lawrence, C. M.; Zhang, N.; Sessler, J. L.; Jayawickramarajah, J., *Chem. Soc. Rev.* **2009**, *38* (6), 1608-1620.

Summary and Conclusion

In this thesis, the author has shown that reversible host-guest inclusion complexes or nucleobase pairs on a microscopic achieve macroscopic morphological change by incorporating supramolecular chemistry with polymer chemistry. Especially, redox stimuli-responsive materials based on redox-responsive inclusion complex between cyclodextrin (CD) and ferrocene (Fc) were mainly described.

In *Chapter 2*, a redox-responsive self-healing material composed of host polymer and guest polymer was studied. Supramolecular hydrogel consisting pAA-6 β CD, which was a poly(acrylic acid) modified with β -CD, and pAA-Fc, which was a poly(acrylic acid) modified with ferrocene, formed stable supramolecular hydrogel by just mixing aqueous solutions of both polymers. Host-guest interaction plays a crucial role to bridge between host polymer and guest polymer to form the hydrogel. Both competitive molecules and oxidizing agent were able to transfer the gel to sol state, and reducing agent brought it back to initial gel state. By utilizing reversible supramolecular crosslinks, the supramolecular hydrogel showed self-healing property due to recovery of host-guest inclusion complexes. The self-healing property is semi-quantitatively estimated by measuring mechanical strength. The self-healing is tunable using redox stimuli in accordance with the redox state of Fc moieties.

In *Chapter 3*, a redox-responsive artificial muscle was studied. Supramolecular crosslinks between β CD and Fc were introduced into chemically cross-linked hydrogel network (β CD-Fc gel). This gel showed solvent-, chemo-, and redox-responsive swelling and shrinking property. By changing solvent from DMSO to water, the β CD-Fc gel shrunk remarkably. Immersion into aqueous solutions of competitive molecules swelled the gel because of decrease in cross-linking density at the side chain. Oxidizing agent and reducing agent led to swelling and shrinking of gel, respectively. This is because oxidized ferrocenium cation went out of cavity of CD and supramolecular crosslink was partly dissociated. It is discovered that β CD-Fc gel has a function as a redox-responsive actuator which can lift up a weight heavier than the gel itself in the course of oxidation-reduction cycle.

In *Chapter 4*, a macroscopic self-assembly between polymeric hydrogels modified with β -cyclodextrin (β CD gel), ferrocene (Fc gel), and styrenesulfonic acid sodium salt (SSNa gel) was investigated to create dual stimuli-responsive assembly system. Under reductive condition, Fc gel selectively adhered to β CD gel through host-guest interaction. On the other hand, the oxidized ferrocenium (Fc^+) gel selectively adhered to the SSNa gel through ionic interaction under oxidative condition. The adhesion strength was semi-quantitatively estimated by tensile test. Finally, an ABC-type macroscopic assembly using three gels together was successfully formed through two discrete non-covalent interactions.

In *Chapter 5*, formation of macroscopic self-assembly between polymeric gels carrying oligonucleotides or nucleobases was investigated. Hydrogels modified with complementary oligonucleotides adhered to each other in aqueous media. Organogels modified with complementary nucleobases formed an assembly in non-polar organic solvent. Adhesion strengths were semi-quantitatively estimated by tensile test. The adhesion between macroscopic objects through complementary hydrogen bonds was observed in wide range of media from aqueous to organic.

In conclusion, the author demonstrated self-healing property, actuation motion, and macroscopic self-assembly based on reversible complex formation on the surface and inside polymeric materials. The studies of self-healing and macroscopic self-assembly demonstrate the molecular recognition on the surface of polymeric materials to realize the adhesion between the materials. These studies indicate that the molecules with complementarity show a precise recognition property even on the materials. On the other hand, the study of the actuation motion through molecular recognition suggests that the functional guest and host groups on the polymer side chain show the reversible molecular recognition even inside the materials. These studies of supramolecular materials based on non-covalent interactions revealed that molecules on the surface and inside materials have relatively high mobility, which create attractive functions. Of course, the mobility of the molecules depends on the stiffness of materials.

Though switching of supramolecular complexes on a molecular scale is well known, a morphological change on a macroscopic scale is difficult to realize. This work demonstrates that stimuli can control molecular recognition to cause macroscopic change which is directly observable on our own eyes without any special apparatus.

List of Publications

Original papers

1. Redox-responsive self-healing materials formed from host–guest polymers
M. Nakahata, Y. Takashima, H. Yamaguchi, and A. Harada
Nat. Commun. **2011**, 2, 511.
2. Redox-Generated Mechanical Motion of a Supramolecular Polymeric Actuator Based on Host–Guest Interactions
M. Nakahata, Y. Takashima, A. Hashidzume, and A. Harada
Angew. Chem. Int. Ed. **2013**, 52, 5731-5735.
3. Redox-Responsive Macroscopic Gel Assembly Based on Discrete Dual Interactions
M. Nakahata, Y. Takashima, and A. Harada
Angew. Chem. Int. Ed. **2014**, 53, 3617-3621.
4. Macroscopic Self-assembly Based on Complementary Interaction between Nucleobase Pairs
M. Nakahata, Y. Takashima, A. Hashidzume, and A. Harada
Chem. Eur. J. **2015**, 21, 2770-2774.

Other related papers

1. Expansion–contraction of photoresponsive artificial muscle regulated by host–guest interactions
Y. Takashima, S. Hatanaka, M. Otsubo, M. Nakahata, T. Kakuta, A. Hashidzume, H. Yamaguchi, and A. Harada
Nat. Commun. **2012**, 3, 1270.
2. Preorganized Hydrogel: Self - Healing Properties of Supramolecular Hydrogels Formed by Polymerization of Host-Guest - Monomers that Contain Cyclodextrins and Hydrophobic Guest Groups
T. Kakuta, Y. Takashima, M. Nakahata, M. Otsubo, H. Yamaguchi, and A. Harada
Adv. Mater. **2013**, 25, 2849-2853.
3. pH-and Sugar-Responsive Gel Assemblies Based on Boronate–Catechol Interactions
M. Nakahata, S. Mori, Y. Takashima, A. Hashidzume, H. Yamaguchi, and A. Harada
ACS Macro Lett. **2014**, 3, 337-340.
4. Supramolecular Adhesives to Hard Surfaces: Adhesion between Host Hydrogels and Guest Glass Substrates through Molecular Recognition
Y. Takashima, T. Sahara, T. Sekine, T. Kakuta, M. Nakahata, M. Otsubo, Y. Kobayashi, and A. Harada
Macromol. Rapid Commun. **2014**, 35, 1646-1652.

Reviews

1. Supramolecular Polymeric Materials via Cyclodextrin–Guest Interactions
A. Harada, Y. Takashima, and M. Nakahata
Acc. Chem. Res. **2014**, 47, 2128-2140.